AD-A160 311 WHITE LIGHT OPTICAL INFORMATION PROCESSING(U) MICHIGAN 1/2
UNIV ANN ARBOR DEPT OF ELECTRICAL AND COMPUTER
ENGINEERING E N LEITH 31 MAY 85 AFOSR-TR-85-0853
UNCLASSIFIED AFOSR-81-0243 F/G 20/6 NL

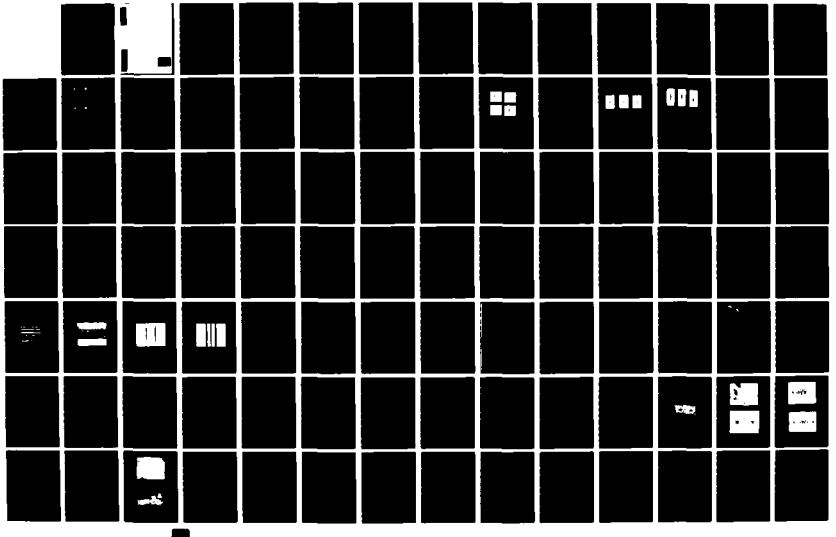

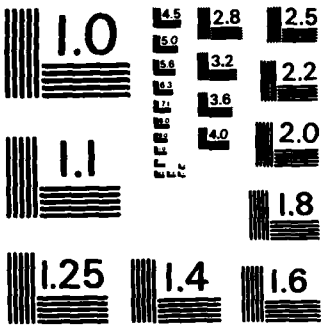

MICROCOPY RESOLUTION TEST CHART
NATIONAL BUREAU OF STANDARDS - 1963 - A

AD-A160311

SECURITY CLASSIFICATION OF THIS PAGE

REPORT DOCUMENTATION PAGE

1a. REPORT SECURITY CLASSIFICATION: unclassified	1b. RESTRICTIVE MARKINGS
2a. SECURITY CLASSIFICATION AUTHORITY	3. DISTRIBUTION / AVAILABILITY OF REPORT
2b. DECLASSIFICATION / DOWNGRADING SCHEDULE	
4. PERFORMING ORGANIZATION REPORT NUMBER(S): report # 7	5. MONITORING ORGANIZATION REPORT NUMBER(S): AFOSR TR-
6a. NAME OF PERFORMING ORGANIZATION: The University of Mich. / 6b. OFFICE SYMBOL (If applicable)	7a. NAME OF MONITORING ORGANIZATION: same as # 8
6c. ADDRESS (City, State, and ZIP Code): Ann Arbor, Mich 48109	7b. ADDRESS (City, State, and ZIP Code)
8a. NAME OF FUNDING / SPONSORING ORGANIZATION: AFOSR/NE / 8b. OFFICE SYMBOL (If applicable)	9. PROCUREMENT INSTRUMENT IDENTIFICATION NUMBER: Grant AFOSR 81 0243
8c. ADDRESS (City, State, and ZIP Code): Bolling Air Force Base, D.C. Bldg. 410 20332	10. SOURCE OF FUNDING NUMBERS: PROGRAM ELEMENT NO. 61102F / PROJECT NO. 2305 / TASK NO. B1 / WORK UNIT ACCESSION NO.

11. TITLE (Include Security Classification): White Light Optical Information Processing

12. PERSONAL AUTHOR(S): Leith, Emmett N.

13a. TYPE OF REPORT	13b. TIME COVERED	14. DATE OF REPORT (Year, Month, Day)	15. PAGE COUNT
final	FROM Sep 30 81 TO Dec 31 84	85-5-31	104

16. SUPPLEMENTARY NOTATION

17. COSATI CODES		
FIELD	GROUP	SUB-GROUP

18. SUBJECT TERMS (Continue on reverse if necessary and identify by block number): optical processing, holography, white light, information processing, phase conjugation, 4

19. ABSTRACT (Continue on reverse if necessary and identify by block number)

Methods for optical processing and holography with light of reduced coherence are described, including the making of holographic optical elements in light of reduced spatial or temporal coherence, phase conjugation with light of reduced coherence, and Fourier transformation spatial matched filtering in spatially and temporally incoherent light.

DTIC ELECTE OCT 15 1985 A

20. DISTRIBUTION / AVAILABILITY OF ABSTRACT: ☐ UNCLASSIFIED/UNLIMITED ☐ SAME AS RPT. ☐ DTIC USERS	21. ABSTRACT SECURITY CLASSIFICATION: unclassified
22a. NAME OF RESPONSIBLE INDIVIDUAL: Lt. Col. Carter	22b. TELEPHONE (Include Area Code): (202) 767 4933 / 22c. OFFICE SYMBOL: C 216

DD FORM 1473, 84 MAR — 83 APR edition may be used until exhausted. All other editions are obsolete.

SECURITY CLASSIFICATION OF THIS PAGE

1

Introduction

During the past 3.5 years we have addressed the problem of performing optical processing and holography in light that is either spatially incoherent, temporally incoherent, or both. We discovered a variety of new techniques and uncovred a variety of applications.

The great advantage of incoherent light, as opposed to coherent, is the noise suppression capability. Another advantage is that this is the light that dominates in the environment, and incoherent systems can thus sometimes use, for the system input, an actual object rather than a photography, or in some cases, a CRT display can be used as the input. Sometimes the use of an incoherent system is cumbersome. The techniques for achieving the incoherent operation may lead to complications. Other times, however, the incoherent techniques are simple. The results, in either case, are generally quite good.

One of the guiding concepts we have followed is that often the operation to be carried out does require coherence, but the coherence need be of only one kind, either spatial or temporal, and if we retain only the kind of coherence that is needed and destroy the other kind of coherence, we can gain the advantages that go with the coherence, but yet retain the favorable SNR that goes with incoherent light. Overall, the techniques that we have developed are diverse, and we judge, likely to prove useful.

2

Research Objectives

This report covers three grant periods. We list the research objectives as given in the three grant proposals

1. Use our white light Fourier transformation process to both construct and use a spatial matched filter, as well as to construct and use other types of complex spatial filters.

2. Analyze the present system limitations and devise ways to improve the system S/N ratio and increase the space-bandwidth product that can be accommodated.

3. Further improve the achromatization through the use of additional dispersive lenses, either refractive or diffractive.

4. Explore methods to extend the achromatization methods to speckle interferometry.

5. Explore various ideas for extending the achromatization methods to spatially incoherent light, that is, to make spatially incoherent light act like coherent light, just as we have made point source white light behave coherently.

6. Demonstrate white light grating interferometry method of phase-amplitude recording using phase and phase amplitude objects from various areas, including engineering and biological.

7. Extend the white light and incoherent optical processing concepts into such areas as robotic vision and phase conjugation, as well as into other areas of image processing.

8. Investigate the SNR for incoherent optical processing systems in the presence of artifact noise, detector noise, and bias build up, and determine the significant parameters, such as space-band width product of the system impulse response.

9. Compare the SNR for the coherent case, polychromatic achromatic coherent case, and the extended source incoherent case, and characterize the situation when the coherent (monochromatic or polychromatic) is advantageous and when the incohernet is advantageous.

10. Examine the trade off between resolution and SNR.

11. Conduct experimental comparisons between coherent and incoherent processing to verify the analytic conclusions.

12. Research the technique for making holographic optical elements in spatially incoherent light, including

    a. Examination of the noise reduction achieved by incoherent illumination.

    b. Development of a theory describing noise reduction, using the concept of a multidimensional transfer function for noise originating at various positions in the optical system used for HOE construction.

    c. Determining of the range of HOE parameters for which our technique is applicable, including the range of conjugate focal planes, and the possibility of making aspheric HOES.

    d. Examination of the aberrations that arise in this new method of HOE construction.

    e. Extention of the incoherent method to the making of reflection HOES.

    f. Development of a comprehensive theory for the creation of HOES in incoherent light.

13. Develop other areas for incoherent light interferometry, including incoherent light holography, the construction of blazed gratings by incoherent methods, the use of incoherent light in phase conjugation methods, and the invention of new ideas for incoherent light interferometry and its application to optical processing.

3
Accomplishments

We gave attention to most of these objectives. Our proposal accomplishments over this period have been:

1. We adapted our grating interferometer method for phase-amplitude recording to the area of phase conjugation. We invented and demonstrated a system for compensation of aberrations in an imaging system by holographically recording the way, generating the conjugate, and sending it through the optical system in a path retracing the original wave. The system aberrations are therefore compensated. The old way of doing this (which incidentally, we invented in 1965) required coherent light, which is rather noisy. The significant development here is that our new methods enables us to do this with light of considerably reduced coherence, thus reducing the noise.

2. We addressed the bias buildup and SNR in incoherent optical processing, making an analysis that indicates that, despite the bias buildup problem in incoherent processing, which can lead to greatly reduced constrast at the output, the incoherent system is generally better than the coherent for SNR. Thus, if we have a sensitive, low-noise detector at the output of an incoherent system, we should do better than if the system were coherent, that is, when we subtract off the enormous bias at the output, we get a very weak signal, but the noise should be, proportionately, even lower.

3. A technique for recording in spatially incoherent light the Fourier transform of an object was developed, where the object is the source distribution. This Fourier transform can be spatially filtered in incoherent light, and either the filtered image or the autocorrelation function can be recovered.

4. A new method of recording the Fourier transform, complete with amplitude and phase, in light that is completely spatially incoherent, was discovered. This method uses a three-grating interferometer, adjusted for broad source operation. It has several important aspects; for example, it works on the amplitude transmittance of the object distribution and it preserves the phase, even though the light is incoherent.
5. We adapted our method for doing reduced-coherence phase conjugation to real time processes, and we conducted experiments to verify the ideas.

6. We carried out an extensive analysis, development and experimental program on the method of recording in spatially incoherent light the Fourier transform of an object. This method, works as if the light were coherent, even though the light is in fact coherent. For example, it works on the light amplitude and it preserves phase.

7. We discovered, a method for making holographic optical elements in spatially incoherent light. In the process, we investigated the SNR achievement in making HOES with incoherent light as opposed to coherent light.

8. The white light spatially incoherent grating interferometry method for recording phase amplitude image was applied to image plane holography with successful results.

9. We examined the noise reduction achieved by making HOES with incoherent light. We found a significant noise reduction in all cases where the corresponding coherent case contained optical elements between the pinhole spatial filters and the recording plate.

10. We found that high diffraction efficiency could be obtained even when the light was spatially incoherent.

11. We found that HOES could be produced in broadband light from a point source and with considerable noise reduction.

12. We demonstrated the nature of the noise reduction process by use of a dye laser that was scanned across its tuning range during the exposure time. The fringes and the signal were found to be stationary, whereas the noise moved across the field as the wavelength changed.

13. We demonstrated an interesting and useful way of viewing the noise in a way separate from the signal. The dye laser was scanned at a slow rate, and multiple pictures were made of the output, with short enough exposure so that the pattern motion due to wavelength chain was negligible. Sequential exposures were then observed as a stereo pair. Whatever patterns were stationary were seen in one plane, while moving patterns (the noise) appeared in other planes at a different depth.

14. We generalized the achromatization process of hologram formation, showing that the achromatization process was in fact far more general than had been previously shown.

15. We conceived a method for forming fringes of arbitrary profile with incoherent light. This method is applicable to making holographic diffraction gratings.

16. We conceived a method for optical tomography with incoherent light.

Of these accomplishments there are two that we regard as significant far beyond all the others. These are items 4 and 7. The recording of a Fourier transformation with incoherent light, which behaves as if it had been made with coherent light, is a development with broad implications, and can be the basis for considerable additional developments. Also, the making of zone plate patterns in extended source light, without the bias buildup that characterizes all previous holographic techniques using broad source light has considerable implication, which we have subsequently been examining.

4.

Summary

The bulk of this work has been reported in journals, and we have therefore compiled this report by using these various publications as the chapters of the report. We summarize the various chapters.

Chapter 5.

Phase conjugation methods are combined with coherence reduction techniques.

Chapter 6.

Signal-to-noise in incoherent systems. We show that SNR improvement in incoherent systems can be simply expressed as the ratio of the redundancy factor of the incoherent process divided by the space of the operation being carried out.

Chapter 7.

A method of making Fourier transform holograms with incoherent light, but in which the process remains linear in amplitude, is given. This is a substantial portion of the dissertation of G. Collins.

Chapter 8.

Holographic optical elements (lenses) are formed in incoherent light with any desired set of conjugate focal planes. Noise and diffraction efficiency measurements are made.

Chapter 9.

Holographic optical elements are made in broadband light by sweeping a dye laser. Significant noise reduction is demonstrated. Stereo imaging methods are used to demonstrate the noise reduction process.

Chapter 10.

The process of achromatization of the holographic process is generalized.

Chapter 11.

This paper introduces some new concepts, including fringe projections and optical tomography with incoherent light.

Chapter 12.

This paper introduces, among other ideas, a method for forming fringes of arbitrary profile with incoherent light.

Chapter 5

Holographic Aberration Compensation with Partially Coherent Light

596 OPTICS LETTERS / Vol. 7, No. 12 / December 1982

Holographic aberration compensation with partially coherent light

E. N. Leith and G. J. Swanson

The University of Michigan, Ann Arbor, Michigan 48109

Received August 23, 1982

The aberration-compensation method of passing the conjugate beam from a hologram through the same optical system used in making the hologram is combined with broad-source interferometer techniques to give, along with the aberration compensation, considerable noise reduction. As with conventional photography, the image is two dimensional.

Aberration compensation by conjugation of a wave is well known in both holography and the relatively new technique of phase conjugation. In the context of holography, a distorting medium, such as an aberrated lens,[1] ground glass,[2] or shower glass,[3] is placed between the object and the recording plate. The hologram records the aberrated wave, and, in the readout process, the conjugate wave is generated. This wave traverses in reverse the path of the object wave, compensating for aberrations in the optical path, and forms an aberration-free image, even when the optical system is severely aberrated. The same method has more recently been demonstrated in phase-conjugation technology.[4]

The process works extremely well. In an early experiment, ground glass was inserted into the object-beam path, completely destroying the image.[2] Yet a sharp image was obtained from the conjugate wave of the hologram. However, the process has the shortcoming of requiring coherent light, which is quite noisy. The use of incoherent light removes the coherent noise, but unfortunately the conjugation process, as originally given, requires coherent light.

Clearly, having both the low noise of incoherent imagery and the aberration compensation of the holographic method would be highly desirable since exchanging a low-resolution, low-noise image for a high-resolution, high-noise one may be dubious. Here we describe a technique that allows the compensation process to be carried out with light of greatly reduced spatial coherence. The method is based on the use of broad-source interferometry in off-axis holography, the making of an image-plane hologram rather than a Fresnel or Fourier-transform hologram of the object, and the fact that the noise typically predominates in high spatial frequencies, whereas the aberrations are slowly varying.

By forming an image rather than recording a hologram, one can eliminate the coherence requirements with respect to the object. If the image contains both phase and amplitude, a spatial carrier can be introduced and thereby permit both to be recorded on photographic film, a process that is like holography, indeed is often termed image-plane holography, but in fact goes back to Ives.[5] In particular, the use of incoherent-light interferometers enables the process to be done with an extremely good signal-to-noise ratio since the incoherence not only reduces noise from scatterers outside the image plane but also, as opposed to most other methods, does not require any optical elements, such as a diffraction grating, to be placed in the object plane.[6] The presence of a grating in the object plane causes whatever noise is on the grating, such as digs and scratches, to appear on the image and is therefore best avoided.

Here we combine the phase-conjugation method with the incoherent spatial-carrier imaging method, producing on the recording medium an image on a carrier as well as a hologram of the aberrations. The spatial coherence of the light is reduced to a degree such that the coherent noise, of relatively high spatial frequency, is substantially reduced, but sufficient coherence is retained that the system aberration, being of low spatial frequency, is duly recorded as a hologram. The lower the spatial frequencies of the aberration, the better this can be done, since the required coherence in holography depends on the spatial frequencies to be recorded.

An optical system for realization of the method is shown in Fig. 1. G_1, G_2, and G_3 are diffraction gratings, all of spatial frequency f_1, forming a three-grating interferometer that produces fringes at the output plane P_o in light that can be both spatially and temporally incoherent. GG is a moving diffuser for spoiling the spatial coherence of the laser beam. The upper beam is formed by the +1 order of G_1, the −1 order of G_2, and the 0 order of G_3. The lower beam is formed by the 0 order of G_1 and G_2 and the +1 order of G_3. The other orders of the gratings are discarded or, even better, are not produced at all, a feat theoretically possible with the proper construction of holographic gratings. For example, a properly designed thick holographic grating will exhibit, because of Bragg effects, only a zero-order beam and one first-order beam. L and L′ are a pair of lenses, each inserted into one of the two beams. The

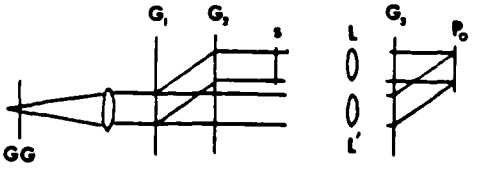

Fig. 1. Optical setup for the process.

0146-9592/82/120596-03$1.00/0

upper lens, L, images the object onto P_o. The lower beam provides a reference function, so that s is recorded on a carrier. Letting $s = |s|\exp(i\phi)$, a complex function, the interference pattern at P_o is

$$|\exp(i2\pi f_1 x) + |s|\exp(i\phi)|^2 = 1 + |s|^2 + 2|s| \times \cos(2\pi f_1 x - \phi). \quad (1)$$

The phase ϕ is accurately introduced into the fringe pattern regardless of the spatial coherence. However, only limited spectral broadening of the source is permitted; otherwise the phase would be lost since the phase delay produced by a thickness Δz in the object is $2\pi\Delta z/\lambda$, which is wavelength dependent.

Let the photographic record, in its original position, be illuminated by a duplicate of the reference beam but traveling in the opposite direction. A beam of light, $|s|\exp(-i\phi)$, is generated, which then forms an image s^* (or $|s|^2$ in irradiance) at the object plane.

Suppose a slowly varying aberration exists in the object-beam path, produced perhaps by the lens L. For convenience, suppose that the phase error resides at a plane where the Fourier transform of s is formed. This is a common procedure, which simplifies the analysis to that of a spatial-filtering operation, with no essential loss of generality. Let the aberration be $U = \exp(i\phi_a)$. Let the object be illuminated by a monochromatic extended source. Each element of the source produces a beam $\exp(i2\pi f_o x)$ impinging upon the object s. For convenience, we drop the third dimension, y. The extension to the third dimension is trivial. The total illumination can then be considered a summation of incoherent beams, each with a different f_o, related to the angle of incidence by $f_o = \sin(\theta_o/\lambda) \cong \theta_o/\lambda$. These various beams are mutually incoherent and thus sum as irradiances rather than as amplitudes.

Each beam interacts with the object, producing the product $s\exp(i2\pi f_o x)$. At the Fourier-transform plane, the field is $S(f_x - f_o)$, where S is the Fourier transform of s, and after passing through the phase aberration becomes

$$U_o = S(f_x - f_o)U, \quad (2)$$

which, at the image plane P_o, becomes

$$u_o = s\exp(i2\pi f_o x) * u, \quad (3)$$

where u is the Fourier transform of U.

The theory of the broad-source interferometer process requires that the function $s * u$ be multiplied by $\exp(i2\pi f_o x)$. If the output image were $(s * u)\exp(i2\pi f_o x)$, it could be regarded as the image of an object distribution $s * u$, illuminated by a plane wave $\exp(i2\pi f_o x)$. The reference beam would similarly contain a term $\exp(i2\pi f_o x)$, the two beams would then form an interference pattern independent of f_o, and a broad source could be used.[8] Thus we ask: Under what conditions can the approximation

$$s\exp(i2\pi f_o x) * u \cong (s * u)\exp(i2\pi f_o x) \quad (4)$$

be made? Fourier transforming this equation yields

$$S(f_x - f_o)U(f_x) \cong S(f_x - f_o)U(f_x - f_o), \quad (5)$$

or, equivalently,

$$U(f_x) \cong U(f_x - f_o), \quad (6)$$

which will be true if U varies sufficiently slowly and if the angular subtense of the extended source, and therefore the maximum f_o, is not too great.

A point at x_o on the signal s gives a point-spread function

$$u_o = s(x_o)u(x - x_o)\exp(i2\pi f_o x) \quad (7)$$

at plane P_o. As before, the exponential term depends on the source element. This is recorded as the hologram component

$$2|s(x_o)||u(x - x_o)|\cos[2\pi f_1 x - \phi(x_o) - \psi_a(x - x_o)], \quad (8)$$

where ψ_a is the phase of u. The interference process has eliminated the source-dependent term $\exp(i2\pi f_o x)$, and the carrier f_1 has come from the reference beam.

The physical description is that each source point projects the signal beam S to a different center position at the Fourier-transform plane; thus the aberration U affects the Fourier transform somewhat differently for each f_o. For slowly varying U, these shifts can be neglected. The assumption of a slowly varying aberration function is realistic except in the case of rather severe aberrations; consequently, it appears that there may be an optimum source-size region where the source is large enough to give significant noise reduction while still enabling the aberration to be recorded.

The readout process, also carried out with a broad source, is conceptually simpler than the recording process, since a coherent reference beam is not required. One plane-wave component of the readout beam is $\exp[-i2\pi(f_1 + f_o)x]$; the f_1 term signifies that the beam travels generally in a direction retracing the original reference-beam path, and the term f_o describes the broadening of the source about the average value f_1. The conjugate beam from the hologram, $s^*(x_o)u^*(x - x_o)\exp -i2\pi f_o x$, is Fourier transformed to produce

$$s^*(x_o)U^*(f_x - f_o)\exp(i2\pi f_x x_o), \quad (9)$$

which is multiplied by the aberration $U(f_x)$. Again, making the approximation $U^*(f_x - f_o) = U^*(f_x)$, we have $UU^* = 1$, the aberration cancels, and an unaberrated image appears at the output.

The concept was verified experimentally in a setup like that shown in Fig. 1. The gratings were of spatial frequency $f_1 = 200$ cycles/mm, and the lenses L and L′ were identical single-element lenses of focal length 22 cm. The light was obtained by spoiling the spatial coherence of a He–Ne laser by placing a rotating ground glass in the laser-beam path. The size of the effective source is the size of the laser beam at the plane where it intercepts the diffuser. The lenses were stopped so that spherical aberration was negligible. Since the other Seidel aberrations are zero for a point object on axis, the reference-beam lens L′ was essentially a perfect lens. The lens L, since it is imaging a nonzero field, exhibits astigmatism and coma, which serve as the aberration U. To heighten these, the lens L was skewed, so that the object was off axis.

The size of the source should be a compromise. The larger the source, the more the noise is reduced, but if it is too large, the aberration U will not be well recorded.

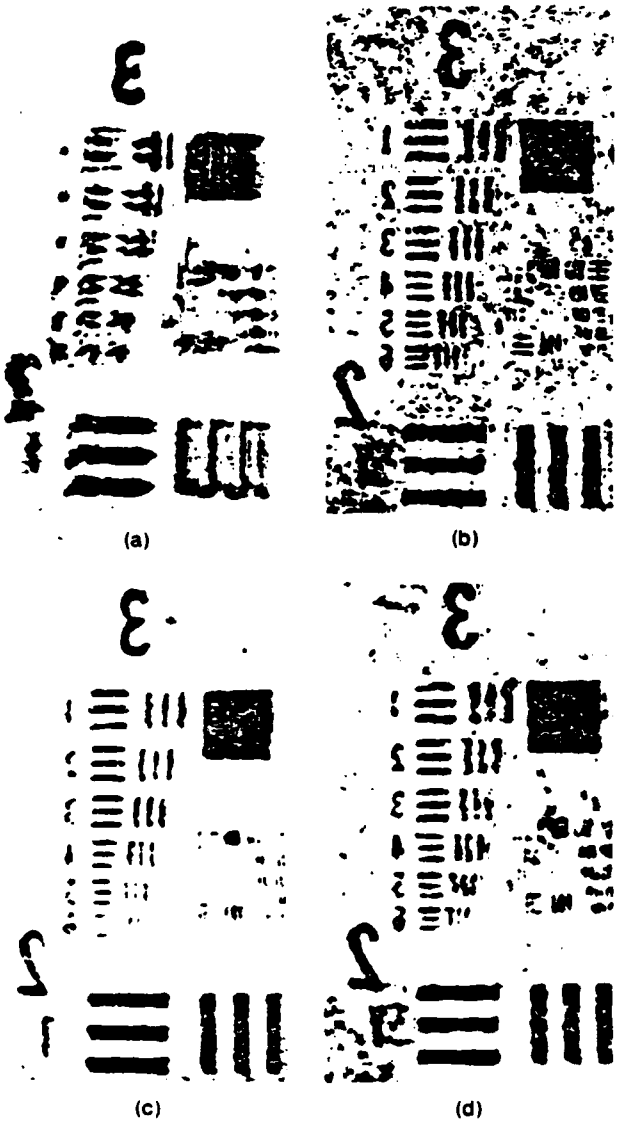

Fig. 2. Experimental results. (a) Conventional imaging of s onto P_o, i.e., point-source illumination, with reference beam blocked. (b) Using point source, making a hologram at P_o, and playing back through L with a conjugate wave. (c) Same as (b) but with an extended source in making and in readout. (d) Same as (b) and (c) but with a broad source for making and a point source in readout.

Various holograms were made, with various sized sources, the size being changed by moving the ground glass axially, thereby changing the size of the beam incident upon the glass. The size used in the experiment was 100 μm, which subtended an angle of 2.5×10^{-4} rad at the collimator. Since the diffraction-limited image size, seen through the collimator, was 2.4×10^{-5} rad, the redundancy factor that is due to the broadened source was about 100, the ratio of the actual source size (in area) to the diffraction-limited source size.

Experimental results are shown in Fig. 2. First the reference beam was blocked, and a conventional image, a part of a U.S. Air Force resolution chart, was recorded at P_o with a broad source and a diffuser [Fig. 2(a)]. The aberration is large. Second, with the ground glass removed, the reference beam was introduced, and a hologram was recorded. The hologram was removed, developed, then placed back in its original position, and a readout beam was introduced, identical with the reference beam but traveling in the opposite direction. The correction achieved is excellent, but there is a great deal of noise [Fig. 2(b)]. Next the source was broadened to its experimentally determined optimum, and a hologram again was recorded. The reconstruction was made as in Fig. 2(b), but with a broadened source of identical angular extent to that used in making the hologram [Fig. 2(c)]. The resolution is essentially the same as before, but there is considerable noise reduction; only the low-spatial-frequency components of the noise remain. Finally, so the relative effects of source broadening in the making and readout steps could be seen, the point-source hologram was read out with a broad source [Fig. 2(d)]. The result is a lesser reduction in noise, giving a reconstruction with noise intermediate between the cases of Figs. 2(b) and 2(c).

The experimental results can be interpreted as the use of two zero-field, or collimating, lenses to give the effect of a conventional, nonzero-field imaging lens. Even in this limited context, the technique has considerable potential value, since zero-field lenses can be simple and inexpensive, yet quite good, and imaging lenses of good quality could be many times more expensive. Other configurations, in which there is no matching lens in the reference beam, may be possible and would give the technique the broader and more-general capability of making an inadequate imaging lens into a better one. Also other interferometers could be used, such as a Mach–Zehnder interferometer. The grating interferometer, however, has two advantages: it is easier to adjust for broad source fringes and it gives better fringes under broad source illumination.

Also the method carries over to the related area of phase conjugation, in which the potential range of application is far greater because of the real-time capability of the phase-conjugation process.

This work was supported by the U.S. Air Force Office of Scientific Research (grant AFOSR-81-0243) and by the National Science Foundation (grant ECS-790-1647).

References

1. E. N. Leith, J. Upatnieks, and A. Vander Lugt, "Hologram microscopy and lens aberration correction using holograms," J. Opt. Soc. Am. 55, 595 (1965).
2. E. N. Leith and J. Upatnieks, "Holograms: their properties and uses," SPIE J. 4, 3 (1965).
3. H. Kogelnik, "Holographic image projection through inhomogeneous media," Bell Syst. Tech. J. 44, 2451 (1965).
4. C. R. Giuliano, "Applications of optical phase conjugation," Phys. Today 34(4), 27 (1981).
5. H. E. Ives, Br. J. Photogr. (August 3, 1906), p. 609.
6. E. N. Leith and G. J. Swanson, "Recording of phase-amplitude images," Appl. Opt. 20, 3081 (1981).
7. J. W. Goodman, *Introduction to Fourier Optics* (McGraw-Hill, New York, 1968), Chap. 6, Sec. 6.4.
8. E. N. Leith and B. J. Chang, "Space-invariant holography with quasi-coherent light," Appl. Opt. 12, 1957 (1973).

Coherence Reduction in Phase Conjugation Imaging

E.N. Leith, Hsuan Chen, Y.S. Cheng, and G.J. Swanson

The University of Michigan, Ann Arbor, MI 48109

and

I.C. Khoo

Wayne State University, Detroit, MI

Abstract

A method is presented for performing phase conjugation with radiation of reduced spatial coherence, using broad-source interferometry

Coherence Reduction in Phase Conjugation Imaging

The phase conjugation imaging technique has the capability for producing diffraction-limited resolution even in severely aberrated imaging systems. In this technique, various beams are mixed in a non-linear medium. An object-bearing beam, passing through the medium, generates a conjugate beam u^*, which retraces the path of the original beam u, and the aberrations in u^* are then compensated by the aberrations of the imaging system. This process, carried out in real time, is similar to a process developed in static holography in 1965.[1-3]

The process in a basic way requires coherent light, which is poor for imaging. First, coherent light, when interacting with a diffuse material, either by reflection from it or transmission through it, acquires a speckly appearance. Second, any scattering or perturbing structure along the optical path results in noise that overlays the image.

There appears to be basically two alternatives in imaging through an aberrating system. First, we can carry out the imaging process in a conventional way, using incoherent light, thereby achieving a good signal to noise ratio, but degraded resolution. Second, we can carry out the process in a phase conjugation process with coherent light, thereby achieving improved resolution but a poorer signal to noise ratio.

One solution to this problem was given by Huignard et.[4] In this method, one in effect makes a sequence of hundreds of exposures, each with a different noise function. The recording medium adds these, giving a resultant where the noise is reduced by the averaging process.

We propose a second method, which achieves a comparable result using an essentially different principle. Instead of making a large number of coherent operations in sequence, we perform a single operation with light of reduced spatial coher-

ence, and possibly also of reduced temporal coherence. This method is an adaptation of a method previously described for static holographic imaging through a phase-distorting medium[5]

Description of the Method

The method, in the embodiment we have used for its demonstration, is shown in Fig. 1. Light from a laser source is passed through an interferometer that splits the incident light into two beams, then recombines them. The first element is a beam splitter, and the remaining elements are mirrors that redirect the beams so that they are brought together again at the plane of the phase conjugating medium. One of the two beams is the object beam, which contains an object and an aberrated imaging system, as well as some noise, resulting from such various defects as dust, digs and scratches on the lenses, etc. Lenses L_3 and L_4, arranged in the telescopic configuration, image the object O onto the phase conjugating medium P. Mirror M_4 reflects the reference beam back on itself and it passes again through the conjugating medium, a conjugate beam u^* is generated. The conjugate beam travels through the imaging system in reverse and forms an image.

The object beam carries the image, the aberrations and the noise. ideally, the image information should be perfectly passed, so that a high resolution image can be formed. The phase error, too, should be preserved, so that it can be cancelled in the conjugation process, thus permitting the high resolution that we seek. The noise, however, should be reduced, i.e., smoothed out, so that it no longer degrades the image. We can, for example, reduce the noise by reducing the spatial coherence of the light; indeed, complete spatial incoherence would essentially eliminate the noise entirely. However, the reduction in coherence would also partially destroy the image and phase error information that is to be transferred onto the conjugate beam.

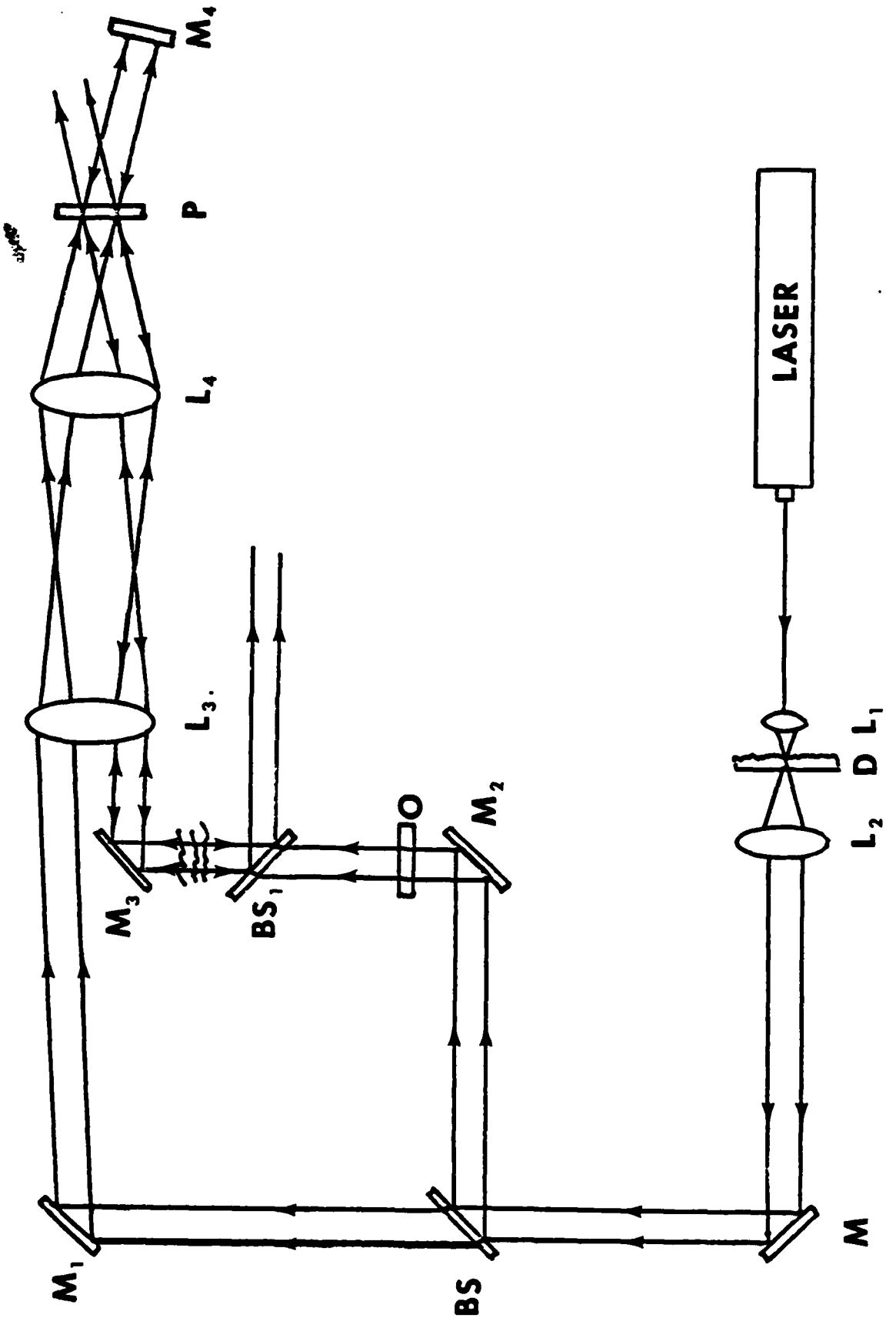

Fig. 1 The experimental setup

However, by forming an image on the conjugation plane, the coherence requirements for preserving the image information become nil--perfectly incoherent light would do. The aberrations, on the other hand, originate at a plane other than the object plane; indeed, the aberration sources are distributed, arising from entire regions rather than from a single plane. Thus, the aberration sources are not imaged at the conjugation plane.

The abberrations, are in general slowly varying; therefore, they require only a low degree of coherence for their preservation. The noise, however, is generally of higher spatial frequency. Therefore, we expect that the spatial coherence can be reduced to a degree such that the noise is significantly reduced, but that the aberration is essentially preserved. Indeed, if the aberrations are varying sufficiently slowly, considerable reduction in coherence is permissible, with good aberration preservation along with an enormous noise reduction.

We can reduce the coherence of the source in one of the many ways; the simplest is to place a rotating ground glass in the beam near the source point. The degree of coherence reduction depends on how far the ground glass is from the source. Another point that is important in the present context is that this method supposes the field to change rapidly compared to the time constant of the conjugation process. Otherwise, the process will be a sequence of coherent recordings, instead of a single recording with partially coherent light.

The reduced coherence will tend to destroy the interference fringes produced at the conjugation plane by the superposition of the object and reference beams. However, the interferometer of Fig. 1, which is basically a modified Mach Zehnder, is capable of broad source operation. The production of fringes under broad source illumination is an important aspect of classical interferometry, and is discussed in texts on interferometry.[6] If the beams are adjusted so that the corresponding rays in the two

beams, i.e., rays that come from a single ray impinging on the beam splitter, are brought back together, then the two beams will interfere in this plane even when the source has reduced coherence. It has been shown that, for the Mach Zehnder interferometer, the number of fringes obtained from a monochromatic extended source is approximately[7]

$$N = \frac{1}{(2\Delta\vartheta)^2} \tag{1}$$

where $\Delta\vartheta$ is the angle subtended by the source at the collimating lens L. This relation allows a large number of fringes, perhaps, several thousand, even for a source that is many times larger than what the system would see as a point source.

Experimental Results

To perform the experiment, we first construct a controlled aberration by coating a portion of a glass slide with optical cement to a thickness of about 100-200 microns. The coating, rather irregular in thickness, provided an aberration that varied from region to region. The object beam, a few mm. in diameter intercepted, only a portion of the aberration plate, and by moving the plate, a suitable aberration could be injected into the beam.

The system was first tested using conventional, static holography, that is, using photographic plate instead of a phase conjugation material. The object was a grid of 4 fine slits of width 1 mm. The hologram was developed and replaced in its original position, the object beam was blocked, and the reference beam was reflected by a mirror M_4 back through the system, providing the required conjugate wave. Photographs of the reconstruction (Fig. 2) show the process works as expected. The aberrated image is shown in 2a, just as it appears at the plane of hologram formation. Figures 2b and 2c show the reconstruction with light of reduced coherence in both the making and readout steps. Figure 2b differs from 2c, in that the hologram was used in a liquid

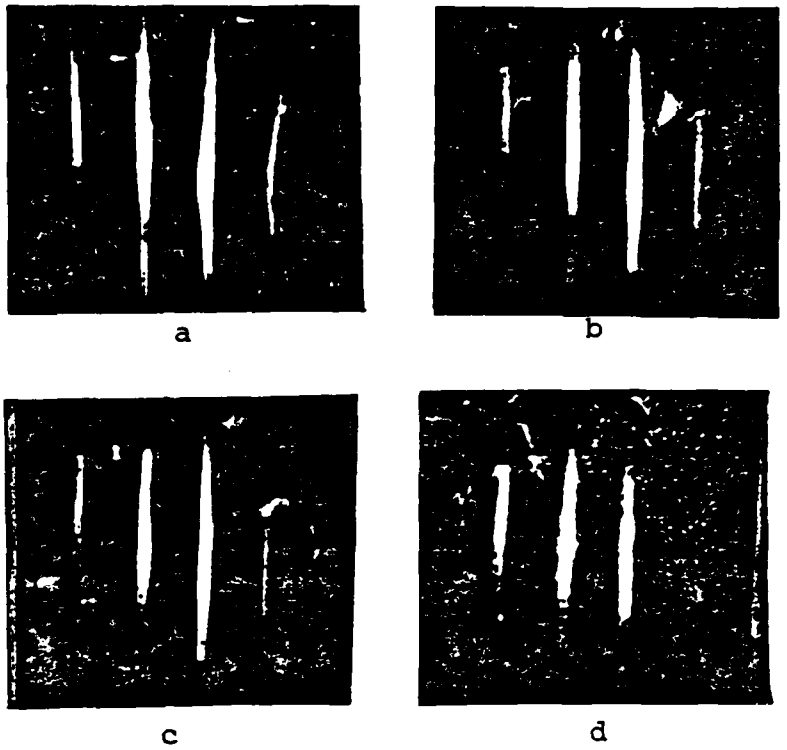

Fig. 2. Experimental results, using conventional (i.e., static) holography. (a) conventional (not holographic) imaging with partially coherent light through the aberration. (b) imaging using holography and reduced coherence. Also, a flat glass plate was coupled to the emulsion surface using an index matching fluid. (c) same as b, but without the glass plate. (d) imaging using holography and complete spatial coherence.

gate, that is, a glass plate was fluid-coupled to the emulsion side of the hologram in the reconstruction process. This greatly reduced the noise from surface defects on the emulsion. Finally, Fig. 2d shows the result when the process was carried out with coherent light. The phase error compensation is very good, but the noise level is high.

By rotating the mirror, M_4 the reference beam could be aimed in various directions, so that the conjugate beam path could be shifted, thus making the phase error compensation imperfect. When this was done, the principal effect was to produce curvature in the slit images, sometimes with some slight broadening (Fig. 2) The mirror was adjusted until the slit images became straight, whereupon the system was assumed to be properly adjusted.

For the real time, or phase conjugation process, a thin film of nematic liquid crystal was used as the phase conjugation medium,[8] in conjunction with an argon laser (5145 A line) with an optimum power of 3.0 watts. The laser was divided equally into the reference and object beams. The total laser power (object, reference and reconstruction beams all together) incident on the nematic film, after passage through the optical system, was about 0.2 watts. A second beam splitter BS1 was placed between the object and the mirror M_3 so as to separate the phase conjugated image from the object. The liquid crystal MBBA (p-methoxbenzylidene-p-n-butylaniline) was homeotropically aligned, with the director axis parallel to the plane defined by the two incident beam propagation vectors (reference and object) and the optical polarization of the beams was normal to the director axis. For this configuration, the nonlinearity arises from the thermal indexing effect[9] (i.e., d n /dT, where n is the refractive index for the ordinary ray, and T the temperature. The diffraction efficiency for the MBBA film was about 0.1 percent at room temperature, but it can be increased by raising the temperature to close to the nematic → isotropic transition. Typically a diffraction (or wavefront conjugation) efficiency of about 3 percent is obtainable.

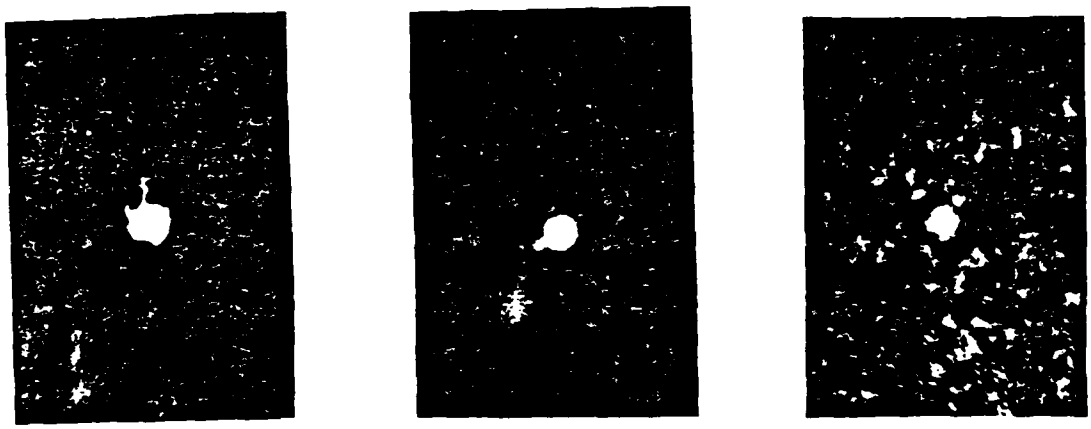

Fig. 3. Phase conjugation results, using a circular aperture for the object. (a) photographic record of the object, after imaging through the aberrating medium, and using light of reduced coherence. (b) phase conjugation imaging with light of reduced spatial coherence. (c) same as b, but with completely coherent light.

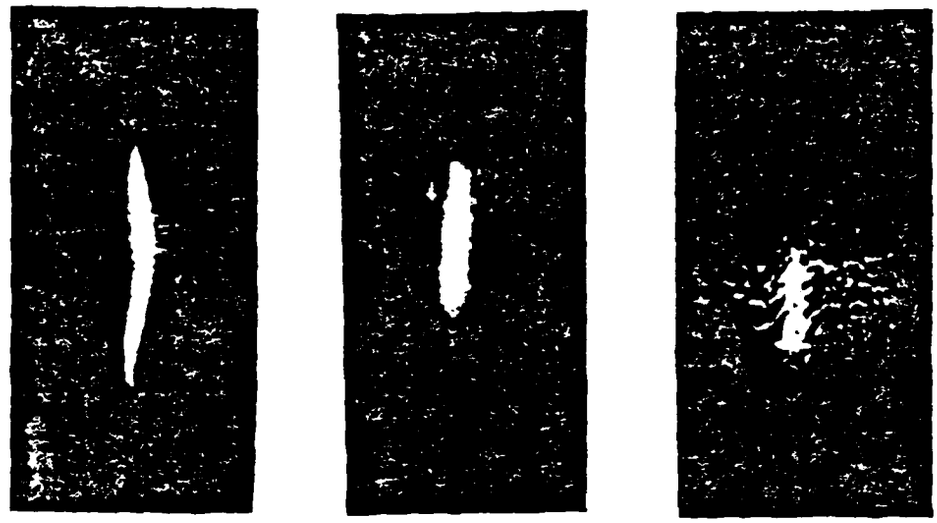

a b c

Fig. 4. Image of a slit (a) formed with incoherent light, (b) formed using phase conjugation with light of reduced coherence, (c) formed using phase conjugation with completely coherent light.

We show experimental results using two different objects. Figure 3 shows results using as an object just the laser beam, a circular distribution of light about 1 mm. in diameter. The aberrated beam, the phase conjugation beam using light of reduced spatial coherence, and the phase conjugation beam using coherent light are shown in Figs. 3 a,b, and c, respectively. The noise reduction in the incoherent case is quite evident.

Figure 4 shows similar results, except that the object was a slit. Again, the phase conjugation image using light of reduced spatial coherence has resolution just about as good as for the coherent case, and the signal to noise ratio is much superior.

This work was supported by the National science foundation (Grants ECS-790-1647 and ECS 802-6775 and the air force office of Scientific Research (Grant AFOSR-81-0243).

C

REFERENCES

1. E.N. Leith, J. Upatnieks and A. VenderLugt, "Hologram microscopy and lens aberration correction using holograms," J. Opt Soc. A. *595(1965)*.

2. E.N. Leith and J. Upatnieks, "Holograms, their properties and users," SPIE J. *4* 3(1965).

3. H. Kogelnik, "Holographic image projection through inhomogenious media," Bell System. tech. J. *44* 2451 (1965).

4. J.P. Huignard, J.P. Herriau, P. Aubourg and E. Spitz "Phase-conjugate wavefront generation via real-time holography in $Bi_{12}SiO_2$ crystals, Opt. Lett. *4* 21 (1979).

5. E.N. Leith and G.J. Swanson, "Holographic aberration compensation with partially coherent light," Opt. Lett *596 (1982)*.

6. M. Born and E. wolf, *Principles of Optics*, pergamon Press, New York; 1959. Cpt. 7.

7. F.D. Bennett "Optimum Source Size for Mach-Zehnder Interferometer," J. Appl. Phys. *22* 184 (1951).

8. I.C. Khoo and S.L Zhuang, Wavefront Conjugation in Nematic Liquid Crystal Film," IEEE Trans. QE 18 246 (1982).

9. I.C. Khoo, "Theory of Optically Indexed Molecular Reorientation and Quantitative Experiments in Wave Mixing and Self-Focusing of Light," Phys. Rev. A, *25* 1636 (1982).

Chapter 6

Analysis of SNR in Incoherent Optical Processing

Analysis of SNR in Incoherent Optical Processing

1. Introduction

Over the past two decades there has been considerable discussion as to the relative merits of coherent and incoherent optical processing (1-3). It has been noted that the incoherent system has many channels for the transmission of the same information, giving a redundancy that leads to noise suppression. Recent analysis by Lowenthal and Chavel supports this conclusion in a detailed and quantitative way (4,5) and suggests that, whenever possible, incoherent processes should be used rather than

the coherent.

What kind of optical processing operations can be done incoherently? Essentially, any linear space invariant operation can be done either coherently, or incoherently. Although there are many systems for doing either coherent or incoherent optical processing, there are two that stand out as being rather basic ones, and our discussion is in terms of these. The first (Fig. 1), produces what is sometimes called the spatial domain synthesis, or convolution. The signals is imaged onto a reference function, or impulse response, r, and at the plane P, on axis, the function

$$g = \int srdxdy \tag{1}$$

is generated. By moving s through the aperture, the output becomes either

a convolution or a cross-correlation, depending on how s is inserted. If a cylindrical lens is used in combination with L_3, the operation is one dimensional, being either

$$g = \int s(x-x',y)r(x,y)dx \tag{2}$$

or

$$g = \int s(x'-x,y)r(x,y)dx \tag{3}$$

the former being a cross-correlation, and the latter a convolution. For the two dimensional case, a two-dimensional scanning movement of s is required, yielding a 2-dimensional correlation or convolution.

If coherent light is used, the system is linear in amplitude, whereas with incoherent light the system is linear in irradiance. A special case occurs when a point

or line source of white light is used; the system then behaves as a coherent system, even though the light is temporarily incoherent.

Complex functions s and r can be handled by placement on a carrier; $s \rightarrow s_b + |s| \cos(2\pi f_o x + \varphi), r \rightarrow r_b + |r| \cos(2\pi f_o x + \varphi_r)$ where s_b and r_b are bias terms, and Φ , Φ_r are the arguments of s and r respectively. This method applies equally whether the system is coherent or incoherent. There are two problems; the output is on a carrier f_o, and is accompanied by a strong bias, $\int s_b r_b \, dx$. In the coherent case, the bias is removed by spatial filtering at the focal plane of L_1 and the carrier is removed by a combination of spatial filtering at the focal plane of L_1 and the detection process at the output. For the incoherent case, such filtering is not available; thus the output signal is on a carrier and is accompanied by a bias, both of which have to be removed electronically. The second basic case (Fig. 4.2) is called the frequency domain synthesis or spatial filtering method. A mask at the focal plane of L_1 is a spatial filter, and the output is the input signal modified by the filter. Again, complex values for s and r can be realized by placing s and r on spatial carriers. For the incoherent case, the transfer function becomes the autocorrelation function of the spatial filter mask. It had at one time been believed that, with the incoherent system, arbitrary transfer functions were not possible; the only realizable transfer functions were those that could be written as an autocorrelation function. Lohmann showed that this supposition is not true[2] and described a basic method for arbitrary complex filters for incoherent spatial filtering. Thus, the incoherent frequency domain synthesis is just as general as the incoherent spatial domain synthesis. The output, as in the spatial domain synthesis,comes with a bias and a carrier, and therefore requires electronic detection to separate the signals from the bias and remove the carrier.

2. Bias Buildup

The bias term is more than just an inconvenience requiring electronic dctection and filtering to remove. It can be overwhelming, leading to poor SNR, even though the system incoherence has made the noise level very low. Any comprehensive discussion of the SNR of coherent vs incoherent systems must take into account this bias term.

We disuss the bias buildup in terms of several examples, starting with relatively simple, specific cases and progressing to the more general cases.

In the 1960's, a number of researchers developed methods for making Fresnel or Fourier holograms in spatially incoherent light. Typically, an interferometer was used, which converted every point of the object into a structure

$$a_o^2[1+\cos(2\pi f_o+\beta x^2] \tag{4}$$

in the case of the Fresnel method, or

$$a_o^2(1+cos02\pi f_1 x) \tag{5}$$

in the Fourier case. Here, a_o is the object amplitude, f_o is a constant carrier, the same for all object points, β is a constant, and f_1 is a carrier different for each object point. If the object consists of N discrete points, which for simplicity we take to be of equal spacing and equal amplitude, then the Fresnel hologram is formed by recording an irradiance distribution.

$$I=a_o^2\sum_{n=1}^{N}\{1+\cos[2\pi f_o(x-nx_1)+\beta(x-nx_1)^2]\} \tag{6}$$

If we assume all N signals overlap, then the bias term increases or builds up arithmetically, i.e., proportional to N, whereas the root mean square amplitude of the signal builds up as $\sqrt{N}$, so that the fringe contrast, the ratio of rms amplitude of the fringes to the bias, is proportional to $1/\sqrt{N}$. Thus, high contrast fringes are obtained only for the case of one or a few object points; for the case of several hundred object points, the contrast is vanishingly small. Experience has shown that for more complex objects, such as continuous tone objects, the SNR of the reconstructed image is very poor, despite the expected noise advantage of using incoherent light.

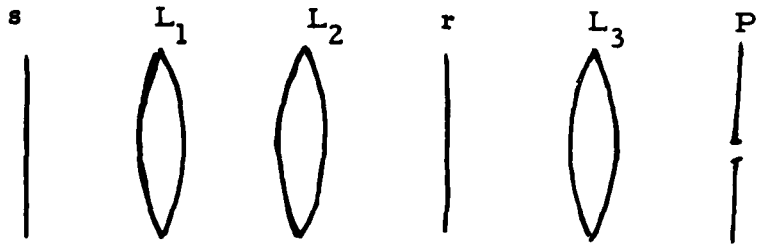

Figure 1

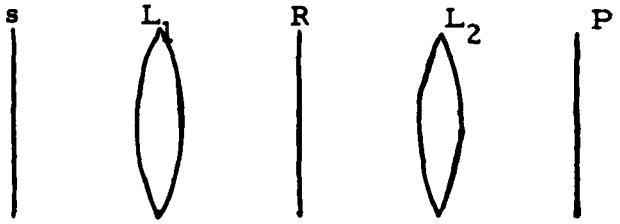

Figure 2

These results can be duplicated using the basic convolving system of Fig. 1 . The signal s is an array of slits , representing the delta-function object points. The reference function is a cylindrical off-axis Fresnel zone plate. The output irradiance is recorded as a function of time through a slit at x = 0 while the object s is moved through the aperture.

The incoherent convolving system can also be used for the reconstruction process, the compression of the dispersed signals into point images. The hologram previously constructed is used as a signal s, and the same reference function used for making the hologram is used for compression. The bias buildup that occurs in forming the hologram was produced by the overlapping process. Since the present process is one of compressing overlapping signals, one might suspect that the mechanism for further bias buildup is absent, but analysis shows this is not the case.

Let the signal, have transmittance

$$T_s = s_b + a_0 \sum_{n=1}^{N} \cos[2\pi f_0 (x - nx_1) + \beta (x - nx_1)^2] \tag{7}$$

and the reference function r have transmittance

$$T' = \tfrac{1}{2} + \tfrac{1}{2}\cos(2\pi f_0 x + \beta x^2) \tag{8}$$

where we take $r_b = 1/2$*. We place the recorded signal in the system of Fig. 1. If we choose coherent operation, then the above functions represent amplitude transmittances. For an incoherent system, the above are to be intensity (or irradiance) transmittances. We form the cross-correlation of the two signals, producing at the output

$$X = \tfrac{1}{2} s_b L + \sum \tfrac{1}{2} L a_0 \, sinc\left[\frac{\beta L (x' + x_1)}{\pi}\right] \cos\left[2\pi f_0 (x' + x_1) - \beta x' (x' + x_1)^2\right] \tag{9}$$

where L is the aperture, or integration interval; this is just the usual holographic image, but on a spatial carrier f_0 and on a bias. The signal to bias ratio is a_0 / s_b If we assume that the spacing x_1 is equal to the resolution, this ratio is also approxi-

mately the mean signal to bias ratio. The corresponding ratio on the hologram is $\sqrt{N}a_o s_b$. Thus, the signal to bias ratio has been reduced in the same manner as in the hologram making process.

The physical basis of this enormous bias buildup can be understood in a rather physical, yet quantitative, way. We consider first the conventional image formation process in a hologram (Fig. 3).

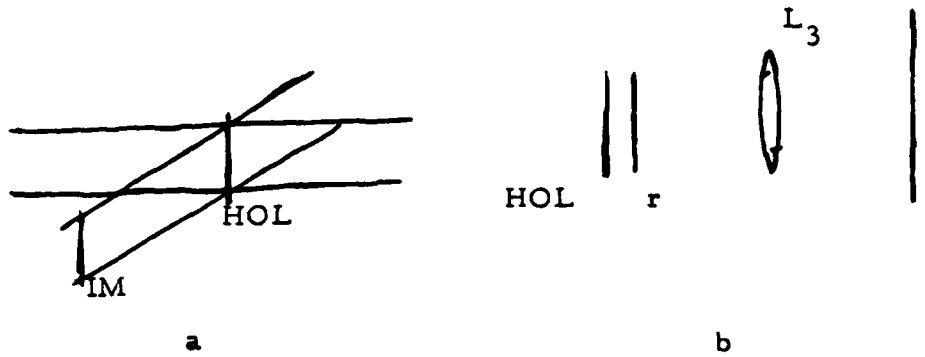

Fig. 3

Fig. 3a shows the conventional hologram reconstruction process. The field on readout consists of a bias term s_b and the image term u, as well as a conjugate term not of interest here. The ratio of mean intensity of the image wave to the bias wave is $|u|^2/s_b^2$. The wave u propagates to the image plane, forming an image s. The energy is unchanged in the process. If we assume for simplicity that the image is the same size as the hologram aperture, the signal to bias ratio is unchanged, since $|s|^2=|u|^2$. By using off-axis holography, the bias term is separated from the image. If the basic Gabor in-line method is used, the bias and image terms overlap.

Next we reconstruct with the convolutional system previously discussed (Fig. 3b). Conceptually, we may think of the reference function $\frac{1}{2}+r$ as overlaying the

hologram, rather than being imaged on it. The bias term 1/2 is a multiplier that gives a resultant bias $\frac{1}{2}s_b$. The r portion is a zone plate, of which the positive focal length term $\exp[-j(2\pi f_o x + \beta x^2)]$ is used. The portion $\exp[-j(2\pi f_o x)]$ has a prism effect, bringing the image wave u into the line with the bias term. The quadratic term, in combination with the lens L_3, constitutes a telescope taking the virtual image, which forms at the front focal plane of the zone plate lens, and reforming it at the back focal focal plane of L_3, with magnification $M = F_3 / F_zp$, where F_zp is the focal length of the zone plate lens, and also the focal length of the hologram.

For the one dimensional case (which for convenience is what we consider), the image brightness is reduced in proportion to the magnification, giving a brightness distribution s^2 /M, and a mean irradiance s^2 /M.

Now consider what the process does to the bias term. As shown in Fig. 4 the reference mask attenuates the bias level by a factor $r_s = 1/2$. The lens L_3 focusses the light into a sinc function of Rayleigh-criterion width $l = 2\lambda F_3 0 / L$, which we approximate by a rect function of width l.

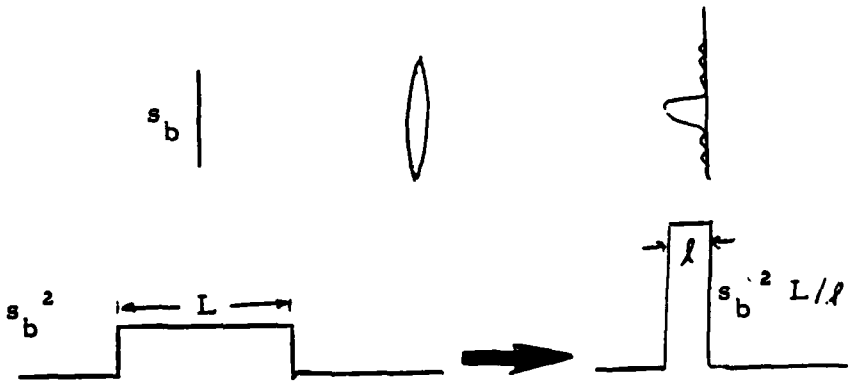

Fig. 4

The increase of brightness is in the ratio $L / l = L^2 / 2\lambda F_3$, giving a bias irradiance level

$$I_b = s_b^2 L^2 / 2\lambda F_3 \tag{10}$$

The signal to bias irradiance ratio is then

$$R = \frac{s^2 F_{zp} / F_3}{s_b^2 L^2 / 2\lambda F_3} \tag{11}$$

The zone plate focal length F_{zp} is $\pi / \lambda\beta$, giving

$$R = (s^2 / s_b^2) \quad (2\pi / \beta L^2) \tag{12}$$

The space bandwidth product of an image point, as recorded on the hologram (or equivalently, of r) is readily shown to be $N_h = \beta L^2 / \pi$ giving

$$R = (\overline{s^2} / s_b^2 y N_h \tag{13}$$

We thus see a large bias buildup factor, equal to the space-bandwidth product of the point spread function of the process performed.

Physically, what has happened is rather simple. The system has conducted the signal part to the output plane with essentially no change in brightness beyond that produced by a magnification factor. The bias term, however, has been concentrated into a small region, with a consequent buildup in intensity proportional to SW. This bias term remains fixed at the sampling point for the entirety of the processing, while the processed image crosses the sampling aperture, one resolution element at a time.

With coherent illumination, the bias term can be removed by various means, including spatial filtering at the focal plane of L_1, or a sideways displacement of the sampling slit so as to avoid the bias term. However, when the illumination is incoherent, neither option is available. The usual way to remove the bias is then by temporal filtering of the detector output, an option made possible because when the input signal and reference function signals are on a spatial carrier, the output will be on a temporal r carrier. The process requires detecting a low contrast signal, a process that can be quite noisy. The bias term traveling through the system will generate arifact noise from scatterers in the optical system, and signal-dependent detector noise will be enormously icreased. Thus, the lower noise level of the incoherent system

is offset by the decreased signal level. If the bias buildup factor dominates, then, the incoherent method is in fact worse that the coherent.

The above results can be obtained on a basis divorced from optics. We consider the convolution process

$$(s_b+s) \quad * \quad (\tau_b+r)=\int_{-L/2}^{L/2} s_b\tau_b+F\{(SR)\} \tag{14}$$

where, for τ_b = 1/2, the first term becomes Ls_b /2.

Now, let

$$\begin{aligned} r &= \tfrac{1}{2}\cos(2\pi f_o x+\beta x^2 \\ &= 1/4\exp j\ (2\pi f_o x+\beta x^2)+1/4\exp -j(2\pi f_o x+\beta x^2) \end{aligned} \tag{15}$$

The Fourier transform of r is

$$R=1/4\frac{\sqrt{\pi}}{\sqrt{r}}\left[\exp -j\frac{(f-f_o)^2}{4\beta}+\exp j\ \frac{(f+f_o)^2}{4\beta}\right] \tag{16}$$

or, for the single sideband case,

$$R=1/4\frac{\sqrt{\pi}}{\beta}\exp -j\frac{(f-f_o)^2}{4\beta} \tag{17}$$

After filtering, the signal energy is attenuated by a factor $\pi/16\beta$, or $\pi/8\beta$ for the double sideband case. The signal to bias ratio of the output is then

$$\frac{I_{sig}}{I_{Bias}}=\frac{s^{\bar{2}}(\frac{\pi}{8\beta})}{1/4s_b^2L^2}=\frac{s^{\bar{2}}}{s_b^2}\frac{\pi}{2\beta L^2}=\frac{s^{\bar{2}}}{s_b^2}\frac{1}{2N_h} \tag{18}$$

which, (except for a factor 2) agrees with the previous result.

This result can be demonstrated on a rather general basis. Let the Fourier transform of r be R. From Parseval's theorem we have

$$\int_{\frac{-L}{2}}^{\frac{L}{2}} r^2=\int_{\frac{-W}{2}}^{\frac{W}{2}}|R|^2 \text{ or } Lr^{\bar{2}}=W|R|^{\bar{2}} \tag{19}$$

For a high contrast mask, τ_b + r, with τ_b = 1/2, we expect $r^{\bar{2}}$ to be of the order of 1/4, giving

$$|R|^{\bar{2}} = L/4W \tag{20}$$

The filter R thus gives an irradiance attenuation of L / 4 W. If we take the statistics of the output signal s_o to be the same as that of the input signal s, then

$$s_o^{\bar{2}} = Ls^{\bar{2}}/4W,$$

and we have for the signal to bias irradiance ratio

$$\frac{I_{sig}}{I_{bias}} = \frac{s^{\bar{2}}(L/4W)}{1/4s_b^2L^2} = \frac{s^{\bar{2}}}{s_b^2} \tag{21}$$

The full benefit of the reduced noise resulting from the incoherent illumination is thus fully realized only for processing operations where the space bandwidth product is unity. The most commonplace example is conventional image formation. The bias buildup phenomenon is entirely absent, regardless of the system resolution, and it is clear that the use of coherent illumination would be foolish in all but exceptional circumstances, such as the unavailability of incoherent illumination. Other operations which involve a modification of the image corresponding to an r with space bandwidth product of the order of one, include image subtraction, psuedocolor generation, placement of a signal onto a spatial carrier (i.e., image plane holography), phase contrast recording, etc. Excellent successes have been reported using incoherent light for these processes.

On the other hand, operations that have a large space bandwidth product, such as spatial matched filtering and image deblurring, would appear to be best done in the coherent mode, using spatial incoherence in one dimension if the operation is one dimensional, or using temporally incoherent light in the achromatic, or coherent processing mode.

A special case arises when the operation to be performed is a Fourier transform, since this operation is not characterized by a point spread function h that is convolved with the object. However, one can proceed in an analogous manner and get similar results. Let the object be of extent L, and let ℓ be either the size of the smallest detail

on the object, or the smallest detail that the optical system can resolve. For the latter case, $\ell = \lambda F / A$, where F is the focal length and A the aperture of the lens. The spatial frequency bandpass of the lens is thus $W = A / \lambda F$, and the space bandwidth product of the system (object aperture plus lens) is $N = LW = LA/F = L/\ell$. If ℓ is limited by the fineness of object detail, the result is the same, except that the space bandwidth product N is attributed to the object rather than to the object-lens combination.

A number of methods exist for performing a Fourier transform with incoherent light. An object resolution cell centered at x_o thus transforms into a cosine transform $\frac{1}{2} + \frac{1}{2}\cos 2\pi f_x x_o$, 0 instead of into $\exp j 2\pi f_x x_o$, as in the coherent case. Again the bias buildup occurs, with the number of overlapping responses being the space bandwidth product N.

The reduction in processed image contrast must be considered when calculating the SNR. The gain, assuming fully incoherent illumination, is[5]

$$G = \sqrt{N} \tag{22}$$

where N is the space bandwidth product of the optical system:

$$N = S_o S_p / \lambda^2 d^2 \tag{23}$$

where S_o is the area of the object, S_p is the area of the pupil plane, and d is the lens focal length. The gain, when considering the contrast loss, becomes

$$G' = \sqrt{N} / N_h \tag{24}$$

The largest possible impulse function space bandwidth product, N_h, that can be achieved in the optical system is N. Thus, for this case, there is no gain at all with the use of incoherent light. On the other hand, if we consider that N for an optical system is generally of the order of 10^6, whereas N_h, for a typical matched filtering operation, is of the order of 10^3, and for linear deblurring operations, of the order of 10, it is apparent that in principle, gains of the order of $G' = 10$ to 100 are available for these applications. However, these improved SNRs will be accompanied by a greatly reduced

contrast, so that, with the decrease of signal (or setup) noise, the detector noise becomes of increased concern.

SNR improvements of the order 10^2 or 10^3 essentially eliminate setup noise as a problem, but the low contrasts result in detection problems. Finer grain and therefore slower films are required, or perhaps very low noise non-photographic detectors are required.

3. Comparison with Spectroscopy

The choice between coherent and incoherent optical processing is thus not at all clear-cut. One might ask the question, are there any optical processing areas where both coherent and incoherent optical processing have been extensively considered. There are perhaps two.

The first is the optical processing of synthetic aperture radar data, in which a complex, holographic-like signal is convolved with a complex reference function that is zone-plate-like in structure. The earliest-conceived processors, of the 1954 period were incoherent. In the following years, coherent optical processors dominated, but many incoherent-type opptical processors were conceived[10,11]. For the most part, these were never highly developed, and even today, with the emphasis on incoherent processing, are in no way a challenge to the coherent. The principal reason is that the noise improvement through redundancy is introduced in another way. The systems collects more data from each object point than can be coherently processed, so the actual processing, although fundamentally coherent, is in fact a mixture of coherent and incoherent, integrated together in a process called tracking[12]. It is remarkable that the resulting radar imagery, although produced from data that was obtained by a coherent process (a coherent radar) and processed in a coherent optical system, using apoint source of laser light, is completely free from the artifact noise associated with

coherent systems.

Another, far more interesting example of the competitiveness of two modes is found in spectroscopy. This is perhaps the most important example of optical processing, and it exists in two basic and important forms,--grating spectroscopy and interferometric spectroscopy. They have each found a niche and are highly complementary. We would like to identify the former with coherent processing and the latter with incoherent.

In interferometric spectroscopy, an interferometer, such as a Michelson or a variant thereof, splits a beam from an extended source into two parts and recombines them with a time displacement. Each wavelength component λ_o is converted into a response

$$I(\tau)=\tfrac{1}{2}I_o\left[1+\cos 2\pi c\frac{\tau}{\lambda_o}\right] \tag{25}$$

or

$$I(x)=\tfrac{1}{2}I_o\left[1+\cos 2\frac{\pi}{\lambda_o}x\right] \tag{26}$$

where τ is the time difference between the two beams, and $x = c\,\tau$ is their displacement. For a multiplicity of wavelengths, the output is asummation of terms of the form of Eqs. (25) or (26), and for a continuous distribution, the irradiance is

$$I_\tau=\int_0^\infty L(\lambda)d\lambda+\tfrac{1}{2}\int_0^\infty L(\lambda)\cos 2\frac{\pi}{\lambda}xd\lambda \tag{27}$$

where L is the irradiance spectral density distribution. The wavelength resolving process is completed by detecting the signal thus generated, with subsequent Fourier transformation in a digital computer. This process is obviously an incoherent operation, and is in fact wholly analogous to the previously noted forms of incoherent holography, whereby an incoherent object distribution is split into two images by an interferometer and each point in the one image produces a beam that interferes with the

beam from the corresponding point of the other image.

The grating case is more subtle. The formation of a wavelength spectrum with a grating and lens, or a curved grating, with its own focal power, an obvious analog to a Fourier transform of a spatial signal with a coherent light beam, is described by the operation

$$I_\tau = \int_0^\infty L(\lambda)d\lambda + \tfrac{1}{2}\int_0^\infty L(\lambda)\cos\frac{2\pi}{\lambda}x\,d\lambda \tag{27}$$

where L (λ) is the irradiance spectral distribution of the source, exp $j2\pi f_o x$ represents the spatial Fourier component of the grating used for dispersing the light, A is the system aperture, and the final term is the Fourier kernel produced by a lens of focal length F.

If we apply the linearity condition that if $f_i \rightarrow g_i$, then $\sum f_i \rightarrow \sum g_i$, where f_i are the inputs and g_i the outputs, and if we assume that the f_i s are not overlapping as a functions of λ ,but that the $g_i s$ are, then clearly the system is quite linear in irradiance and is thus a wholly incoherent system. On this basis, both types of spectroscopy techniques are incoherent; in terms of our context, they differ in that the grating method is an operation with a unity space bandwidth product at the output recording plane, whereas the interference method has a space bandwidth product much greater than one. Thus, the one is afflicted with bias buildup, whereas the other is not.

However, the grating case has an obvious similarity to the coherent optical Fourier transformation of a spatial signal with a coherent light beam, and the illumination source, being a slit, has spatial coherence. The system is in fact a summation of many such Fourier transformations. In particular, for the case of a discrete spectrum, where the responses g_i have no overlap, the issue of whether the system is coherent or incoherent becomes moot, and the system can be perfectly well regarded as a coherent Fourier transforming device. Indeed the substitution $f_1(\lambda) = y$ and $f_2(\lambda) = x$ into Eq. 27 yields

$$\int\left[\int\sqrt{L(y)}e^{2\pi f_z y}\right]e^{j2\pi f_z z'}df_z \tag{28}$$

where $L'(y)=L(y/Ff_0)=L(\lambda)$. The bracketed term is the Fourier decomposition of a function $I(f_z)$; thus, the integral can be written

$$\int d(f_z)e^{2\pi f_z z'}df_z \tag{29}$$

which is the in the form of the Fourier transform of a spatial function. Thus, although an incoherent system, the grating spectroscope has a considerable resemblance to a coherent system, and under certain very realistic circumstances can be treated like one.

Of principal interest is how the noise, particularly the setup noise, behaves in such a system. We show that with respect to such noise, the system performance closely parallels that of an achromatic coherent. Optical processing system[13,14] . In such a system (Fig. 5), the

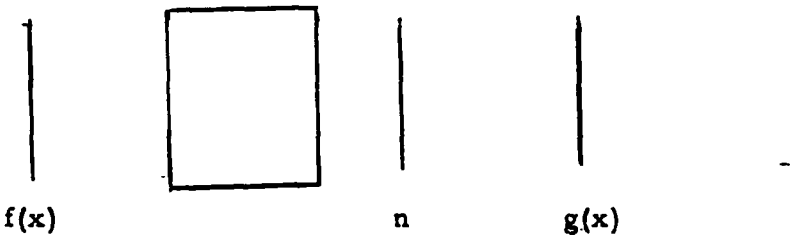

Fig. 5

transformation that carries f to g is identical over a range of wavelengths, so that the output g formed from one wavelength is in registry with that formed from the other wavelengths. However, a noise signal n, residing in another plane, produces at the output a wavelength-dependent spatial structure that becomes smeared when the illumi-

nation is spectrally broad. Thus, setup noise is diminished.

The achromatic coherent optical processor can assume many forms, depending on the application. However, the above observation is always true and is the essence of these systems. The mismatch variation may be in the form of a scale factor change, which produces a spatial-frequency- dependent and a sometimes position-dependent smoothing effect; low spatial frequencies may not be adequately smoothed. It was shown (15) that when the optical system contains a diffraction grating, for example in the form of a signal f residing on a spatial carrier, there will be, in addition to a wavelength scaling effect, a lateral dispersion which can enormously increase the smoothing effect of the polychromatic light. Looking back at the source through the grating, one sees the source broadened into a spectrum; the effectively broader source gives a reduced lateral (i.e., spatial) coherence. Thus, by use of the grating, temporal incoherence is partially converted into spatial incoherence. It is well known that spatial incoherence gives better noise suppression than temporal incoherence. Thus, the grating improves the noise suppression capability of the spectrally broad spatially coherent light.

The reduction in noise is readily seen by the following analysis, which considers the case where the smoothing is by λ-*dependent* lateral displacement; other cases can be similarly analyzed. The field impinging on the noise plane, for a single wavelength, can be written u. Letting the transmittance of the noise plane be 1 + n, where $n << 1$, the light distribution at the output plane is $u'(1+n')$, where u' and $u'n'$ are u and un propogated to the output plane. The irradiance distribution is

$$I = |u'|^2 + |u'|^2(n' + n'^*) \tag{30}$$

If the system has N degrees of freedom, produced by spectral broadening of the source, that is, if N is the number of resolvable wavelengths in the source, as seen through the optical system, then each wavelength component produces a pattern of

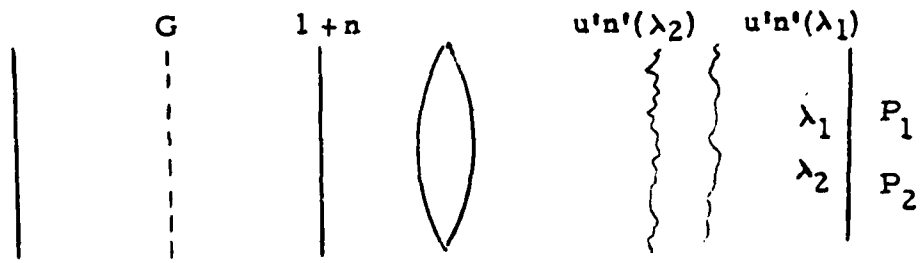

Figure 6

the form of Eq. 30. The constant term builds by a factor N, the fluctuating term by a factor $\sqrt{N}$ giving a noise reduction factor of $\sqrt{N}$.

In the grating spectrometer case, the light impinging on the noise plane is brought to focus. Again, we take the source to have N resolvable components. Impinging at a point P_1 (Fig. 6) are the direct light for the wavelength λ_1, as well as the noise light for all N wavelengths. Only the noise light $u'n'(\lambda_1)$ interferes with the direct light to produce a term of the form of Eq. 30. The other noise terms do not, and their noise contribution is hence negligible.

To relate this system to the optical processing case, we compare this system with a hypothetical system in which all of the $u'n_i'$ interfere with the λ_1 light. This could be realized, for example, by replacing the broad spectrum slit source with a spatially broad coherent source. Such a system, although performing no useful function we can think of, does serve as the fourth element of our comparison. Thus, in terms of noise, the achromatic optical processing system is to the coherent as the grating spectrometer is to this broad-source system. The noise suppression in the two broad spectrum cases is $\sqrt{N}$ compared to the monochromatic counterparts.

The direct identification of two basic kinds of optical processing with the two major kinds of spectroscopy is potentially significant, since a vast body of research in spectroscopy becomes relevant the to the smaller area of optical processing. It would have perhaps been more significant if the purely coherent optical processing, as opposed to the achromatic coherent, could have been tied to spectroscopy, but it appears that the purely coherent has no counterprt in spectroscopy. Also, it may be that other kinds of noise, such as detector noise, could be treated within this analogy. Although setup noise is the dominant noise in coherent processing, it is a much lesser factor in achromatic coherent processing, especially when the operation is one-dimensional and the source is a line source, with coherence in only one dimension, and

it is overshadowed by other noise in incoherent processing. It appears also to be a minor factor in spectroscopy.

There remains a final significant observation. Noting that the grating vs. interference spectroscopy situation is analogous to the achromatic coherent optical processor vs. incoherent optical processing, and also noting that, in theory, achromatic optical coherent optical processing is better in all respects than the coherent and is at a disadvantage only in the practical sense of being cumbersome and more difficult to implement, it follows that if interference spectroscopy has in some circumstances a competitive advantage over grating spectroscopy, then incoherent optical processing, even for situations where processing operation has a large space bandwidth product ($N<<1$), can be advantageous over achromatic optical processing, and even more so over purely coherent processing.

Chapter 7
Formation of Fourier Transform Holograms in Spatially Incoherent Light
(Condensed from the Ph.D. Dissertation of G. Collins)

7.1 Overview of the Incoherent Holographic System

We introduce here a holographic system for use in spatially incoherent illumination.

The basic system consists of the interferometer shown in Figure 1. The incident illumination is from a spatially extended (incoherent) source and is quasi-monochromatic. It is assumed that the source is not so spatially broadband that the beams cannot be separated within the interferometer. The ideal system behavior, predicted as a limiting case by a Fourier optics analysis which ignores the beam separability requirement, requires that the incident illumination be completely (spatially) incoherent as would be the case if the source were infinitely extended. In actual practice, the beam separability requirement can be satisfied, as the idealized behavior is approximated to any desired degree of accuracy, by constraining the spatial bandwidth of the object amplitude transmittance to be suitably narrowband with respect to the spatial carrier frequency of the gratings.

The basic interferometer, composed of the gratings G1, G2, and G3, is the grating equivalent of the classical Mach-Zehnder interferometer. The grating G1 splits the incident light into two beams: an object beam, derived from a diffracted order, and a reference beam, derived from the undiffracted or zero order. The object beam propagates to the grating G2 where it is redirected to become parallel with its original directon. It intercepts the object transparency, which assumes the role played by a test section in conventional interferometry, and propagates onward. The reference beam propagates to the grating G3 where it is redirected, by diffraction, to intercept the object beam.

The basic three grating interferometer is initially set up so that, without the object present, high contrast fringes are obtained at the $z = 0$ plane under broad source conditions. It is essential to the proposed technique that the interferometer be capable of forming, under conditions of broad source illumination, spatially invariant, high contrast, strongly localized interference fringes of arbitrary spatial frequency.

With the object transparency inserted into the system, each spatial frequency of the amplitude transmittance acts as a grating

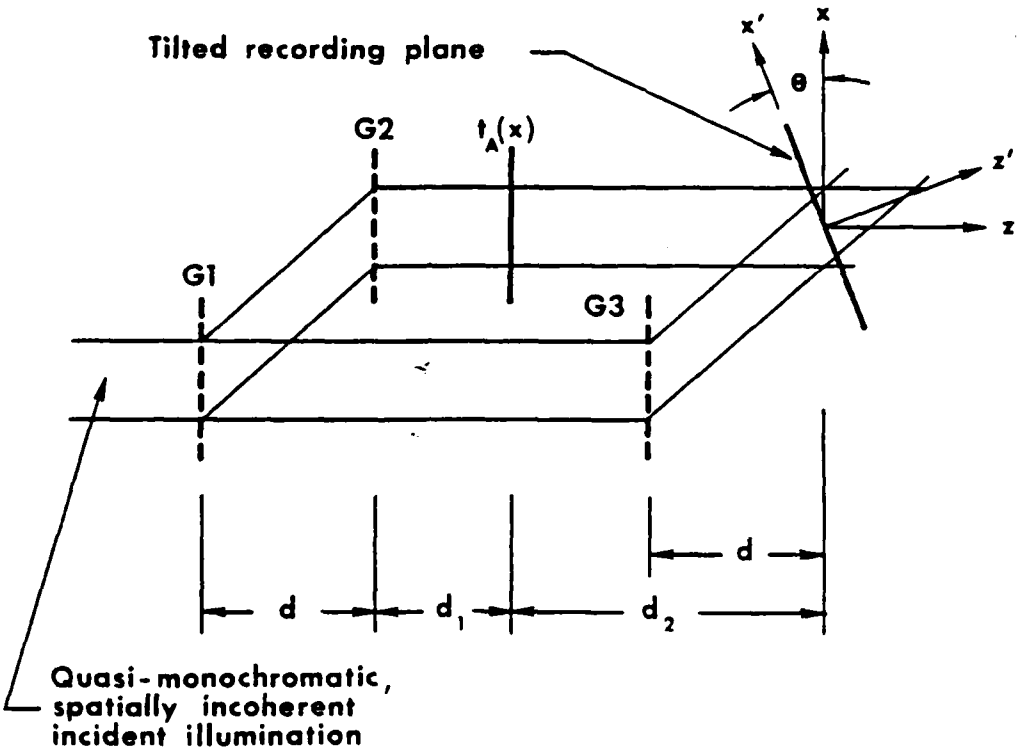

Figure 1

The interferometric system for recording holograms in quasi-monochromatic, spatially incoherent illumination. G1, G2, and G3 are gratings of spatial frequency f_g. t_A is the complex amplitude transmittance of the object.

of the interferometer. In short, the system is capable of essentially arbitrary wavefront construction within this plane. To avoid any possible confusion here (arising from the fact that there are in reality many wavefronts if one associates a wavefront uniquely with some particular point radiator on the extended source) we note that the reconstructed wavefront is, in a sense, an equivalent wavefront. The equivalence, however, is to that wavefront which would be obtained in an equivalent, but completely coherent system.

The similarities of the proposed system and technique to conventional coherent holography are quite striking, and go well beyond simple functional equivalence (as wavefront reconstruction techniques). For example, the Mach-Zehnder interferometer employed here has often been used for coherent holography. In fact, with coherent illumination, the proposed system (including the titled recording plane) could obviously be used to record a conventional hologram. The hologram recorded in this manner would differ from the incoherently recorded hologram, but, if attention is confined to the imaging process within the plane of the interferometer, the differences are slight. Aside from the bias terms, which are potentially of significance only when considering the signal-to-noise ratio, the primary difference is in the additional Fourier transform relationship impressed upon the image term in the incoherent (interferometric imaging) method. Functionally, this is an insignificant difference. Its only impact is to alter slightly the reconstruction technique.

7.2 Experiments

Having developed the basic theory the experimental philosophy was quite simple. The experiments were intended only to verify qualitatively the most fundamental and important aspects of the theory. The basic idea was simply to demonstrate those features of the proposed technique which would qualify it as a true incoherent counterpart to conventional coherent holography.

The experiments had three primary objectives. First and foremost was simply the demonstration of the basic imaging capability of the proposed technique. Second, the linearity of

the technique in the complex amplitude transmittance of the object transparency needed to be demonstrated. This is one of the most fundamental characteristics which distinguish true holography from the various pseudo-holographic techniques which have been proposed for use in spatially incoherent light. The latter are, without exception, linear in the intensity distribution of the object and thus are not true incoherent counterparts to coherent holography. Finally, the ability of the proposed system to image the longitudinal, as well as the transverse, structure of nonplanar objects was to be demonstrated. This characteristic is important because it is a fundamental property of coherent holography. It is also very important because it distinguishes this technique from most broadband compensation techniques. Most broadband compensation techniques, for either the spatial or the temporal domain, are modified imaging systems and are constrained to operation upon a single object plane. In other words, the compensation is for a specific, fixed object plane only.

Two experiments were devised to test the holographic capabilities of the proposed technique. The first, imaging a complex transparency (in this case a bleached ronchi ruling) was designed to verify that the fundamental technique actually works on the complex amplitude associated with the object transparency. The second, imaging a simple two dimensional (in the x' and z' dimensions) object scene in the x' and z' dimensions, was developed to demonstrate that depth information was preserved in the recording and reconstruction processes just as it is in conventional coherent holography.

It is important to note that although both experiments deal with the phase, they are really quite independent in what they demonstrate. For example, depth information can be recorded by incoherent systems which are totally insensitive to the phase in transmission or reflection of an object; i.e., systems which linear in the intensity. An example of this is the well known pseudo-holographic technique for producing holograms of self luminous objects by shadowcasting Fresnel zone plates. Thus, merely preserving depth information does not demonstrate that the system is linear in (or works on) the complex amplitude (transmittance/reflectance associated with the object.

Conversely, demonstrating that the system is linear in the complex amplitude associated with the object does not say anything about whether or not depth information is preserved in the recording process. The demonstration of the system linearity in complex amplitude is not quite as straightforward or simple as it would seem. The system for doing this is in Figure 2.

The object for the experiment was a segment of a bleached ronchi ruling of spatial frequency 1ℓ/mm. A photograph of the ruling is shown in Figure 3. The ronchi ruling was chosen for several reasons. It is one dimensional and simple, its sharp edges are good for qualitative evaluation of the image, and it allows reasonable control of the frequency content (and the SBW) of the object/image. Its periodic nature was also useful and convenient for the spectrum evaluation part of the experiment. The ruling was bleached to generate a phase, as well as amplitude, object. This made the object amplitude transmittance complex. The bleaching was controlled such that the first two diffracted orders were significantly brighter than the undiffracted zero order. In the power spectrum of the object, the first two diffracted orders are separated from and symmetric about the undiffracted or zero order (which corresponds to zero spatial frequency in the object) and are thus easily distinguishable. Because of the bleaching process they are much stronger than the zero order. This is exactly what is needed for the evaluation of the recorded spectrum. Note that the power spectrum of the intensity transmittance would be just the reverse of this in that the diffracted orders would appear much weaker than the zero order.

The first part of the experiment consisted of evaluation of the general image quality. The hologram was constructed using the system described previously and shown in Figure 1. The image was reconstructed using the system described previously and shown in Figure 2. The reconstruction aa photographed through a microscope is shown in Figure 4. It should be noted here that only a portion of the ronchi ruling shown in Figure 3 was used in the hologram construction process, the rest was masked off. The reconstructed image is a pretty good replication of the original object. For example, allowing for the effects of exposure and

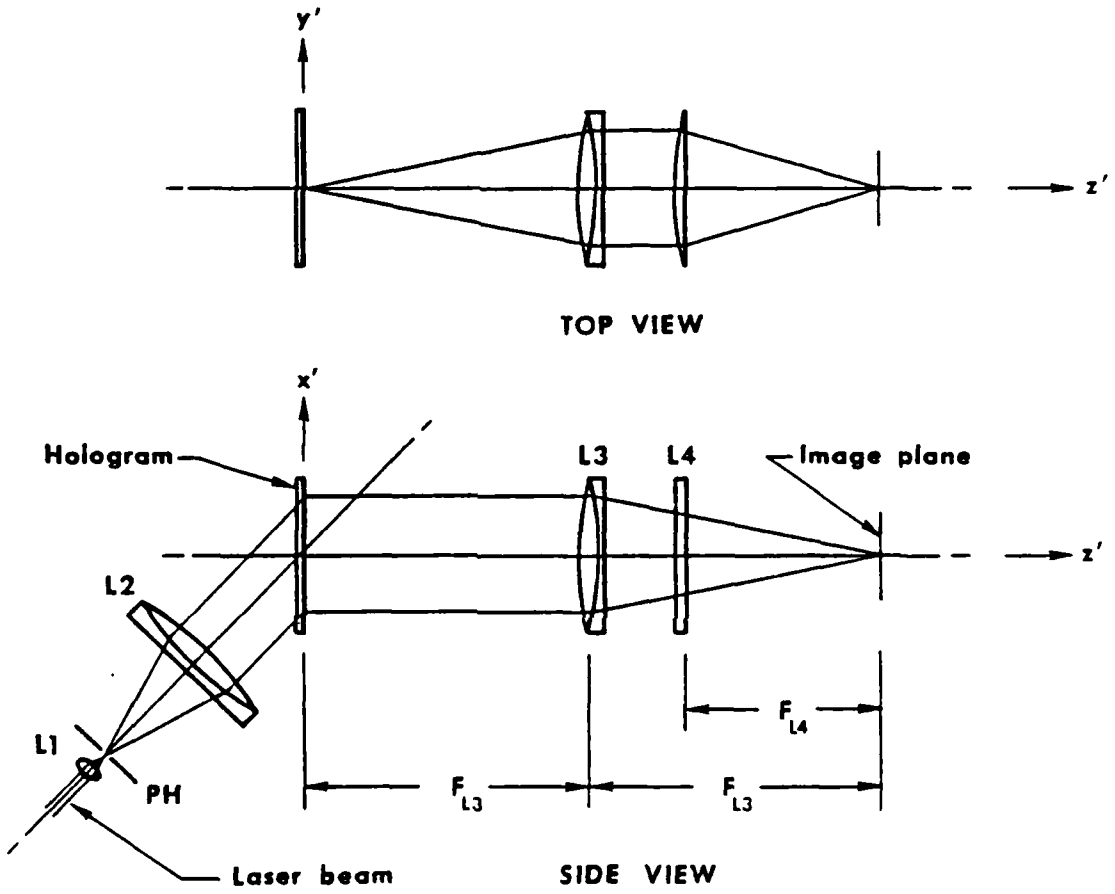

Figure 2

The coherent system used for image reconstruction in the experiments.

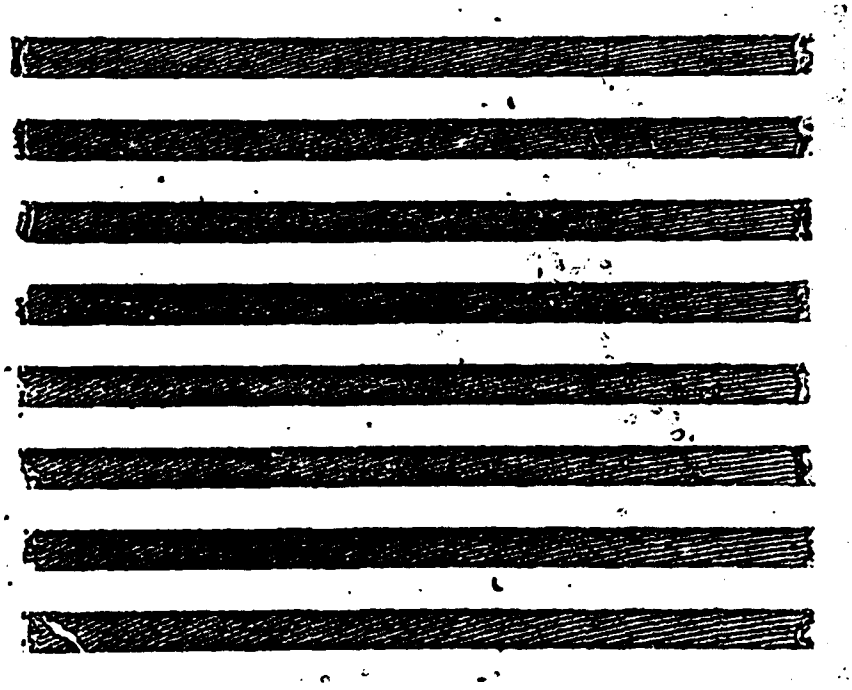

Figure 3

The bleached ronchi ruling used for the demonstration of linearity in complex amplitude.

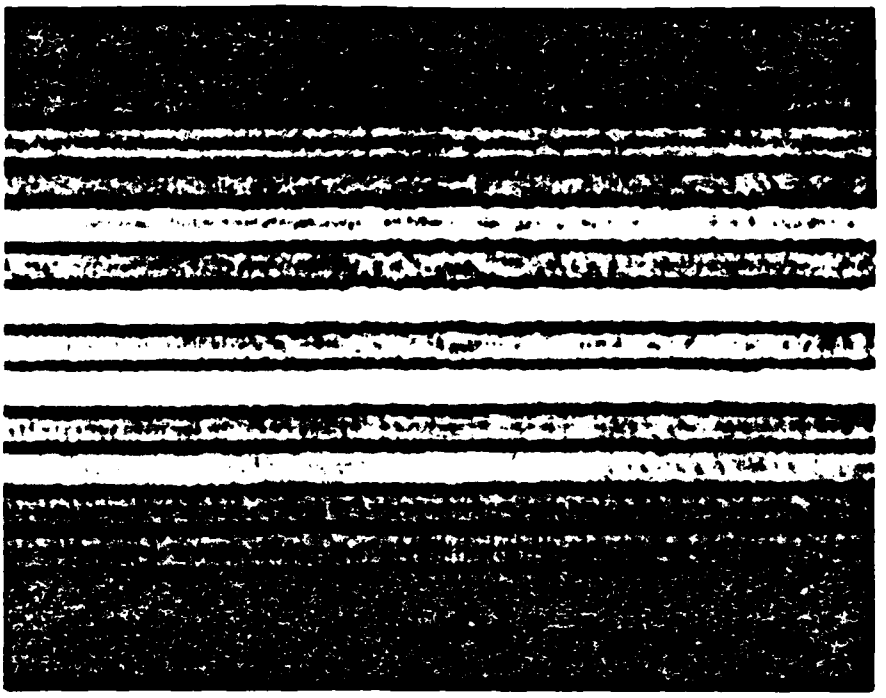

Figure 4

The reconstructed image of the ronchi ruling

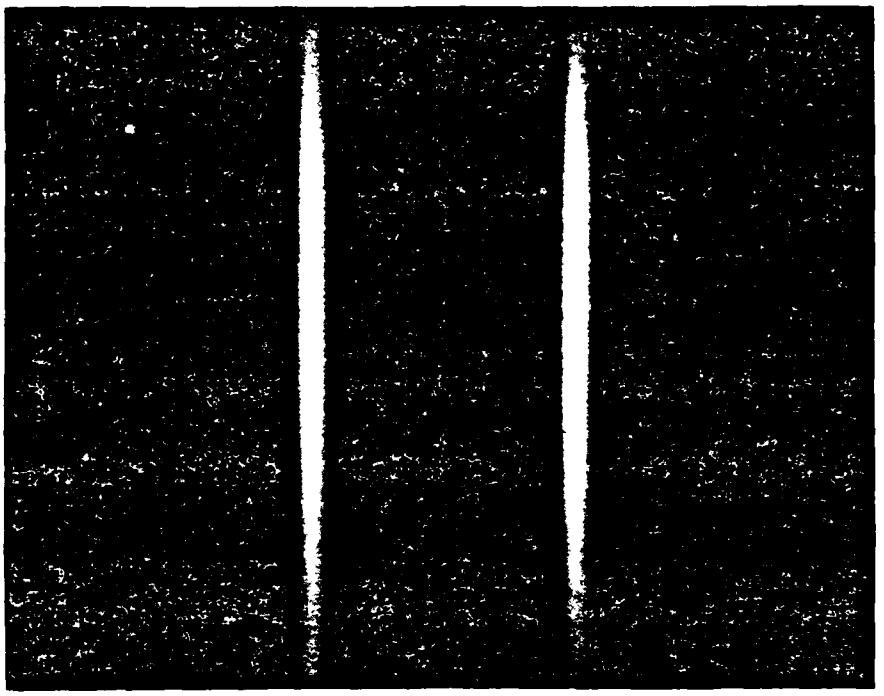

Figure 5

The modulation recorded on the hologram of the ronchi ruling. The exposure was such that the zero and first diffracted orders did not saturate (over expose) the film.

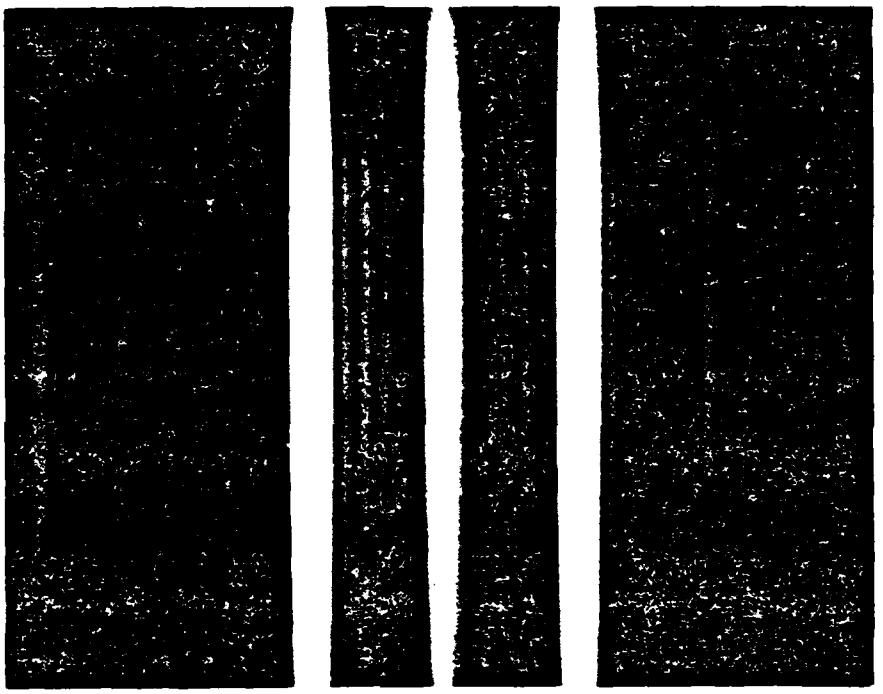

Figure 6

The modulation recorded on the hologram of the ronchi ruling. This photograph was deliberately overexposed in the zero and first diffracted orders to allow the detailed side lobe structure to be examined.

development in the hologram construction and the print processes, the relative contrast between the bars of the object has been well preserved. There is some edge enhancement (note the pronounced edges of the bars) which is probably due to nonlinearities in the recording process. The justification for this will become more apparent when the spectrum is examined. The resolution is also relatively good; the line width at the bar edges may be taken as the width of the minimum resolvable element.

Of particular interest in the reconstructed image is the noise. Note that two dimensional noise such as the emulsion defects in the original object has been wiped out. This is due to the one dimensional nature of the imaging process. The noise has essentially been smeared in the direction orthogonal to that in which the imaging takes place. There is clearly coherent artifact noise present. Note for example the faint ringed diffraction patterns clustered near the center. This is due to the coherent reconstruction technique employed. What is most notable about the reconstructed image is that, in general, the signal to noise ration is very good, and we would not really expect to do much better (if at all better) using a coherent holographic method. The bias buildup problem, which plagues incoherent optical processing in general and which is especially acute in incoherent (pseudo) holographc techniques, has apparently had a negligible effect here. This is probably for the most part due to the somewhat limited SBW of the object, which, on the basis of the apparent resolution and the size of the object field, can be estimated roughly to be of the order of 60 to 70 (resolution elements).

The modulation recorded on the hologram was then imaged using the modified reconstruction system discussed earlier. This resulted in the two photographs shown in Figures 5 and 6. These two figures differ only in the exposure of the initial photograph of the image.

Figure 5 was exposed such that the first diffracted orders (plus and minus one diffracted order) one the undiffacted zero orders are not saturated (overexposed). It essentially demonstrates that these diffracted orders are much stronger than the zero order. Thus, as discussed earlier, the complex amplitude

transmittance of the object was at least bipolar. More importantly, it demonstrates that the object for the initial recording process was in fact the complex amplitude transmittance of the object transparency.

Figure 6 was overexposed in the zero and first diffracted orders. It does, however, allow the detailed sidelobe structure of these terms to be examined and the presence of additional diffracted orders to be detected. because of the extreme dynamic range involved, these features could not be incorporated in the first photograph (Figure 5). Figure 6 illustrates several important features. First, it essentially demonstrates the diffraction limited nature of the recording process. As a brief aside from this, note that the phase errors which precluded integrating over the orthogonal dimension will not be apparent in this photograph since they are phase errors. Given this, it might be questioned whether or not Figure 6 really demonstrates diffraction limited performance. The answer to this would be that it does since the phase errors are in the direction orthogonal to that in which the (diffraction limited) interferometric imaging process take place. In other words, they are not truly part of the imaging process since we are only concerned with imaging in the orthogonal dimension. A diffraction limited image will in fact result when the imaging system used for the reconstruction (such as the anamorphic system described earlier) does not integrate in the orthogonal dimension, i.e., when it images in this dimension.

Figure 6 (in combination with Figure 5) also demonstrates the large dynamic range of the modulation. It can be inferred from this that essentially the same sort of dynamic range problems as is encountered in coherent holography where recording a Fourier transform hologram (such as a matched filter) will be found here also. This is not too surprising since in each case the distribution being recorded is the Fourier transform of some object distribution. while control over the bias cannot be exercised in this case as it can be in a coherent system, a problem with nonlinearities in the recording process still results, and in fact the anticipated results are much the same for the two cases (although more extreme for the coherent case). In

the incoherent system being tested here each spatial frequecny of the original object generates localized fringes in one plane and bias throughout the rest of the fringe box. For the ronchi ruling used as the object in the experiments, the bias in the fringe box will be almost entirely due to the zero and first diffracted orders (and especially the first diffracted orders) since these are far and away the predominant terms of the object's spectrum. The contrast (between signal and bias) for these terms will thus be very high, but it will be much reduced for other diffracted orders. Because of the limited dynamic range of photographic film, very high contrast signals will be recorded much more nonlinearly than low contrast signals. In particular, if the signal and bias are approximately the same, and if the average (spatial) or bias exposure has been set for the middle of the linear segment of the film transfer characteristic, the recorded signal will be limited at both of its extremes (assuming it to be oscillatory in nature). If other much weaker signals are also present, they can still be recorded quite linearly. The net effect in the recording, aside from the distortion of the stronger signals, is to increase the (relative) contrast of the weaker signals relative to the stronger signals. Since the stronger signals correspond to lower spatial frequencies in the present case, the result of the nonlinearity of the recording process is to emphasize somewhat the higher spatial frequencies. This same phenomena occurs in the coherent case, and especially in the generation of spatial matched filters, where it is usually deliberately enhanced by a suitable choice of reference to object beam ratio. The higher pass affect was evident in the reconstructed image of the ronchi ruling (Figure 4) where the edges of the bars were enhanced somewhat.

Lastly, Figure 6 provides an alternative demonstration of the high S/N noted in the reconstructed image of the object. Note that even far down in the sidelobes of the diffracted (and undiffracted) orders, the S/N appears quite good.

Chapter 8

Construction and Evaluation of HOES Made in Light of Reduced Coherence

Reprinted from Applied Optics, Vol. 23, page 942, March 15, 1984

Construction and evaluation of HOEs made in light of reduced coherence

Emmett N. Leith and Stacy Leon

Using interferometers adjusted for extended source operation, it is shown that holographic optical elements (HOEs) can be constructed with any designed conjugate focal planes. Noise and diffraction efficiency measurements show that the reduced coherence method can yield HOEs of high diffraction efficiency and good SNR.

I. Introduction

Fringes formed in light of reduced coherence, either spatial or temporal, are less noisy than fringes formed with coherent light. However, in general, fringes formed in light of reduced coherence are usually limited in various ways; the fringes may be of lower contrast, be fewer in number, exist only over a small region, or it may prove difficult or impossible to modulate the fringes, that is, form fringes of nonuniform spacing such as a zone plate pattern. Here we describe two complimentary optical systems with which we can modulate fringes to obtain zone plate patterns made using interferometry with a spatially broad monochromatic source. Such interferometrically recorded zone plate patterns are often called holographic optical elements (HOEs) or diffractive optical elements and have been finding increasing application. Diffraction efficiency and the noise level of these elements are also discussed.

II. System

Initial experiments of this type were discussed by Swanson, who described a method for modifying the grating interferometer so as to form zone plate structures instead of grating structures.[1] In this method lenses are placed in each branch of the interferometer to image a common plane at the same magnification but with different curvature being given to the interfering wave fronts. The interferometer configuration is shown in Fig. 1. For example, lenses L_2 and L_3 may be in the telescopic (or afocal) configuration, so that P_1 is imaged to P_{out} so that a plane wave at P_1 becomes a plane wave at P_{out}. Lens L_1 also images plane P_1 onto P_{out} but so that the wave impinging on P_{out} is a diverging spherical wave of radius F, the focal length of the three lenses being used. The two beams interfere under broad source monochromatic illumination, but the fringes, being the result of interference between a plane and spherical wave, form, after recording, a diffraction lens of focal length F. Thus to make low noise diffractive lenses, we have at P_1 a uniform distribution of light. No structures are placed at P_1, since such structures inevitably contain noise (dirt, scratches, etc.); thus the fringe pattern is very clean when the light source is of reduced spatial coherence.

Important to the incoherent HOE construction method is the range of HOEs that can be achieved. We would like to be able to produce any focal length. This is relatively easy. More important is to achieve any range of conjugate focal planes. Noting that if we desire the object and image distances to be d_{ob} and d_{im}, respectively, for best results the HOE should be made with two interfering beams converging to or diverging from points at these same distances. To achieve any possible set of d_{ob} and d_{im} is a more difficult problem. It is by no means *a priori* evident that it has a solution.

For convenience of analysis, suppose the optical systems within the two branches of the interferometer are removed; the justification is that the interferometer itself need not be part of the analysis. All we must do to have these optical systems function in the interferometer is to impose a few constraints on them so that their presence would not disrupt the fringe forming capability of the interferometer. These two optical systems are shown in Fig. 2. The top system images plane P_1 to P_{out}, the fringe forming plane, and the lower system images P_1 to P_{out}; L_{sys} and L_{sys} are imaging systems. We consider here the various forms that these systems can take and the capabilities and limitations of these forms.

The authors are with University of Michigan, Department of Electrical & Computer Engineering, Ann Arbor, Michigan 48109.
Received 18 November 1984.
0003-6935/84/060942-06$02.00/0.

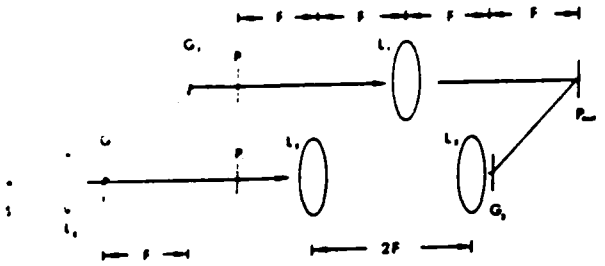

Fig. 1. System for making HOEs in extended source light.

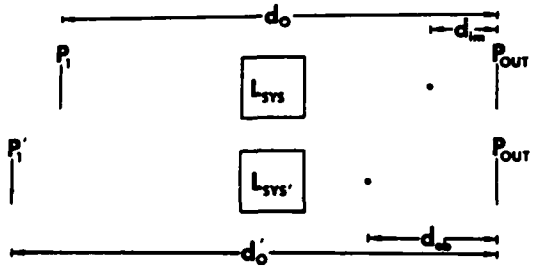

Fig. 2. Basic concept.

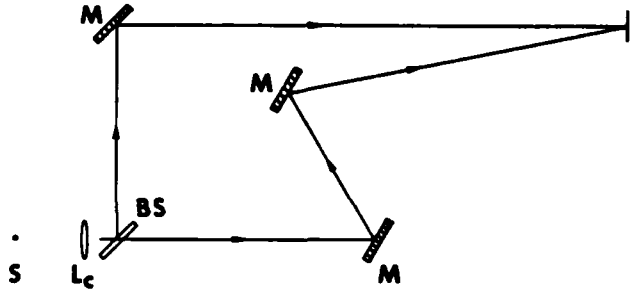

Fig. 3. Modified Mach-Zehnder interferometer for HOE construction.

To obtain interference with a spatially incoherent monochromatic source, we require that at P_{out} both beams have undergone the same amount of Fresnel diffraction and that the magnifications of the two beams be equal. Now the Fresnel diffraction process occurs between the source plane and planes P_1 or P_1'. Since P_1' and P_1 are each imaged to P_{out}, the Fresnel diffraction process stops at P_1 and P_1'. Thus it is necessary that planes P_1 and P_1' be equally distant from the source. Otherwise the interference would be weak or absent. Since the diffraction paths stop at P_1 and P_1' we must allow for the optical path from P_1 to P_{out} and P_1' to P_{out} to be different, a condition that gives a useful flexibility in the realization of HOEs with arbitrary conjugate focal planes. Indeed it is in general necessary to image over different distances in each arm of the interferometer, that is, the distance from P_1 to P_{out} must be different from that from P_1' to P_{out}. Since the distances source to P_1' and source to P_1 must be equal, it follows that the total optical paths must in general be unequal, the path difference being the difference between the $P_1 - P_{out}$ and the $P_1' - P_{out}$ paths.

We have considered two optical systems that fulfill the above requirements. One is a modified version of a grating interferometer setup described by Swanson, and the other is a modified version of the Mach-Zehnder interferometer (Fig. 3) where the final beam splitter is replaced with a mirror. Both systems have advantages and drawbacks.

The required optical path difference can be generated in various ways. Such generation is easy in the modified Mach-Zehnder interferometer by simple positioning of the various mirrors. To generate a large path difference requires a high degree of monochromaticity, so that the beams can travel unequal path lengths and still interfere. This idea can be taken to an extreme by making the path length difference equal to twice the laser cavity length and compensating for Fresnel diffraction by imaging over the path length difference with appropriate lenses and unity magnification. This system will produce high contrast fringes in broad source monochromatic illumination. Besides the requirement of a high degree of monochromaticity, another disadvantage of this system is that the number of fringes is limited, being given by $N = 1/(2\Delta\theta^2)$,[2] where $\Delta\theta$ is the source subtense at the lens (not shown) that collimates the light incident on the interferometer. For a large $\Delta\theta$ the number of fringes may be inadequate. There is no similar constraint for the grating interferometer, which can produce a completely unlimited number of fringes regardless of source subtense.

Actual physical path length differences need not be introduced to compensate for differences in Fresnel diffraction. Inserting a cascade of appropriate unity magnification telescopic imaging systems into the grating interferometer will produce the desired Fresnel diffraction compensation. The disadvantage with this system is that multiple lenses introduce more noise and more aberrations, both of which will reduce fringe contrast.

A completely general mathematical analysis of the systems is somewhat tedious and does not easily yield a simple physical viewpoint. There are basically two ways of describing the process physically. Each branch of the optical system images the plane P_1 (or P_1') but with a quadratic phase factor. Alternatively we can say that each optical system in addition to imaging the plane P_1 (or P_1') images the source. The distances d_{ob}, d_{im} (Fig. 2) from the source image to the plane P_{out} become the designed conjugate focal planes of the resulting HOE. This viewpoint can lead to some basic insights as to what range of d_{ob}, d_{im} is possible.

For example, if the incident beam is collimated, where L_{sys} and $L_{sys'}$ of Fig. 2 become imaging lenses in each branch of the interferometer for imaging P_1 and P_1' to P_{out}, the source image is found at a distance of one focal length downstream from the imaging lens. Thus, by appropriately adjusting the focal lengths F_1 and F_2, any set of conjugate focal planes is possible subject to the constraint that both source images are formed to the left of P_{out}. This constraint always leads to a HOE designed as a negative lens. This is a severe restriction, as almost all practical lenses are positive lenses. Be-

Fig. 4. Imaging by lens of two axial points.

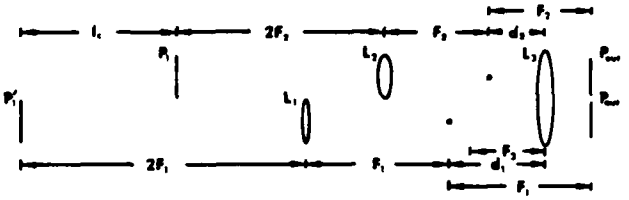

Fig. 5. General configuration for HOE construction.

sides there is no justification for using an incoherent system for producing a negative HOE, since this can always be accomplished just as well and in a much simpler manner by conventional means, with light diverging from two pinholes a distance d_{ob} and d_{im} from the recording plate, and with no optical elements between either pinhole and plate, there will be no coherence induced noise.

The challenge is thus to cause one of the beams to be converging at P_{out}, i.e., have either d_{ob} or d_{im} be a negative quantity, thus producing a positive HOE. The philosophy of accomplishing this is the following. A lens can be considered as always preserving the sense of the image (Fig. 4). That is, two points, A and B, separated axially are always imaged into points A' and B' with no axial inversion (i.e., B and B' both form to the right of A and A', respectively). Suppose we consider a dynamic situation in which A' and B' are imaged continually farther from the lens, which can be accomplished by bringing the object points A and B continually closer to the lens. When B reaches the front focal plane of the lens, B' goes to infinity and further movement of B toward the lens results in B' coming in from $-\infty$.

We thus have achieved one of the goals. We have effectively inverted A and B, although the principle stated above has in a sense not been violated, since both A and B always moved in the forward axial z direction without one overtaking the other; we see that the path is cyclic with the positive and negative ends being connected at infinity. Adding more focal power, either with shorter focal length lenses or the addition of more lenses, merely moves A and B (here the source plane and the plane being imaged) to new positions along the z track.

To apply this viewpoint to the HOE problem, we identify planes A and B with the source image and P_{out}, respectively, and we place a second lens in each branch of the system, which reimages both the source point and P_{out}. The viewpoint given above then seems to suggest that the constraint on positive focal length HOEs should be no greater than that for negative HOEs. For analysis we return to Fig. 2. P_1 and P_1 are both to be imaged at P_{out} with equal magnification. The separations $P_1 - P_{out}$ (labeled d_0) and $P_1 - P_{out}$ (labeled d_0) can be anything, including negative values, since it is immaterial what planes are imaged to P_{out} as long as the distance $d_0 - d_0$ remains equal to the interferometric path difference, and indeed this path difference can be altered in any way we choose.

Considering Figs. 2 and 4 one can see that the addition of one more lens, which accepts both beams (Fig. 5), will produce any positive HOE desired. The conjugate focal planes are given by d_{ob} and d_{im}, where

$$d_{ob} = \frac{d_1 F_3}{d_1 - F_3} \quad d_{im} = \frac{d_2 F_3}{d_2 - F_3}.$$

Simply by varying F_3, d_1, and d_2 one can achieve any range of conjugate focal planes desired for a positive lens. The constraints for the HOE to be a positive lens are $F_1 > F_2$ and $d_2 < F_3 < d_1$. The diffraction path length difference for this HOE forming system is seen to be $l_c = 4(F_1 - F_2)$ in Fig. 5. Thus when using the Mach-Zehnder interferometer we require the coherence length to be $> l_c$, the required physical path length difference between the two arms of the interferometer (Fig. 3). Likewise l_c is the extra path length difference over which we must image to obtain equal diffraction path lengths when using the grating interferometer of Fig. 1 integrated with the optical system of Fig. 5.

Here we have considered two systems: the grating interferometer, which is limited in fringe contrast by the number of lenses introduced into the system; and the modified Mach-Zehnder interferometer, which is limited in the number of fringes obtainable and by the coherence length of the laser being used. With these two systems almost any range of positive HOEs desired can be obtained using broad source monochromatic illumination.

III. Diffraction Efficiency

We desire that the diffraction efficiency of HOEs made with light of reduced coherence be comparable with those made with coherent light. Thus the fringe contrast of HOEs should be high over the entire recording area and for even the highest spatial frequencies. Theoretically such a high contrast fringe pattern will be produced, but any such system defects will tend to lower fringe contrast as the source is broadened.

Various HOEs were recorded with the interferometric arrangement of Fig. 1, both for coherent illumination and for illumination of reduced coherence. The HOEs thus produced had a mean spatial frequency of 300 cycles/mm, the highest and the lowest spatial frequencies being 100 and 400, respectively. Three source sizes were used: a point source and sources of angular subtense of 0.010 and 0.005 rad measured at the collimator.

A set of HOEs was made for each of the three source sizes, and the diffraction efficiency was measured. The results, shown as the diffraction efficiency vs exposure curve of Fig. 6, indicate that diffraction efficiency has decreased somewhat with increasing source size but not significantly. High diffraction efficiency (say 80–95%) could be obtained by either bleaching or recording on

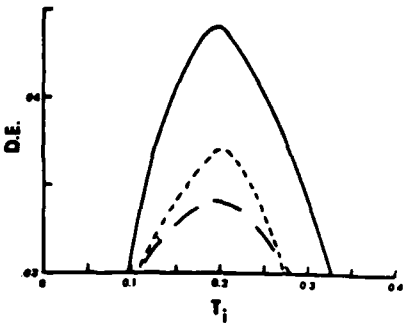

Fig. 6. Diffraction efficiency vs intensity transmittance. Solid curve—using coherent source. Dotted curve—using source of angular extent of 0.005 rad. Dashed line—as before but with angular extent of 0.01 rad.

dichromated gelatin for the optimal exposures of any source size used.

It appears that the greatest loss of diffraction efficiency arises from system imperfections, such as field curvature, which cause the surface of fringe localization to depart from the ideal planar shape, and the recording plate will, therefore, be at some places outside the surface of highest fringe contrast. Assuming that such aberrations were absent, there remain two factors that affect diffraction efficiency. First, the noise reduction is a smoothing process wherein spatial frequency energy representing noise is converted to an ambient background. This results in a loss of fringe contrast and resulting diffraction efficiency. Since the noise, even in a rather noisy fringe pattern, has a power that is only a small fraction (a few percent) of that in the signal, the contrast loss for this effect should be similarly small. On the other hand, the presence of noise means locally that the beam ratio may be different from the nominal or average beam ratio, and the fringe contrast is thus lowered. In addition, the resulting local mean exposure may not be optimum, again providing lower diffraction efficiency. Thus, as we broaden the source, we find factors that decrease the diffraction efficiency and others that increase it, and it appears that rigorous analysis is required to ascertain how these opposing factors balance.

IV. Noise

To investigate the noise, various types of data were collected. First, HOEs were made using the grating interferometer setup of Fig. 1 with an extended source of 0.005-rad size. Second, HOEs were made the same way but with a nonbroadened source. The results show the enormous noise reducing effect of the coherence reduction, but the comparison is not entirely realistic, since the interferometer contains noise sources, such as gratings, that would not be present in the normal HOE-forming system. Thus to test the efficacy of the method the comparison should be made with coherent illumination in a conventional HOE-forming system.

We have distinguished two HOE-forming systems, each rather simple. In one, interference is obtained between two divergent beams and in the other between a diverging and converging beam. The former produces a HOE designed for use as a negative lens and the latter a HOE designed for use as a positive lens. In the former case, light emanates from two pinholes with no optical elements between pinhole and recording plate. Thus the entire pattern should be quite free from setup noise except for backreflections from the recording plate, and experience shows that with good film backing this can be negligible. In the second case, a lens must be placed downstream from the pinhole in one of the beams; this lens is unavoidably a noise source. Since positive lenses are far more common than negative lenses, the system with the noise producing lens will be the usual case.

In general, noise on either of the two interfering beams will be recorded and will appear in the beam generated by the hologram. However, this noise can be minimized by proper hologram construction procedures. Suppose one of the beams has a noise $n(x,y) = |n| \exp(i\Phi)$, i.e., both an amplitude and phase component. On the basis of conventional first-order theory, both the amplitude and phase components of the noise will be modulated onto the fringe pattern and will appear in the reconstructed beams. However, it is possible to reduce considerably, sometimes almost eliminate, the amplitude component $|n|$. If diffraction efficiency is plotted as a function of exposure, the resulting curve typically shows a broad flat maximum. Thus, if one aims to record at the center of the maximum region but misses the proper exposure by a small amount, the diffraction efficiency is not affected.

Now, suppose one of the two beams has an amplitude noise $|n|$ of small magnitude, so that the beam has a spatial fluctuation across it of perhaps 10%. Consequently, the total exposure received by the recording plate will vary by some similar amount, or actually less, if the other beam is uniform. But, since the diffraction efficiency is insensitive to these exposure variations, the noise amplitude fluctuations $|n|$ will not appear in the reconstructed beam; i.e., amplitude noise is suppressed. This suppression may be in fact only partial, since the fluctuations alter not only the exposure but also the fringe contrast, and the lowered contrast results generally in HOEs of lower diffraction efficiency.

However, the noise suppression that results can be rather dramatic. For example, we recorded a fringe pattern of $\sim$1 cm^2 ten separate times on different portions of a plate with different exposures. The exposed areas that had the highest diffraction efficiency were also found to diffract the most uniformly. Thus the nonlinearities of the recording process indeed offer a significant mechanism for suppression of amplitude noise.

In the first noise experiment, the HOEs were photographed through a microscope at various magnifications, results being shown in Fig. 7. Figures 7(a) and (d) show the HOE made in the grating interferometer with an extended source at two different magnifications, and Figs. 7(c) and (d) show the same but with a point source. The noise is setup noise produced by defects in the optical elements. The pictures show how effectively the higher spatial frequency noise is eliminated,

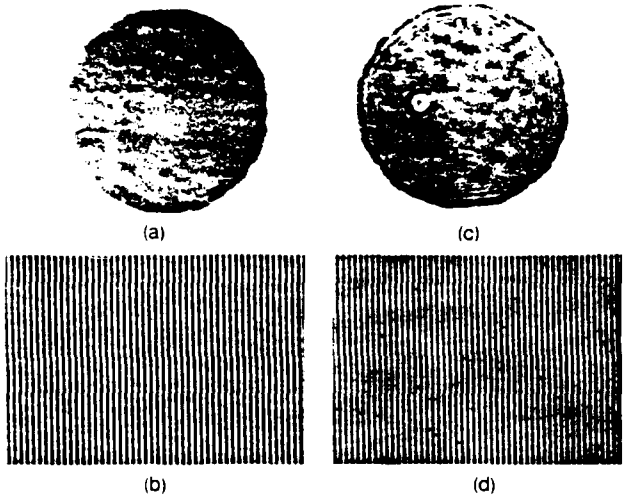

Fig. 7. Magnified image of HOE surface using 0, +1, and −1 orders: (a) extended source, low magnification; (b) higher magnification; (c) as in (a) but using a point source; (d) as in (b) but with a point source.

whereas the very low spatial frequency noise is only partly removed by the reduction in spatial coherence. Not shown is the result for a HOE made in the conventional setup, both for the case of no lens in either beam beyond the pinholes, in which case the hologram is quite noise free, and for the case of a lens in one beam, yielding a result intermediate between the coherent and the incoherent cases of Fig. 7.

Of greater significance is the amount of noise to be seen in the first diffracted order. Indeed, it is conceivable, although unlikely, that none of the noise visible on the photograph of Fig. 7 is present in the first diffracted order. To examine the first diffracted order, a white light source of moderate, but not large, extent (a microscope illuminator) was used, the HOE was reimaged through a unity magnification telescopic system, and a spatial filter removed all diffractive orders except for one first-order beam. The results, not shown here, are comparable with Fig. 7. It was also found that the highest diffraction efficiency exposures gave the least amplitude noise $|n|$.

Since practical HOEs are phase holograms and since the amplitude-to-phase transformation amplifies the noise, we bleached some HOEs and repeated the observation of the first order. At low magnification, noise similar to that of Fig. 7 was observed.

Higher magnification revealed, however, yet another noise, much finer and basically different in appearance. This is shown in Fig. 8. Figure 8(a), made with a coherent beam containing no optical elements downstream from the pinhole, revealed a noise-free field, except for a few spots and some grain noise, both produced by the film that recorded the beam. Similarly, Fig. 8(b) shows the result for a grating interferometer containing various lenses and gratings using an extended source. There is a small trace of noise that we attribute to the HOE (the low frequency mottling, not the much finer grain noise). Figures 8(c)–(e) show the result for the conventional case with a single lens in one beam. The noise level is considerable. In Fig. 8(c), the camera is focused on the emulsion, whereas in Figs. 8(d)–(e), the focus is moved slightly to one side of the emulsion, of the order of 0.5 mm. Again the small black spots are not relevant. The noise is enormously greater for the defocused position. The noise thus appears to be predominately phase noise. It almost completely disappears when the emulsion was covered using a cover glass with xylene between the two glass surfaces. The noise thus is found to be a surface relief, and the emulsion surface thus exhibits an orange peel effect. This seems somewhat curious, since the bleaching process ($R10$ bleach) produces a phase image primarily of the refractive-index modulation type, and the brightness of the first diffracted order was only slightly affected by the liquid gate.

A search for the origin of the noise revealed that it arises from two causes, first, from diffraction from the aperture edge of the lens, and, second, from noise on the lens. The effect could be duplicated with no lens, just

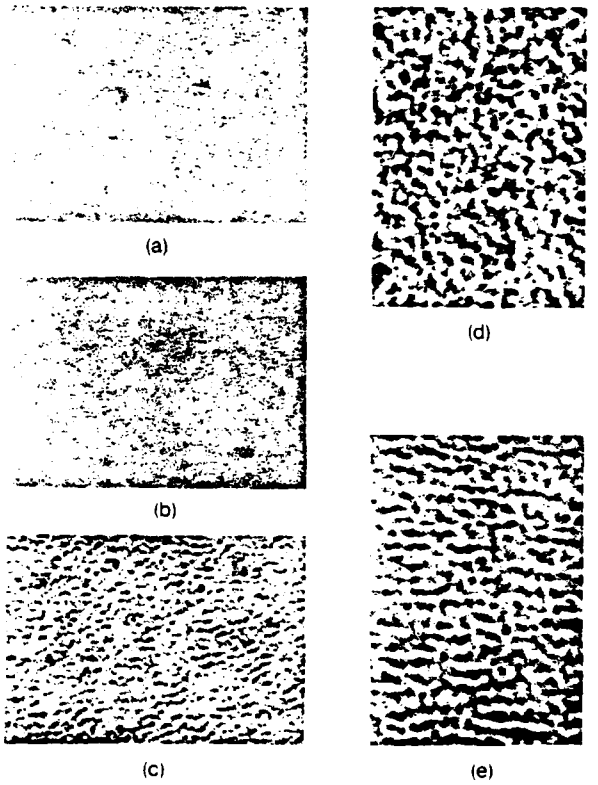

Fig. 8. Magnified image of surface of HOE imaged in one first-order only: (a) HOE made with two diverging beams and no optics between pinhole and recording plate. No noise visible except for some emulsion defects on HOE surface. (b) HOE made with grating interferometer and lenses in system. Faint noise (mottling) is seen. (c) HOE made in conventional system with one lens in one beam. Some noise is seen. (d) Microscope focused to one side of image plane (~0.1 mm); noise is greater. (e) Same as (d) but on other side of image plane.

a diffracting aperture (iris) in the beam, or by a large diameter lens, producing no edge diffraction but having some scattering centers (dirt etc.) on and in the glass.

We also observed the zero order and found again the same noise but less intense. We looked for traces of such noise on the unbleached HOEs but failed to find any. Our presumption is that the noise is present on the unbleached plate but at a level too low for observation. The bleaching process amplifies the noise bringing it up to a visible level.

These noise measurements, by no means exhaustive, indicate that whenever scattering structures are present in one of the two beams in a HOE making system, the reduced coherence method will remove almost all the noise, except that of very low spatial frequency. However, if there are no scattering structures, the use of coherent light will do quite well and is preferred because of the simplicity.

V. Concluding Comments

The results presented here, although by no means exhaustive, clearly indicated that HOEs made with light of reduced coherence can have diffraction efficiency comparable with HOEs made by the conventional coherent methods and may have a significantly better SNR. Also the reduced coherence methods are quite versatile.

Finally, we recount a point that is central to this paper: Two HOEs that have the same focal length and are thus described to first order by a phase function $\exp[j\pi(x^2 + y^2)/\lambda z]$ are generally not the same. The HOE made with beams of curvature C_1 and C_2 will have aberrations different from one made with beams of curvature C_3 and C_4. The differences are manifested by the presence of higher-order terms in x and y, where the coefficients depend on the location of the source points. There is an important corollary to this observation. As the source point is broadened, we expect the higher-order terms to be improperly recorded, resulting in loss of diffraction-limited performance as well as reduced fringe contrast. Thus there are limits to the source broadening process. These aberrations have already been studied to some extent in the doctoral dissertation of Swanson.[3] Our intent is to explore them further and discover what limits they impose on the broad source HOE technique.

We acknowledge a number of useful discussions with Yih-Shyang Cheng, who in particular indicated some advantages of a Mach-Zehnder interferometer for this application.

This work was supported by the Air Force through grant AFOSR 81-0243.

References

1. G. W. Swanson, Opt. Lett. **8**, 45 (1983).
2. F. D. Bennett, J. Appl. Phys. **22**, 184 (1951).
3. G. W. Swanson, "Partially Coherent Imaging and Interferometry Based on Diffraction Gratings," Ph.D. Thesis, U. Michigan (1983); available from University Microfilms.

Chapter 9

Formation of HOES in Spectrally Broad Light

The Construction of Holographic Optical Elements in Broad Spectrum Light

S. Leon and E. Leith

The University of Michigan, Ann Arbor, Michigan 48109

Abstract

An achromatic Fourier transforming system is analyzed in a manner which gives new physical insight. A matched spatial filtering experiment is performed comparing noise performance of a coherently produced matched filter and one made using broad spectrum light in an achromatic Fourier transforming system. The broad spectrum light is obtained by scanning a dye laser through its tuning range, thereby simulating a polychromatic point source. The system is applied to the construction of low noise holographic optical elements.

Introduction

The processing of optical data by optical means has been pursued by those in the field of optical data processing because of the parallel processing capabilities of optical processors. A well known optical processor is the Fourier transforming system described by a single lens which produces a two dimensional Fourier transform of a two dimensional object illuminated with coherent light. In order to reduce the effect of coherent noise inherent in this Fourier transforming system an achromatic Fourier transforming system was developed by Katyl[1] that permits the Fourier transform to be produced with a polychromatic point source.

The achromatized Fourier transform can be recorded as a Fourier transform hologram by incorporating the transforming process into an achromatized interferometer, produced from diffraction gratings, as described by Collins.[2] A Fourier transform hologram produced under polychromatic illlumination exhibits a large increase in signal-to-noise ratio (SNR) over the coherent case. The SNR improvement is exhibited both in the reconstruction of the Fourier transform hologram and in the autocorrelation function when the hologram is used as a matched spatial filter.

This paper has three objectives. First, we describe the achromatization of the Fourier transforming process in a manner that differs from the treatments by Katyl and by Collins, and offers, we believe, considerable physical insight, using basic concepts of physical optics. Second, when integrated into a grating interferometer, we show that this Fourier transforming system can be used in the construction of low noise holographic lenses (or HOEs). HOEs have found an increasing number of

uses in optics, in the form of gratings, diffraction lenses, etc. The need for low noise HOEs has stimulated research in the area of HOE formation with light of reduced coherence. Finally, we investigate the nature of the noise reduction process.

The Achromatic Fourier Transform

The Fourier transform, a Fraunhofer diffraction pattern of an object S, always occurs in the plane where the source is imaged (Fig. 1). However, the mask S, through which the source is imaged, generates new waves which, when projected back to the source plane, form a virtual object that is wavelength scaled. This distribution is imaged in the process of producing the Fourier transformation. For example, let S be a diffraction grating of spatial frequency f_o . Light impinging on the grating forms various orders, which project back to the source plane as additional object points, separated laterally from the actual source point. These source points have a lateral location proportional to wavelength. In the paraxial approximation the lateral position of these points is $x = F_c \lambda f_o$. Now, the two lenses, L_c the collimator and L_F the Fourier transform lens, together reimage the source plane to the Fourier transform plane. The magnification is $M_1 = F_F/F_c$, the ratio of the Fourier transform lens and the collimator lens focal lengths, since the source is at the front focal plane of L_c and the image forms at the back focal plane of L_F.

To achromatize the process, the magnification M should be inversely proportional to wavelength in order to compensate for the wavelength dependence at the source plane. We let L_F be a zone plate lens, or HOE, as

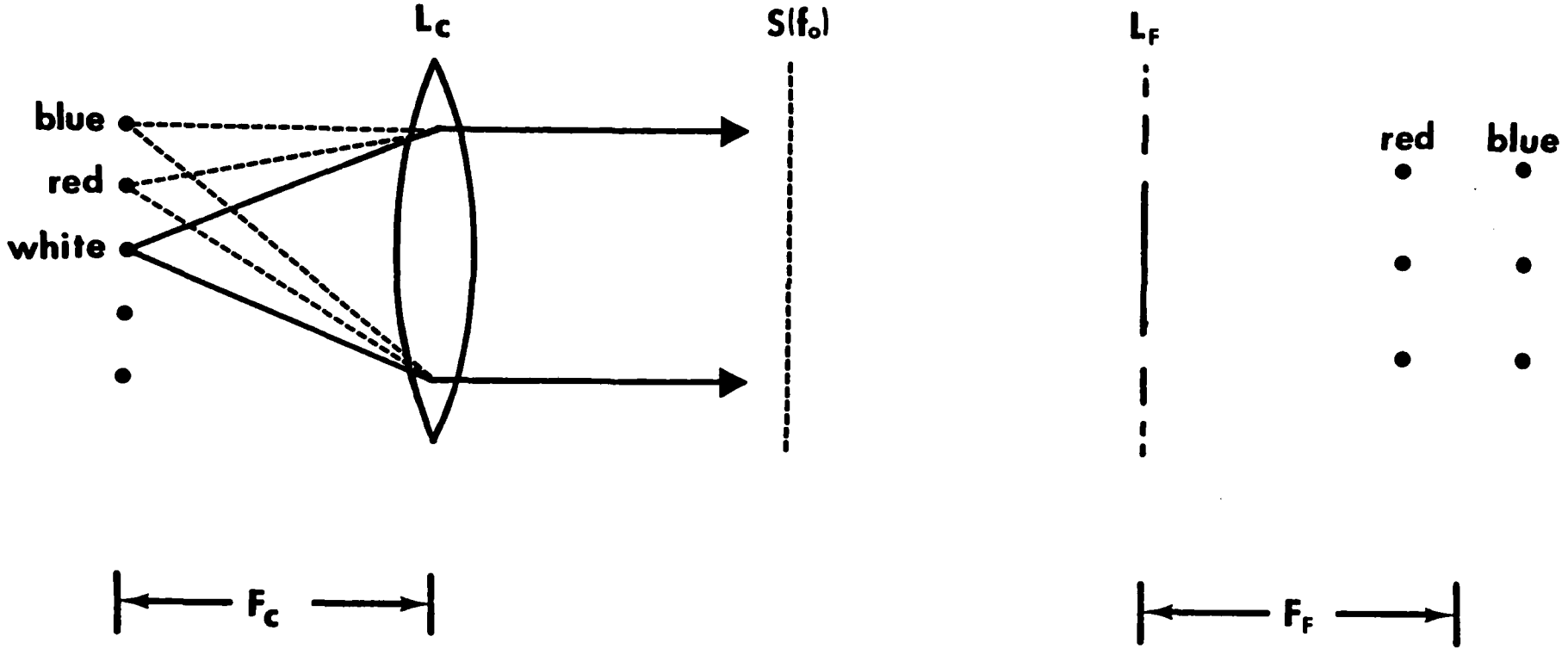

Fig. 1 An optical system which compensates for the wavelength dependence of the scale of the Fourier transformation of a grating, $S(f_o)$, by introducing a zone plate, L_F, as the Fourier transforming element. However, since F_F is a function of wavelength, L_F introduces a longitudinal dispersion.

described by Katyl.[1] The HOE has a focal length inversely proportional to wavelength: $F_F = F_{Fo}(\lambda_o/\lambda)$ where F_{Fo} is the focal length at the wavelength λ_o. The magnification becomes $M_1 = (F_{Fo}/F_c)(\lambda_o/\lambda)$ and the new, wavelength independent, lateral position of the imaged source points is $M_1 \cdot x = F_{Fo}\lambda_o f_o$. The result is a Fourier transform with scale independent of wavelength. Instead there is now a longitudinal dispersion; for shorter wavelengths, the HOE has longer focal length, and the source image is then farther from the HOE than it is for longer wavelengths (Fig. 1).

We require a second lens system that will appropriately shift the image positions as a function of wavelength, while keeping the magnification wavelength independent. We now invoke the concept of the shift lens. We show (Fig. 2) two lenses, L_1 and L_2, separated by the sum of their focal lengths. For all object positions the magnification is just the ratio of the focal lengths, F_2/F_1. Next, consider a third lens, L_s, placed at the common focal plane of L_1 and L_2. This lens will cause the image to shift position, but the magnification is left unaltered. This can be shown readily by simple algebra. Alternatively, we can argue from basic principals. The lens L_s is in fact a spatial filter. The operation it performs is linear and spatially invariant. Therefore, it cannot introduce magnification, since if it did, it would not be invariant. This argument should be quite compelling to those who have familiarity with spatial filters. Those not convinced by this heuristic argument may prefer just to

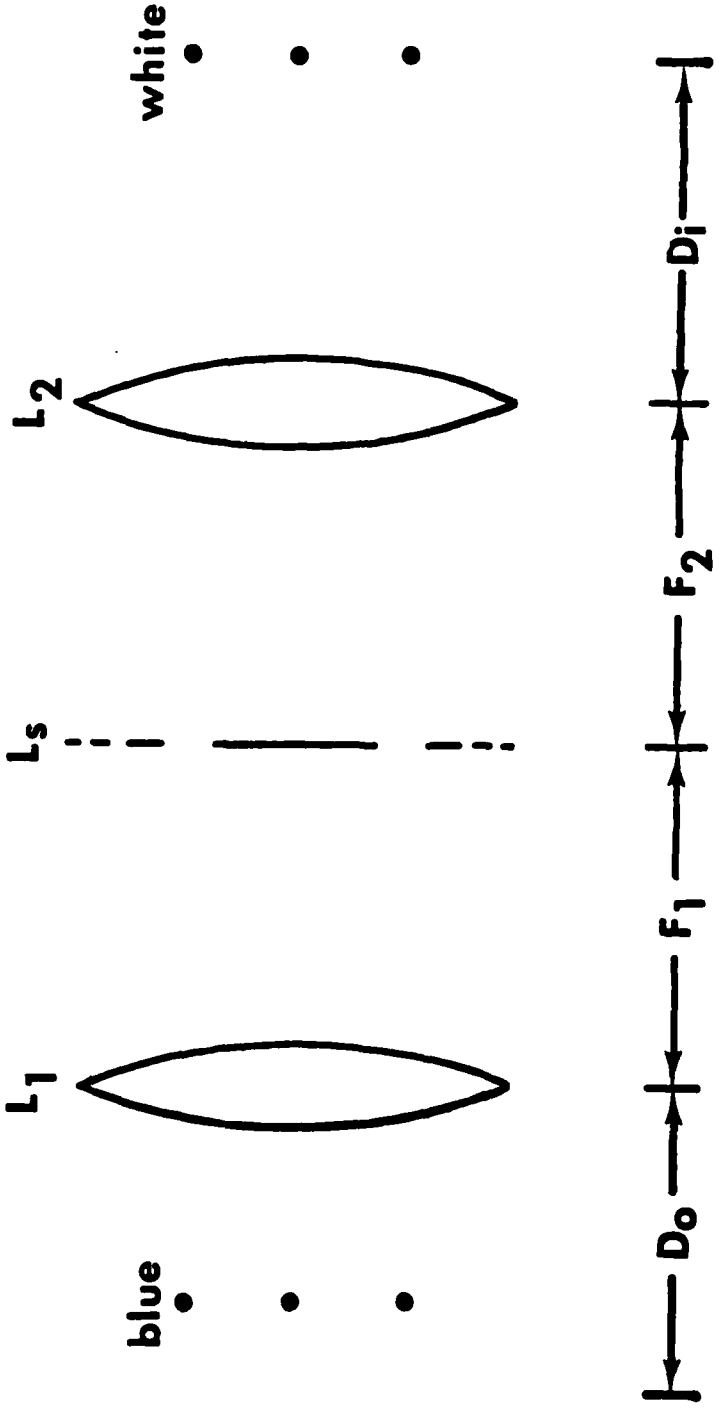

Fig. 2 A spatial filtering system which uses the shift lens concept to compensate for longitudinal dispersion

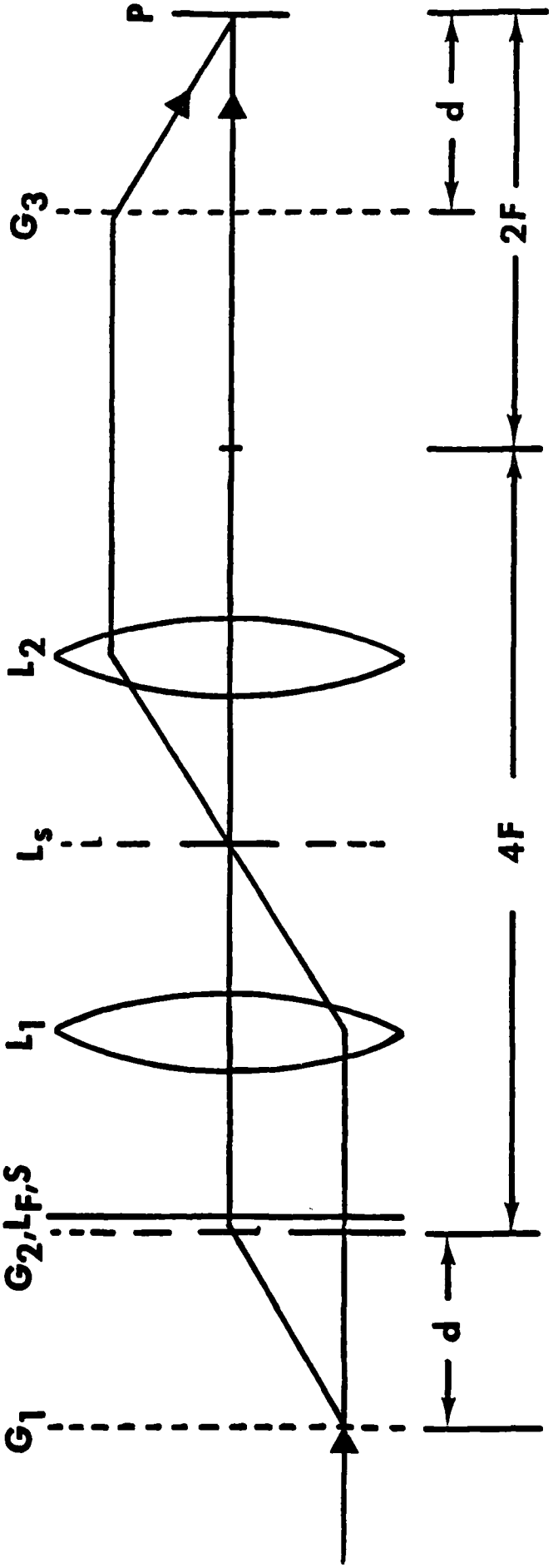

Fig. 3 The final optical system, combining Figs. 1 and 2, as described by Collins[2].

calculate the magnification of this three lens system, which is $M_2 = -F_2/F_1$.

If we use a zone plate lens (HOE) for the shift lens we can produce longitudinal dispersion, which calculations show will be proportional to wavelength. The image distance, D_i in Fig. 2, is given by,

$$D_i = F_2 + F_2^2/F_1 - (F_2/F_1)^2 D_o - (F_2^2/F_{so})(\lambda/\lambda_o) \qquad (1)$$

with $F_s = F_{so}(\lambda_o/\lambda)$ and F_{so} is the focal length at the wavelength λ_o. Alternatively, the already dispersed image (Fig. 1), can be compensated by this second lens system of Fig. 2. The total Fourier transform system is the combination of Fig. 1 and Fig. 2 in tandem, where L_F and L_s are shown as HOEs. The broad spectrum Fourier transform is displayed as the white source image in Fig. 2. The compensation is only approximate and is useful only over a small bandwidth, say about 400 Å, since L_F disperses as $1/\lambda$, whereas the shift lens system, L_1, L_2, and L_s, disperses in proportion to λ.

The final step is to insert these optical systems into a grating interferometer in order to produce a Fourier transform hologram. We must do this without destroying the interferometer's fringe forming capability[3]. This requires that the two branches of the interferometer be well matched; thus, both beams should pass through all of the lenses. The final system, as given by Collins, is shown in Fig. 3. The lens L_F is combined with the grating, G_2, as a single unit. The reference beam is

unaffected by the lenses L_F and L_S (the zero order is used), and the hologram is recorded at plane P. Under these conditions the optical system in Fig. 3 is used to construct Fourier transform holograms (matched spatial filters).

Matched Spatial Filtering

The use of Collins' system for the construction of matched spatial filters is well documented but no comparison was done between a coherently produced matched filter and one made using the achromatic system. The comparison made here uses the same optical system for both the coherent and polychromatic case. Although this comparison is somewhat unfair to the coherent Fourier transform because of the large number of coherent noise producing optical elements involved (more than would be present in a conventional, coherent Fourier transforming system), the comparison is nonetheless useful in demonstrating the coherent noise suppression capabilities of the achromatic system.

Our experimental system is identical to Collins' except that we use a dye laser as a polychromatic point source.[4] The dye laser is scanned through its tuning range of about 400Å at a variable speed so as to compensate for amplitude variations inherent to the spectrum of the dye being used. The use of a dye laser allowed us to view the noise smearing process of polychromatic illumination in real time. When viewed through a microscope one observes the Fourier transform and accompanying fringe pattern, which together form the hologram, to be perfectly motionless as the wavelength is varied. The noise, however, is observed to fluctuate. The hologram is then recorded with the sweep speed sufficiently high so

that all wavelengths get recorded; the sweep time can be set equal to the exposure time, or there can be many sweeps during the exposure time.

The noise fluctuations fall into three catagories. First, there is an effect manifested by light from a strong, isolated scattering center. The resulting Fresnel, or bull's-eye pattern is observed to pulsate, growing in size as the wavelengths are swept in one direction, then contracting as the wavelengths are swept the other way. The entire bullseye pattern is visible because these scatters are located close to the output plane. Second, there is a lateral motion which also originates from such scatterers. These scatterers are located far from the output plane. Thus, only the outer edge of the bull's-eye is seen, which exhibits this lateral translation. A third effect which is observed is that the pattern may not translate at all, but may change in appearance; the individual speckles come and go, an effect often called boiling. All three effects have been observed, sometimes separately, sometimes in combination. In any case the noise is smoothed by the multiplicity of wavelengths. The process of scanning through the wavelength spectrum instead of having all wavelengths present simultaneously gives good physical insight into the noise reduction process.

We recorded the output of the Fourier transforming system as a motion picture. We note that a pair of frames, not necessarily adjacent ones , can be viewed as a stereo pair with interesting effects (Fig. 4). The noise, if it is translating and not boiling too much, will in a stereo viewing system, appear to form in an image plane other than where the fringes and Fourier transform appear. Figure 4 should be observed as a stereo pair. This can readily be done by placing a piece of cardboard normal to the plane of the

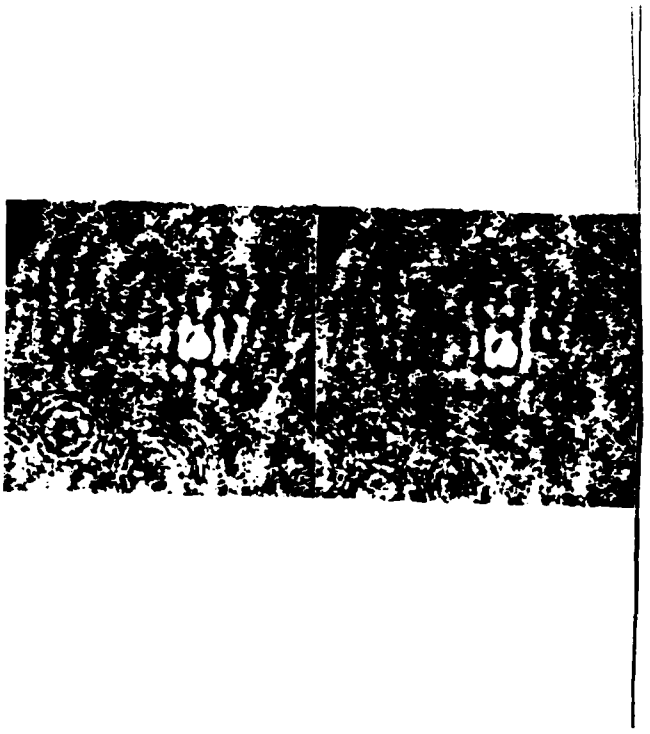

Fig. 4 Stereo pair of pictures, show separation of signal and noise.

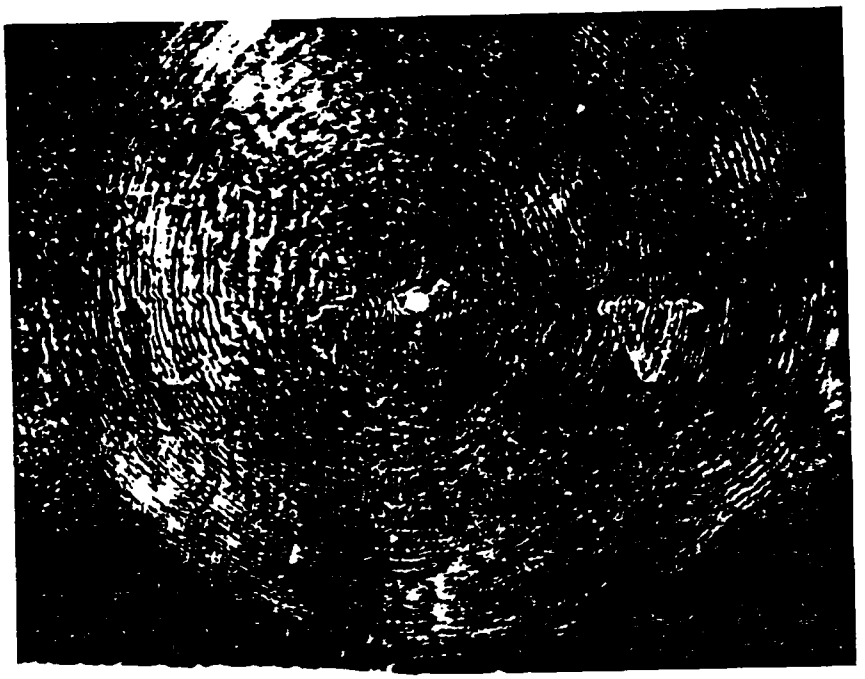

a.

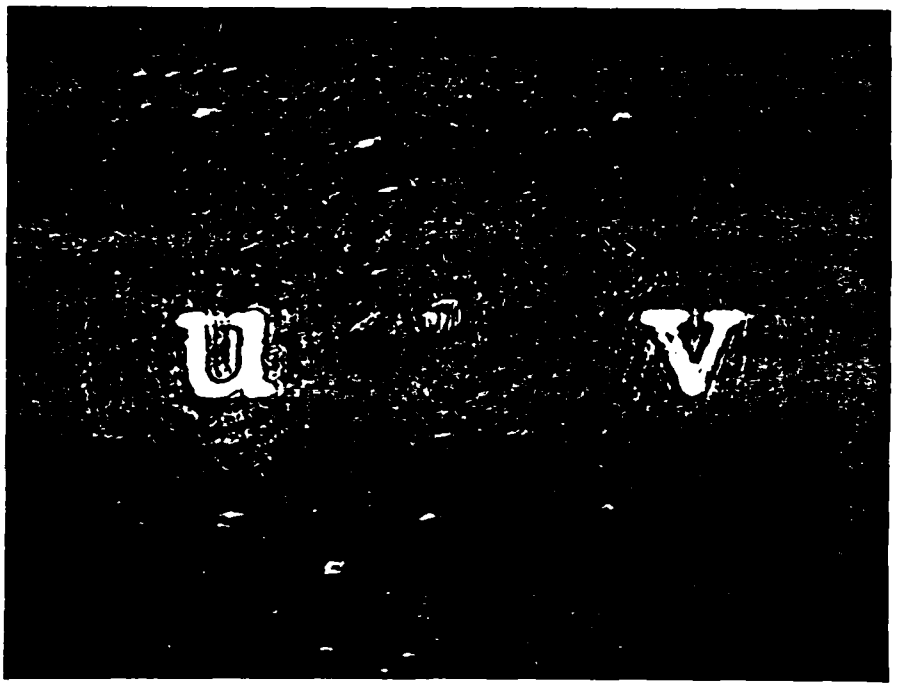

b.

Fig. 5 The reconstruction of a Fourier transform hologram. a. The coherent case. b. The polychromatic-point source case.

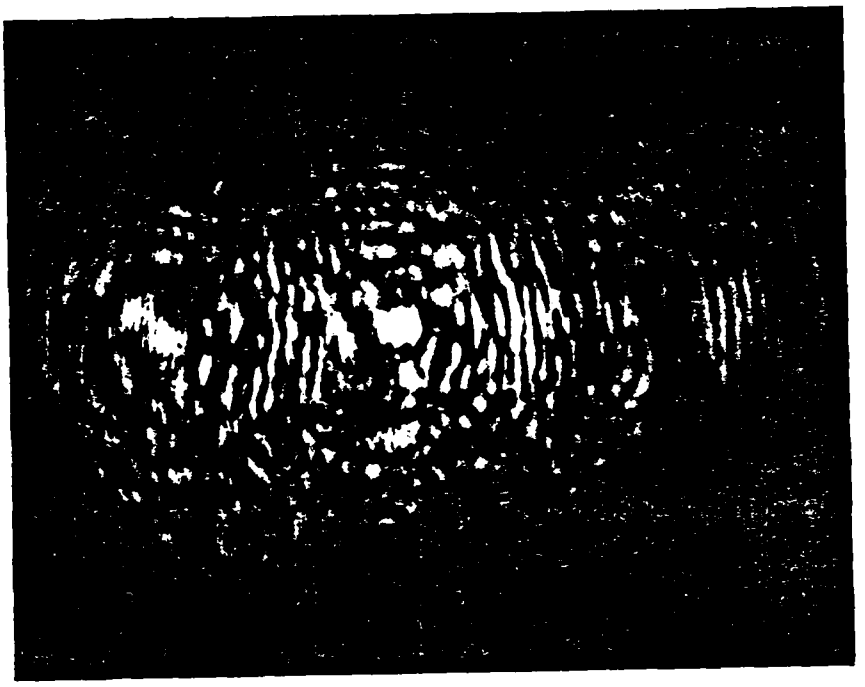

a.

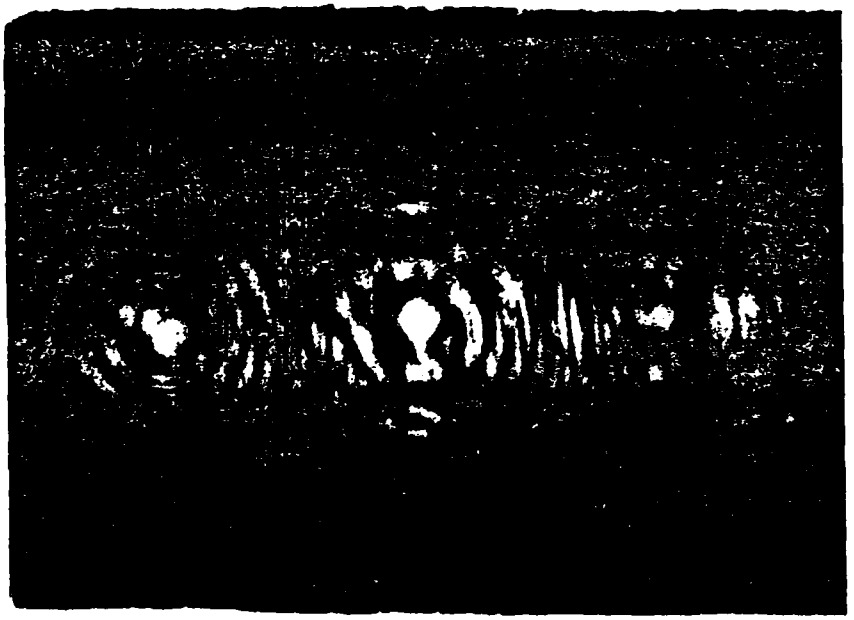

b.

Fig. 6 The autocorrelation function of the letter combination **u v**.
a. The coherent case. b. The polychromatic point source case.

page, extending from the page surface to the nose, oriented such that the left eye sees only the left picture, and the right eye only the right picture. The signal, which includes the bright spot and some lobing structure with the accompanying fringe pattern (possibly the fringe pattern, or spatial carrier, may be too fine to be resolved in the published image), is seen to be raised above the noise background. A pair of bull's-eye patterns, in the lower left, are seen to be somewhat above the signal plane. The two images are from adjacent frames produced by wavelengths separated by about 20 Å. When nonadjacent frames were used, the stereo depth was increased, as expected, but decorrelation of the noise (the boiling effect) resulted in a partial loss of the stereo effect. The overall effect was less impressive.

We made two comparisons of the noise suppression capabilities of this optical system; *reconstruction of the object being* Fourier transformed and the autocorrelation function produced when the Fourier transform hologram is used as a matched spatial filter. The reconstruction, for both the coherent and polychromatic case, is seen in Fig. 5. The noise suppression here is considerable. An unwanted diffracted order from HOE L_3 is coherently recorded in Fig. 5a, whereas in Fig. 5b, the polychromatic case, this unwanted order is almost completely smoothed out, demonstrating the capability of this system to eliminate coherent noise.

The autocorrelation function produced when the Fourier transform hologram is used as a matched spatial filter is seen in Fig. 6. For both cases, Fig. 6a the coherent filter and Fig. 6b the polychromatic, we see the bright central spot due to the autocorrelation of the letter combination **u v**

and also the sidelobes which are the crosscorrelations between these letters. The side-by-side comparison clearly demonstrates the superiority of the achromatic system. The noise level of the achromatically produced one is much less and is less likely to produce confusion in an object recognition scheme.

Construction of HOEs

In order to form a HOE of the off-axis zone plate type (or diffraction lens) we take the Fourier transform of another zone plate structure, or alternatively, the Fourier transform of a spherical wave. We use one diffracted order of the zone plate, which provides a spherical wave. Writing the wave in its paraxial form, we have

$$s = e^{i\pi(x^2+y^2)/\lambda F_I} \qquad (2)$$

where F_I is the focal length of the zone plate or HOE providing the wave. This wave Fourier transforms into another spherical wave u_0, given to within a constant by

$$u_o = e^{i\pi(x^2+y^2)/\lambda F_o} \qquad (3)$$

where F_o and F_I are related by $F_o = -F_F^2/F_I$. F_F is the effective focal length of the lens performing the Fourier transformation, i.e. the focal length of a single lens that would have performed an equivalent Fourier transformation. In terms of the actual lenses in the system, as shown in Fig. 3, we have

$$F_o = F^4/F_s F_I \qquad (F_1 = F_2 = F) \qquad (4)$$

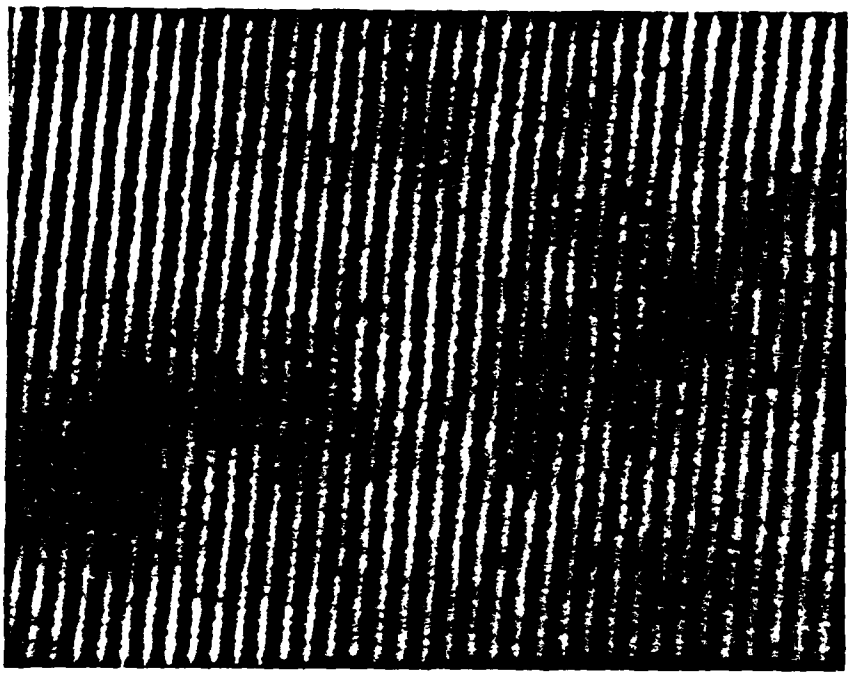

a.

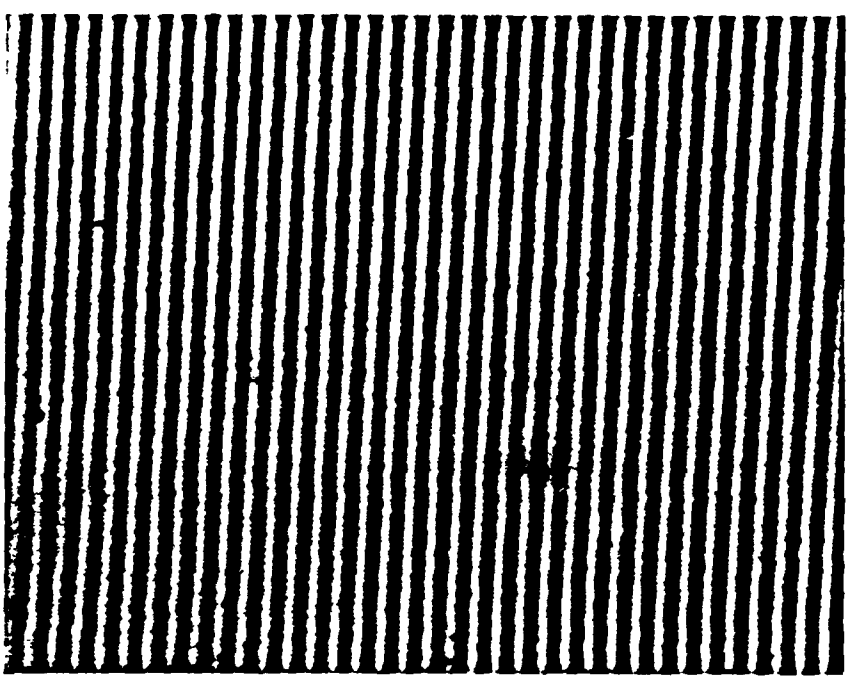

b.

Fig. 7 Off axis zone plates, under high magnification (300 lines/mm), recorded under a. coherent illumination b. polychromatic-point source illumination.

In the system of Collins, the object plane also contains G_2, which is an off-axis zone plate that serves both as the second grating of the interferometer and as the first zone plate lens for the achromatic Fourier transforming system. If we simply make G_2 a zone plate of incorrect focal length, the residual focal power, beyond that required for the achromatization of the Fourier transformation process, constitutes the object to be Fourier transformed. For example, if the required focal length is F_F and the actual focal length F_A, then the wavefront emerging from the zone plate can be written as

$$e^{i\pi(x^2+y^2)/F_A} = e^{i\pi(1/F_F + 1/F_I)(x^2+y^2)/\lambda} \qquad (5)$$

The HOE thus formed achieves noise reduction in two ways: first, the noise due to dust and dirt on the intervening optics is smeared by the wavelength dependence of the diffraction process; second, point defects on the zone plate being Fourier transformed are smoothed by the reciprocal spreading property of the Fourier transformation; that is, a point scatterer, which represents a concentration of noise, is spread by the Fourier transformation process into a low level noise of broad extent. The resulting noise reduction in HOEs thus formed is shown in Fig. 7.

Conclusion

The capabilities for optical processing with polychromatic point source illumination is versatile and can replace coherent optical processing systems in many cases, with an improvement in SNR. The construction of

low noise Fourier transform holograms and HOEs are only two of what we believe are many possibilities for polychromatic optical processing systems to replace coherent systems.

This work was supported by the Air Force Office of Scientific Research (Grant No. AFOSR 81-0243).

References

1. R. H. Katyl, "Compensating Optical Systems, Part 3: Achromatic Fourier Transformation," Appl. Opt. 4 1255-60 (1972).

2. G. D. Collins, "Achromatic Fourier Transform Holography," Appl. Opt. 20 3109-19 (1981).

3. E. N. Leith and G. J. Swanson, "Achromatic Interferometers for White Light Optical Processing and Holography," Appl. Opt. 19 638-44 (1980)

4. Steven Case, Private communication, 1981.

Chapter 10

Generalization of the Holographic Achromatizing Process

Generalization of Achromatized HOE Formation

Katyl first described optical systems consisting of Fresnel zone plates (FZPs) and conventional imaging lenses in tandem for producing achromatized Fourier and Fresnel transformations[1]. Similar systems have been used by George and Morris[2,3] and by Collins[4,5]. We describe a generaliztion of the technique, especially for the achromatization of Fresnel transformations, thus enabling holographic optical elements to be formed in broad spectrum light.

The basic concept is shown in Figs. 1 and 2. Figure 1 shows a conventional FZP. For simplicity we treat the case of the in-line zone plate, since the off-axis zone plate behaves the same way, and the analysis becomes immensely complicated for the off axis case. We consider a plane wave of polychromatic light impinging on the FZP, which is given as $1/2 + 1/2 \cos [\pi(x^2 + Y^2)/\lambda_o F_o]$, where F_o is the focal length for illumination with light of wavelength λ_o. Let the incoherent light be of unity amplitude. The positive-lens portion of the field emerging from the zone plate is $1/4 \exp[-j\pi(x^2 + y^2)/\lambda_o F_o]$. We observe that this expression is independent of wavelength. As the wave travels downstream to its point of focus, the expression becomes wavelength dependent. The focal length, under illumination with light of wavelength λ, is

$$F = \frac{\lambda_o}{\lambda} F_o \tag{1}$$

where, letting $\lambda = \lambda_o + \Delta\lambda$, we have

$$F \quad F_o/(1 + \frac{\Delta\lambda}{\lambda_o}) \equiv F_o(1 - \frac{\Delta\lambda}{\lambda_o}) \tag{2}$$

where the final step involves an approximation, valid for $\Delta\lambda/\lambda_o < 0.1$

We next consider the lens system of Fig. 2, consisting of a broadband point light source, a collimating lens L_1, and three additional lenses L_2, L_3, and L_4, with L_2 and L_4 being FZPs. We

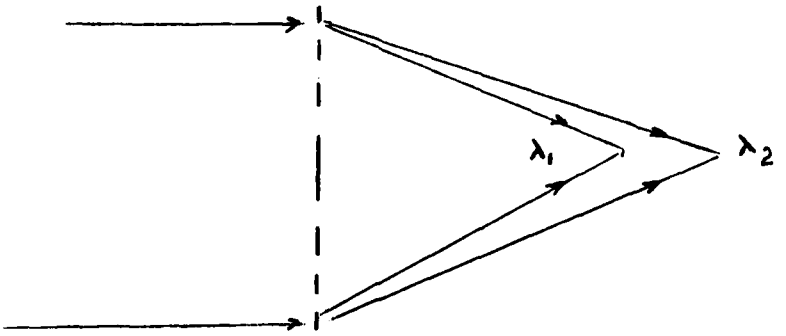

Fig. 1. A Conventional Fresnel Zone Plate, Showing wavelength Variation of Focal Length

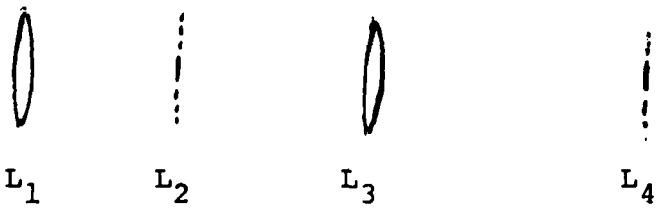

Fig. 2. System for General Analysis

consider this combination, since it has been used previously in achromatized configurations, especially for Fourier transformation. We now generalize the previous results. The generalization procedure suggests that other basic configurations can also produce achoromatization, leading to yet broader generalizations.

The basic idea involved here is to attempt to find a plane where the radius of curvature of the wavefront is inversely proportional to wavelength. At this plane, the phase distribution will be independent of λ, just as in Fig. 1, at the field immediately to the right of the zone plate. If a reference beam, produced achromatically using a grating interferometer, is introduced at this plane, the result is a fringe pattern independent of wavelength.

We note that we could satisfy this condition and yet not be quite achromatic, since the phase distribution could have a constant phase term (constant in x,y) but be wavelength dependent:

$$\mu = \exp - \alpha[\pi(x^2 + Y^2)\lambda_o F_o + \phi(\lambda)] \qquad (3)$$

in which case the achromatization would be incomplete, unless the reference beam had a compensation λ-dependent term $\theta(\lambda)$ such that $\phi(\lambda) - \theta(\lambda)$ were λ independent. This problem is addressed later.

The principal aim is to produce a light distribution that upon recording becomes a HOE. This calls for simply imaging a point polychromatic source, but in a dispersive system such that the image is dispersed longitudinally, in accordance with the requirement given above. We then consider the additional requirement needed in order that a more complex hologram, corresponding to a distributed object rather than a point, can be formed under broad-band illumination.

Analysis

We carry out a simple analysis, using the Newtonian form of the lens equation, $F^2 = d_{ob}\, d_{im}$ where F is the focal length, and d_{ob} and d_{im} are the object and image distributions, measured from the lens focal planes. We assume the source to be at the focal plane of a collimating lens. This puts the signal at ∞ as seen by lens L_2, which is a FZP.

From Fig 2, ant the Newtonian lens formula, we have

$$D_1 = F_{10} + d_{10} = F_{10} \frac{\lambda_o}{\lambda} + d_1 \tag{4}$$

where

$$d_1 = d_{10} + F_{10} (1 - \lambda_o/\lambda)$$

F_1 = focal length of L_1, FZP

F_{10} = focal length of L_1 at $\lambda = \lambda_o$

d_1 = separation between focal plans of lenses L_1 and L_2

$d_{10} = d_1$ at $\lambda = \lambda_o$

Similarly, we have

$$D_2 - F_{30} + d_{20} = F_{30} \frac{\lambda_o}{\lambda} + d_2 \tag{5}$$

where $d_2 = d_{20} + F_{30} (1 - \frac{\lambda_o}{\lambda})$

and $$D_3 = F_{30} + Z_{io} = F_{30} \frac{\lambda_o}{\lambda} + Z_i \tag{6}$$

where $Z_i = Z_{io} + F_{30} (1 - \lambda_o/\lambda)$

For a 3-lens system, we have

$$Z_i = \frac{d_i f_3^2 Z_o - f_1^2 f_3^2}{Z_o(d_1 d_2 - f_2^2) - d_2 f_1^2} \tag{7}$$

If we taken the object (i.e., the source) to be at ∞, Eq. 7 reduces to

$$Z_i = \frac{d_1 f_3^2}{d_1 d_2 - f_2^2} \tag{8}$$

Substituting in the relations given by Eqs. 4-6, we have

$$z_i = \frac{[d_{10} + F_{10}\,(1 - \frac{\lambda_o}{\lambda})]\;F_{30}{}^2(\frac{\lambda_o}{\lambda 1})^2}{[d_{10} + F_{10}\,(1 - \frac{\lambda_o}{\lambda})]\;[d_{20} + F_{30}\,(1 - \frac{\lambda_o}{\lambda}) - F_2{}^2} \tag{9}$$

and

$$D_3 = F_{30}\,\frac{\lambda_o}{\lambda} + z_i \tag{10}$$

Letting $\lambda - \lambda_o = \Delta\lambda$, and using Eq. 9, we have

$$D_3 = F_{30}\;\frac{\lambda_o}{\lambda_o + \Delta\lambda} + (d_{10} + F_{10}\;\frac{\Delta\lambda}{\lambda}\,F_{30}{}^2\,(\frac{\lambda_o}{\lambda_o + \Delta\lambda})^2 \tag{11}$$

After using the relation $1/(1 + \Delta\lambda/\lambda_o) \cong 1 - \Delta\lambda/\lambda_o$ in various places, this can be put into the form

$$D_3 = F_3 + \frac{F_3^2}{d_{20} - F_2{}^2/d_{10}} - \frac{\Delta\lambda}{\lambda_o}\;[F_{30} - \frac{{}^2F_{30}\,d_{10}}{d_{10}\,d_{20} - F_2{}^2} - F_{30}\,\frac{{}^2F_{30}\,d_{10}{}^2 + F_2{}^2\,F_{10}}{(d_{10}\,d_{20} - F_2{}^2)^2}\;(1$$

Finally, we want to put this in the form

$$D_3 = D_3' + (1 - \Delta\lambda/\lambda_o)z_o \tag{13}$$

When this is done, we make the following interesting interpretation. At a distance D_3' from the final lens, the distance to the plane of focus has a variation $(1 - \Delta\lambda/\lambda_o)\;z_o$. This is precisely the condition specified by Eq. 2; a wave having such a distribution has a phase independent of wavelength. At this plane, the wavefront is achromatic, and interference with a reference beam will form a FZP in polycromatic light, to within the approximations made in the derivation.

To put Eq. 12 into this desired form, we write

$$D_3 = F_{30} + \frac{F_{30}{}^2}{d_{20} - F_0{}^2/d_{10}} - z_o + z_o - z_o\,\frac{\Delta\lambda}{\lambda_o} \tag{14}$$

Where z_o is the coefficient of $-\Delta\lambda/\lambda_o$ in Eq. 12, i.e., z_o is the radius of curvature of the wave at $\lambda = \lambda_o$.

$$D_3 = \frac{F_{30}^{\ 2}\, d_o}{F_2^{\ 2}\, d_{10}\, d_{20}} - F_{30}^{\ 3}\left(\frac{F_{30}\, d_{10}^{\ 2} + F_2^{\ 2}\, F_{10}}{F_2^{\ 2} - d_{10}\, d_{20}}\right) + Z_o\left(1 - \frac{\Delta\lambda}{\lambda_o}\right) \qquad (15)$$

Equation 15 indicates that at a position D_3', given by the first 2 terms of the right hand side of Eq. 15, the field is achromatized, and interference at that plane between the spherical wave and a plane wave yields a FZP whose focal length is z_o at $\lambda = \lambda_o$.

From the Equation

$$z_o = \frac{F_{30} - 2\, F_{30}^{\ 2}\, d_{10}}{d_{10}\, d_{20} - F_2^{\ 2}} - F_{30}^{\ 2}\,\frac{(F_{30}\, d_{10}^{\ 2} + F_2^{\ 2}\, F_{10})}{(d_{10}\, d_{30} - F_2^{\ 2})} \qquad (16)$$

it is apparent that a wide range of design possibilities exist. We have a wide range of possible selections for the three lenses, L_2, L_3 and L_4, and the separations d_{10} and d_{20} can be chosen arbitrarlily. It would appear that any desired focal length is attainable.

Chapter 11

Optical Processing in Incoherent Light

Optical processing techniques in incoherent light

E. N. Leith and G. J. Swanson

The University of Michigan
Ann Arbor, Michigan 48109

Abstract

Diffraction Gratings permit many and diverse optical processing techniques to be carried out with light of greatly reduced coherence, either spatial or temporal. Several such techniques are described, including phase-amplitude imaging, fringe projection and tomography.

Introduction

Interferometers formed with diffraction gratings have many interesting properties and uses, all based on their capability for forming fringes in incoherent light, either from an extended monochromatic source, a polychromatic source, or an extended polychromatic source. We have shown this capability for the formation of holograms, for carrying out optical processing such as image deblurring or spatial matched filtering, for recording phase-amplitude object distributions with extremely good SNR, for making high quality holographic optical elements, for projection of high quality fringes, and for tomography. We describe some of the capabilities.

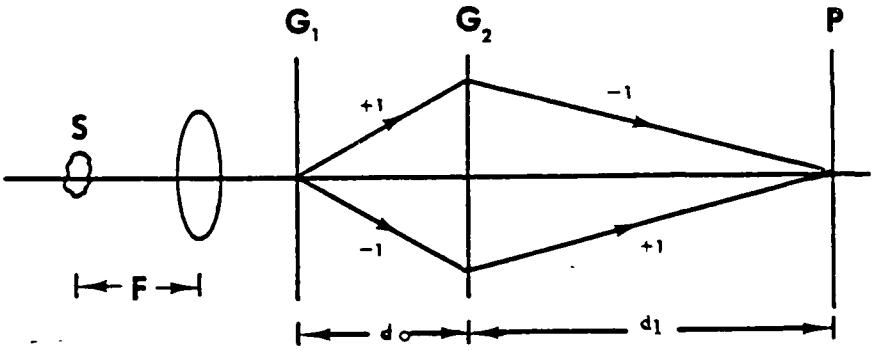

Figure 1

In 1959 Weinberg and Wood described an interferometer formed from two gratings in tandem (Fig. 1). Light falling on G_1 is diffracted into various orders, two of which are selected and propagate to the second grating, G_2. For each of the two beams impinging upon G_2, one diffracted order of G_2 is selected in such a way that the two emerging beams are brought back together. For proper adjustment, fringes are formed in the overlap area, and the fringes can be formed in light from an extended, white light source. As is illustrated in Fig. 1, one beam is produced by the +1 order of G_1 and the -1 order of G_2, with the other beam produced by the -1 order of G_1 and the +1 order of G_2. Numerous other combinations are possible. In any case, the Weinberg-Wood grating interferometer is much like a Mach-Zehnder interferometer, with gratings used in place of the mirrors and beam splitters.

Our method for analyzing the interferometer has been described previously[1]. An element of the source, taken to be at infinity, sends a plane wave $e^{i2\pi f_0 x}$ to the grating G_1, where $f_0 = \sin\vartheta_0/\lambda = \vartheta_0/\lambda$. We neglect the other lateral dimension y, and we ignore constant multiplication factors, thereby simplifying the analysis without losing anything essential. Letting G_1 have transmittance $\frac{1}{2} + \frac{1}{2}\cos 2\pi f_1 x$, we find the field emerging from the grating to be $\exp[i2\pi(f_0 + nf_1)]x$, where n=0, 1, or -1, depending on which diffracted order we choose. This field then propagates to the second grating, and in the process is multiplied by the transfer function of free space, $\exp(-i\pi\lambda z f_x^2)$, where z is the propagation distance and $f_x = (f_0 + nf_1)$. This process is repeated for every grating and for every distance d between the gratings. The field at the output plane is, for a two-grating structure,

AD-A160 311 WHITE LIGHT OPTICAL INFORMATION PROCESSING(U) MICHIGAN 2/2
UNIV ANN ARBOR DEPT OF ELECTRICAL AND COMPUTER
ENGINEERING E N LEITH 31 MAY 85 AFOSR-TR-85-0853
UNCLASSIFIED AFOSR-81-0243 F/G 20/6 NL

END
FILMED
DTIC

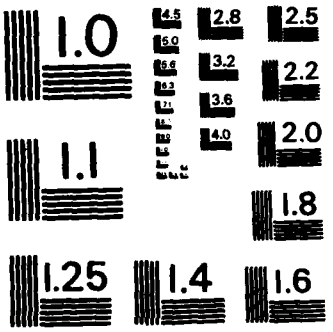

MICROCOPY RESOLUTION TEST CHART
NATIONAL BUREAU OF STANDARDS - 1963 - A

$$u=\exp i\,2\pi(f_o+nf_1+mf_2)x-\pi x\left[d_o(f_o+nf_1)^2+d_1(f_o+nf_1+mf_2)^2\right] \tag{1}$$

where f_2 is the spatial frequency of the second grating, and again, m = 0, 1, or -1. If we have a second beam passing through the interferometer, the field at the output can be written as u', of the same form as Eq. 1, except that we use n' and m'. The two beams combine to give the irradiance distribution

$$\begin{aligned} I=2+2\cos\{&2\pi\left[(n-n')f_1+(m-m')f_2\right]x-2\pi\lambda\left[(n-n')d_of_1+(n-n')d_1f_1+(m-m')d_1f_2\right]f_o\\ &-\pi\lambda\left[(n^2-n'^2)d_of_1^2+(f_1n+f_2m)^2-(f_1n'+f_2m')^2d_1\right]\} \end{aligned} \tag{2}$$

For example, for the interferometer of Fig. 1, we have n = 1, m = -1, n' = -1, and m' = 1, with an output irradiance

$$I=2+2\cos\left[4\pi(f_1-f_2)x-4\pi\lambda d_of_of_1-4\pi\lambda d_1f_o(f_1-f_2)\right] \tag{3}$$

An interferometer formed with a pair of gratings will produce fringes in light from an extended source if the phase term is made independent of f_o, that is, if each element of the source produces fringes in registry with those from the other elements. This condition is readily found by setting the coefficient of f_o to zero, yielding

$$d_1=-d_o/\left[1+\left[\frac{f_2}{f_1}\right]\left[\frac{m-m'}{n'-n'}\right]\right] \tag{4}$$

This equation shows that the fringes are localized under broad source illumination, that is, the fringes form only at a single plane, not over a range of d_1 values. These fringes can be considered to be an image of the first grating, and the second grating is akin to a lens, imaging the first grating, a view that is stressed by rewriting Eq. 2 as

$$\frac{1}{d_o}+\frac{1}{d_1}=\frac{1}{F_g} \tag{5}$$

where F_g, the focal length of the grating is

$$F_g=-d_o\left[\frac{f_1}{f_2}\right]\left[\frac{n-n'}{m-m'}\right] \tag{6}$$

This focal length varies with grating separation and also with the spatial frequency f_1 of the grating being imaged, so it is indeed a rather special kind of imaging process. Further, the image is not formed in a geometrical sense, where all rays from an object point are brought together again at the image. Indeed, only rays produced by one element of the source are recombined; sets of rays emanating from the same object point, but emanating from different elements of the source are in general not recombined at all.

Imaging processes can be achromatized, and such is the case here. For fringes to occur in broad spectrum illumination, we require the fringes to be λ-independent. We note that the fringe spacing is already λ-independent, which is not the usual case for interferometers. We also require that the fringes be in registry for all wavelengths; this requires that the constant-phase terms, the x-independent terms of Eq. 2, be λ-independent. For a point source on axis, the f_o-dependent term phase term is zero, and the remainder of the phase term becomes zero if

$$d_1=-d_0/\left[1+\frac{(m^2-m'^2)}{(n^2-n'^2)}\left[\frac{f_w}{f_1}\right]^2+2\frac{(nm-n'm')}{(n^2-n'^2)}\left[\frac{f_2}{f_1}\right]\right] \tag{7}$$

For the achromatization to occur at the image plane, that is, for simultaneous broad source and broad spectrum fringes, we require the entire λ-dependent term to be zero for all f_o. This is done by simultaneously imposing the conditions of Eq. 4 and Eq. 7, which is readily found to be Eq. 4 along with either the condition $n=n'$ or $m=m'$.

We also note that the usual expression for magnification applies, taking the form

$$M=\frac{(m-m')f_1}{(n-n')f_1+(m-m')f_2}=\frac{d_1}{d_0} \tag{8}$$

Some caution is required in applying this expression. For example, for $f_2=2f_1$ and $d_0=d_1$ in the symmetrical configuration of Fig. 1, we have M = 1, which seems to suggest that the fringes formed will be out of spatial frequency f_1, whereas they in fact are of spatial frequency $2f_1$, as can be seen from Eqs. 2 or 3. The explanation is that the imaging process is akin to a coherent imaging process, i.e., is linear in field rather than intensity. That this is so evident from the consideration that

the fringes are the same as would be formed under coherent illumination. And with coherent illumination, we have the terms $e^{i2\pi f_1 x}$ and $e^{-2\pi f_1 x}$ being propagated to the output plane and combining to form the pattern $u=\cos 2\pi f_1 x$, or $I=|u|^2=\frac{1}{2}+\frac{1}{2}\cos 4\pi f_1 x$. This same pattern is also the object distribution being imaged. Thus, the magnification is indeed 1:1. Therefore, in considering the magnification, one must consider not merely the fringe spatial frequency, but what Fourier component or components of the object are being imaged.

As an imaging device, the grating has a number of significant characteristics relative to a lens. First the phases of the Fourier components are in general altered, so that for a multiple-Fourier-component object, the image does not resemble the object. Second, different Fourier components are imaged to different planes. For most object distributions, these effects are disasterous. For some object distributions, all of the periodic type, these characteristics may not matter. For example, to image a simple, sinusoidal fringe pattern, the grating is quite satisfactory.

This imaging process can be described in part by the consideration that the imaging process is narrow-band, with the MTF consisting of a few discrete lines, or δ-functions.

Also, the grating imaging process is space invariant, that is, rays from one part of the object undergo exactly the same alteration as rays from any other part of the object. This effect sharply distinguishes the grating from a lens and leads to some interesting conclusions. First, the off-axis Seidel aberrations of a lens, such as coma, astigmatism, and distortion, which are tied to the space-variant characteristic of a lens, could in some circumstances be inherently absent from the grating imaging process. Second, one ought to be able to realize extremely low F-number values for an imaging grating, since the grating can be arbitrarily large compared to the focal length, and the larger aperture should not increase either the required tolerance or the aberrations.

Fringe Projection

We consider the problem of projection of fringes onto a three-dimensional object, a requirement arising in such applications as metrology and robotic vision. Suppose the number of fringes to be large, say, several thousand. The fringes are to be high in contrast and as noise-free as possible. Of the many ways to accomplish this, we consider two for comparison. In each case we start with a grating G_1, which is to be imaged onto the object. Let the aperture of G_1 be L, and the spatial frequency be f_1. For simplicity, suppose the grating to be sinusoidal, i.e., rulings of the form $\frac{1}{2}+\frac{1}{2}\cos 2\pi f_1 x$ *with* $I=\frac{3}{4}+\frac{1}{2}\cos \pi f_1 x+\frac{1}{4}\cos 4\pi f_2 x$. Consider first a magnification of unity, then consider fringe enlargement. Figure 2 shows the configurations (a) with a lens, and (b), with a second grating G_2 in place of the lens. For perfectly coherent illumination, the fringes will in each case have perfect contrast provided the aperture is sufficiently great to collect both the -1 and $+1$ orders, and fringe depth will be considerable, i.e., the fringes will not be localized, but will form wherever the beams overlap.

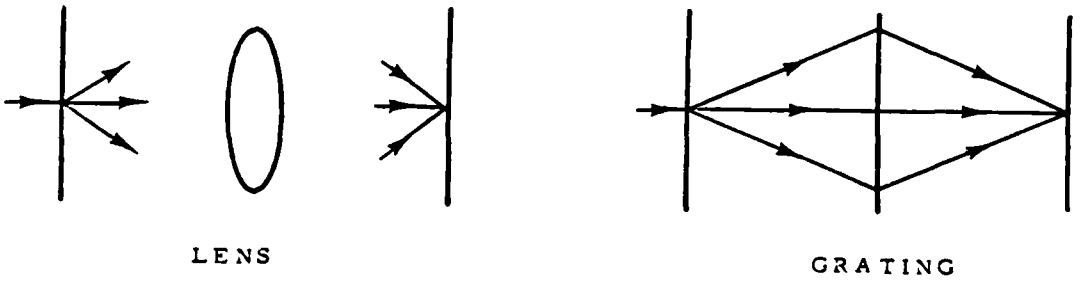

Figure 2

Under broad source illumination, the fringes formed by the grating device, are, using the analysis that led to Eqs. 1 and 2, readily found to be

$$I=\frac{3}{4}+\frac{1}{2}\cos 2\pi\lambda d_0 f_1^2\cos 2\pi f_1 x+\frac{1}{4}\cos 4\pi f_1 x \tag{9}$$

and if we take $d_0=1/\lambda f_1^2$, the fringes become just the original object distribution.

In order that the grating G_2 produce just the three beams that are required, we suppose the grating to be thick enough so that strong Bragg effects are produced, and to be constructed so that both the -1 and $+1$ orders of G_1 impinge on G_2 so as to satisfy the Bragg condition, giving 100 percent diffraction efficiency, and that the 0 order of G_1 not satisfy the Bragg condition, so that no diffraction occurs. Under this circumstance, the light incident on G_2 will form only 3 beams, and no light will be lost into unused beams. Alternatively, the 0 order of G_1 could be blocked, so that only two beams form the fringe pattern. The auxilliary condition $z_0=1/\lambda f_1^2$ is no longer required, giving more flexibility in fringe formation.

If we desire to magnify the fringes, this possibility is available, but the magnification is achieved only by choosing a different grating rather than by adjustment of the object, - image distance, as with a lens. Examination of Eq. 9 shows that for unity magnification, we require $f_2=2f_1$. For large magnification, we require $f_2=f_1+\varepsilon$, where ε is a small number. When $\varepsilon = 0$, the magnification is infinite. We would like to magnify the fringes while retaining at the image of all the fringes on G_1. Therefore, the beam must enlarge in proportion to the fringe spacing. The grating G_2 does not do this, instead, we must form the fringes with diverging rather than collimated beams, in such a way that the ratio of beam widths at the output plane to those at G_1 is just the fringe magnification M. As shown in Fig. 3 the required beam magnification occurs when G_1 is illuminated with a converging beam with center of curvature at G_2. Under this condition, the number of fringes is preserved, except for the factor 2 increase explained earlier.

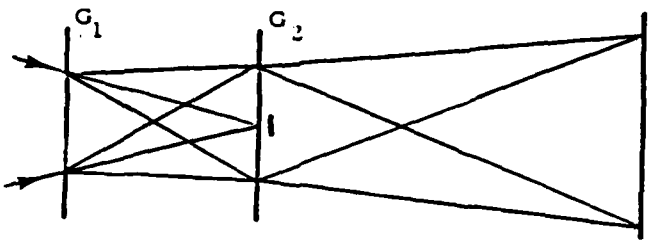

Figure 3

Suppose the beam diverges more, so that the beam magnification is greater than the fringe magnification. Will there be *more fringes* than exist at G_1? Since fringes form wherever the beams overlap, there must indeed be more. From the imaging viewpoint, this seems enigmatic, since we seem to have created some additional fringes beyond those supplied by the object.

To make the beam diverge more, the focal point is brought back to a position between G_1 and G_2. The beam is then somewhat expanded when it intercepts G_2. A rather straight-forward geometrical analysis shows that the number of fringes at the output is just the number of rulings on G_1 plus the number of rulings intercepted Thus, the total number of fringes at the output is just the number each beam intercepts alongs its travels, and we thus have a conservation of fringes.

The grating imaging process has aberrations, the analysis of which are beyond the scope of our treatment here. Some interesting observations can be made. For unity magnification, (e.g., for $d_1=d_0$ and $f_2=2f_{12}$), the process is aberration-free. Aberrations arise when we depart from this symmetrical situation. The aberrations are manifested as a loss of fringe contrast under broad source illumination. The aberrations are space invariant, in that the loss of contrast is the same over the entire field, and the fringe spacing remains uniform over the field, to within the approximation of our analysis.

Grating and Lens Systems in Combination

Some intersting possibilities arise when the grating interferometers are combined with lens systems. For example, it has been found possible to make Fresnel or Fourier transform holograms in light of enormously reduced coherence[3,4]. A particularly simple but effective arrangement is to combine the grating interferometer with an imaging system. Such an arrangement is shown in Fig. 4, using three gratings, all of equal spatial frequency. In this way, the imaging can be done without diffraction occuring between object and image, such diffraction deviation of the object light would introduce aberrations into the image. With a system like this, an image plane hologram of a transparency having both amplitude and phase can be made and the phase perfectly preserved[5]. A powerful advantage of this method is that the lens system does not image the grating at the output plane, a process that would unavoidably incorporate any noise on the grating onto the output image.

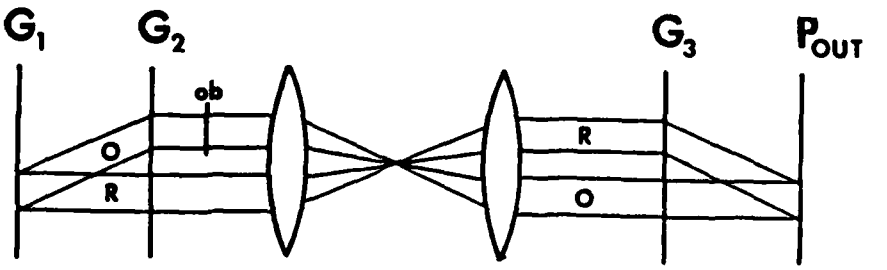

Figure 4

One obvious application is to use a lens for the phase object, and the resulting image plane hologram would be a holographic lens. Again, this method suffers from the problem noted above; any noise on the lens element would be incorporated onto the hologram. A far more satisfactory way has been described. This is to place a lens in one beam while placing a two lens system, in telescopic configuration, in the other beam. Each system images the same plane onto the output. The former system images with a spherical curvature (in the paraxial approximation, the familiar quadratic phase term noted, for example, by Goodman[7]), whereas the latter does not. Thus, the interference is between a plane wave and a spherical wave, and a holographic lens is thus produced. Since the process is carried out with light of greatly reduced spatial coherence and the image formed at the output is just the image of an empty aperture, the interference pattern is essentially noise-free.

Application to Tomography

The grating imaging concept has potential application to tomography. The suggested approach is shown in Figure 5. We suppose the volume V to consist of absorbing or scattering material, of rather weak form, that is, the amplitude transmittance T_a at any small region in the volume is nearly unity. The transmittance $T_a(x,y,z_1)$ at any plane $z = z_1$ can be represented by a Fourier decomposition, which can be approximated by a Fourier series. For simplicity of analysis, we drop as usual the y dimension. The transmittance at $z = z_1$ can then be written

$$T_a(x,z_1)=\sum_{n=0}^{N} a_n \cos(2\pi n f_g x+\varphi_n) \tag{10}$$

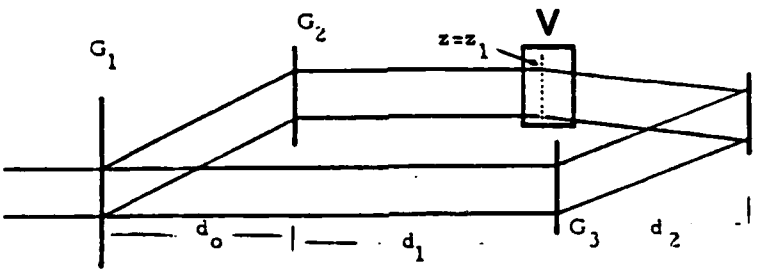

Figure 5

We consider one representative spatial frequency component, $a_n \cos(2\pi n f_g x+\varphi_n)$, and for our analysis, think of it as a grating, which results in fringes being formed in broad-source illumination when the light passing through the object combines with the other beam. The resulting fringe pattern is, using the method of Eq. 1, readily found to be

$$a_n\left[1+\cos\left[2\pi(f_n-f_1)x+\pi\lambda(f_n-f_1)zf_n+\varphi_n\right)\right] \tag{11}$$

with the fringes forming at a plane

$$d_2=\frac{d_0 f_1-zf_n}{f_1+f_n} \tag{12}$$

For a 3-D object, each plane of the object will contribute one Fourier component to this detection plane, in accordance with Eq. 12. The reconstruction of the object distribution from these fringes is thus a two-fold task. First, the fringes have to be detected. This is done by scanning the interference pattern in each of N different planes. The fringes are of low contrast, but because of the incoherence of the illumination, the SNR is quite high. Thus, the detection is done with a low-noise detector. The data gathered is then digitized and processed by computer, which has the task of Fourier analyzing the data and reassembling the Fourier components in the proper way, that is, with the proper phase φ_n, and with all the Fourier components belonging to the object slice at z_n, (which are distributed one at each data plane) being gathered and then added. In this manner, the image is computer-constructed plane by plane.

The optimum spacing between the sample planes at the output will depend on the size of the source. The source size determines the degree of fringe localization, and therefore, the separation between planes that carry different fringe patterns. If the sample spacing is too small, the same Fourier components will be measured at adjacent planes. If the sample spacing is too large, data will be missing. It would appear, then, that resolution in depth depends on the source coherence; the more incoherent the source, the better will be the resolution in depth. On the other hand, the less coherent the source, the fewer will be the number of Fourier components that materialize at a given output plane, and the greater will be the number that do not. The latter will contribute to a bias background thus producing lower signal contrast.

Equation 11 shows the fringe formation process to be wavelength dependent, so monochromatic radiation should be used. On the other hand, for the case $f_n = f_1$, the λ-dependence disappears. Therefore, there is the possibility of

achromatizing the data gathering process by continually changing one of the gratings, so that each Fourier component in turn becomes achromatized. The set of Fourier components throughout the entire project plane that are thus simultaneously achromatized are not the ones that appear in a given output plane, since the achromatized ones are $f_n = f_1$, the same for each object plane, whereas the ones that form at a given plane, as given by Eq. 12, are different for each plane. Thus, only one Fourier component at a time can be detected, rather than a set, and to obtain all the Fourier components, a scan must be made through N different output planes for each selected value f_1.

This method of tomography appears to have many interesting extensions, and will be explored further.

This work was sponsored by the Air Force Office of Scientific Research (grant AFOSR 81-0243) and by the National Science Foundation (grant ECE-790-1C47).

References

1. F. O. Weinberg and N. B. Wood, "Interferometer Based on Four Diffraction Gratings," J. Sci. Instrum. *36*, 227-230 (1959).
2. E. N. Leith and G. J. Swanson, "Achromatic Interferometers for White Light Optical Processing", Appl. Opt. *19*, 638-644 (1980).
3. G. J. Swanson, "Recording of One-Dimensionally Dispersed Holograms in White Light," appl. Opt. 20, 4267-4270 (1981).
4. G. D. Collins, "Achromatic Fourier Transform Holography," Appl. Opt. *20*, 3109-3119 (1981).
5. E. N. Leith and G. J. Swanson, "Recording of Phase-Amplitude Images," Appl. Opt. 20, 3081-3084 (1981).
6. G. J. Swanson, "Recording of Holographic Optical Elements in Spatially Incoherent Light," Opt. Lett *8*, xx-xx (1983).
7. J. W. Goodman, *Introduction to Fourier Optics*, McGraw-Hill, New York, 1967.

Chapter 12

Construction of Diffraction Lenses in Non-Coherent Light

Construction of Diffractive Optical Elements in Non-Coherent Light

E. N. Leith, G. Swanson and S. Leon

The University of Michigan
Ann Arbor, Michigan 48109

Methods are described for producing optical elements, such as grating and lenses, in light of reduced temporal or spatial coherence. The preferred interferometer for producing fringes in light of low coherence is one formed from diffraction gratings. Consi able more noise reduction is achieved.

Introduction

Optical elements are increasingly being made by interferometric means. The optical elements we describe here fall into two classes, diffraction gratings and lenses. Diffraction gratings made by optical interference methods are now offered as commercial products and the market share of this kind of diffraction grating is growing. Lenses made by interferometric means are also assuming increasing importance. Such elements are generally known as HOEs (Holographic Optical Elements). The grating type are produced from uniformly spaced fringes, the lenses from fringes of variable spacing.

It has often been believed that such optical elements could be created only with highly coherent light, since light of lesser coherence was incapable of producing the required number of fringes. Not only is this viewpoint in error, but there is in fact an advantage to making them in light of lesser coherence - a better signal-to-noise ratio (SNR).

Highly coherent light is capable of producing, with ease, many thousands of very fine high contrast fringes. But light of low coherence can produce just as many fringes, equally fine, and of very high contrast, and the fringes can be in fact better from an SNR viewpoint.

There is an adage well-known to those who work with coherent optics: don't let the light be more coherent than your purpose requires. The greater the coherence, the more susceptible the optical system becomes to noise, by which we mean spatial noise, which manifests itself as speckles, bullseye patterns (resulting from Fresnel diffraction by scattering centers such as dust particles, bubbles, etc. in the system), a general smudginess, or a jaggedness or waviness of the fringes. This noise is unavoidable in a coherent optical system, since one can never have an optical system that is perfectly free from such defects.

We are interested in optical systems that produce the fringes without producing the noise. This means reducing the coherence, but without affecting the ability for fringe formation. There are interferometers that can accomplish these objectives quite well indeed.

Spatial and temporal coherence

Coherence is of two kinds, spatial and temporal. Spatial coherence is achieved by means of a small source. Thus, point sources yield spatially coherent light, whereas extended sources yield spatially incoherent light. Temporal coherence is achieved by means of a monochromatic source, hence the term monochromaticity and temporal coherence are often used synonamously. Temporal coherence is achieved by means of a monochromatic source, whereas temporal incoherence is achieved by means of a polychromatic source. Completely coherent light has both spatial and temporal coherence. For the best noise reduction, light should be incoherent both ways.

Uniform fringes, used in grating formation, can be produced by light that is either spatially or temporally incoherent, and even with light that is completely incoherent. Nonuniform fringes, required for the production of other kinds of diffracted optical elements, generally requires one type of coherence but not the other kind.

Intense light having both temporal and spatial coherence became available only with the laser. But the laser has also made available, for the first time, intense light that is spatially incoherent, but temporally coherent, as well as light that is spatially coherent, but temporally incoherent. These two additional kinds of light should not be regarded as merely semidegenerate cases of the completely coherent case, but as light types that have their own unique characteristics. The former type is easily produced by passing a laser beam through a coherence spoiler, such as rotating ground glass; the latter type is

produced by sweeping a dye laser through its tuning range.

Interferometers for incoherent fringe formation

In general, interferometers can be adjusted so as to form fringes in broad source illumination. In the days before the laser, this was the typical way of operating an interferometer. Figure 1 shows a Mach Zehnder interferometer, which splits a light beam into two parts and recombines them downstream. Broad source operation is achieved when rays originating from the same point in the beam that enters the interferometer are recombined at the output. Bennett[1] showed in 1951 that the number of fringes that are achievable is related to the source size by

$$N = 1/2(\Delta\theta)^2 \qquad (1)$$

where $\Delta\theta$ is the source subtense at the collimator; this is the measure of source size. This equation shows that the source can be as great as a few degrees and still produce thousands of fringes, which is far more than enough fringes for most applications, but is often very insufficient for the construction of optical elements; for example, a grating or a diffraction lens might require 100,000 or more high contrast fringes.

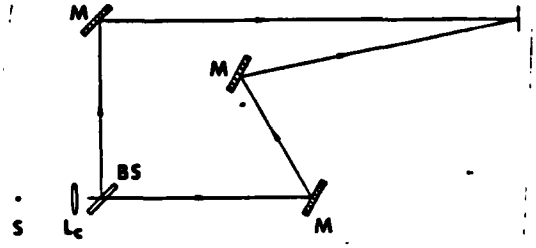

Figure 1. Mach Zehnder interferometer with broad source illumination. S is source

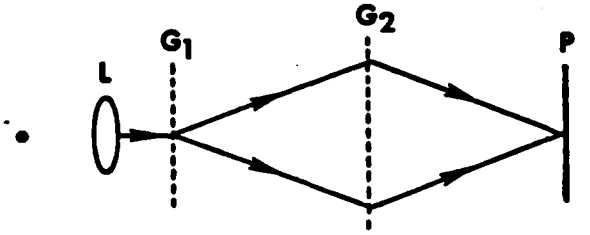

Figure 2. Grating interferometer. S, source; L, lens; G_1,G_2, gratings; P, output plane.

In pre-laser days Eq. (1) was not a practical limitation, since the chromatic limitations were much worse. A typical pre-laser monochromatic source, such as the low pressure 100 watt mercury arc source has sufficient temporal coherence to produce only about a thousand fringes.

More suitable for the generation of the enlarged number of fringes is an interferometer formed from diffraction gratings; Figure 2 shows such an interferometer, as described in 1949 by Weinberg and Wood.[2] G_1 is a diffraction grating that produces a +1 and a -1 order, and preferably no other orders. The upper beam passes through grating G_2, emerging as the -1 order of G_2. Similarly, the lower beam emerges as the +1 order of G_2. The two beams are thus brought together, producing interference. This interferometer has some remarkable broad source and polychromatic source fringe formation capabilities.

In a typical interferometer, the formation of fringes is accompanied by path differences generated between the two interfering beams. In Figure 3, we show two beams, 1 and 2, combining at an angle, thus producing fringes. Suppose that at point A on plane P the two beams have traveled the same path length from the source. The interference at A is then called the zeroth order bright fringe. At point B, the one beam is delayed by $\lambda/2$ (one-half wavelength) and the other advanced by $\lambda/2$, so that we get the first order bright fringe. The number of fringes is thus $n = \ell/\lambda$ where ℓ is the coherence length of the light, which is related to the spectral bandwidth by $\Delta R = \lambda_o 2/\Delta\lambda$.

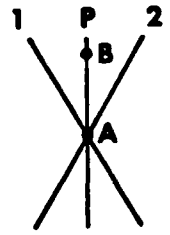

Figure 3. Interference of two waves.

Figure 4. Interference fringes. Left-coherent; right-incoherent.

In the grating interferometer, however, the fringe generation is produced without change of path length between the two beams. Inspection of Fig. 1 shows that the two beams combine everywhere in the fringe plane P with no path difference whatsoever. Thus, it would appear that an almost unlimited number of fringes, limited only by the grating aperture, is obtainable with perfectly white light. First order analysis confirms this, although higher order analysis shows that there are limitations, although for the symmetrical arrangement, where G_2 has twice the spatial frequency of G_1, the achromatization is perfect to all orders of approximation.

We offer a simple explanation for the achromatization. Each wavelength component of the source makes its own fringes independently of the other components. We require only that each λ make fringes of the same periodicity and that all sets of fringes be in registry. The fringe spacing is determined by two factors, the angle at which the two beams combine, and the wavelength. The longer wavelengths are diffracted at higher angles by G_1 and G_2, and therefore they combine at P at greater angles, in just the right amount to compensate for the longer wavelength. Theory shows that fringe position is independent of λ; hence the fringe patterns for all wavelengths are in registry. However, we do not have a correspondingly simple heuristic argument for this.

Similarly, the interferometer can form fringes under broad source illumination, without the limitation of Eq. (1). For a given source size, the number of fringes is limited only by the size of G_1 and G_2, and for the symmetrical configuration of Fig. 2, the source size can in theory be large without limitation; however, practical considerations, such as grating imperfections, will limit the size to a subtense angle of perhaps 10°, which is indeed a very large source.

Figure 4 shows fringes produced by the grating interferometer of Fig. 2, under point source illumination and broad source illumination. The vastly higher fringe quality for the noncoherent case is evident. Appropriate recording of the fringe pattern of Fig. 3b will result in a very noise-free grating.

Gratings for most uses should be blazed so as to concentrate the light into a single order. To produce a blazed grating by interferometric means, the fringes should have a brightness profile other than the simple sinusoidal profile produced by two-beam interference.

We suggest how this can be done (Fig. 5). As before, we have two gratings in tandem, with each grating producing many orders. If grating G_1 produces N orders and G_2 produces M orders, then there will be N^M diffracted orders, although some may be degenerate; for example, if G_2 has twice the periodicity of G_1, the beam formed by the +1 order of G_1 and the -1 order of G_2 will have the same propagation direction as the beam formed by the -1 order of G_1 and the zeroth order of G_2. As these beams propagate they combine in different ways, with different phase relations, to produce a resultant that is different at different planes.

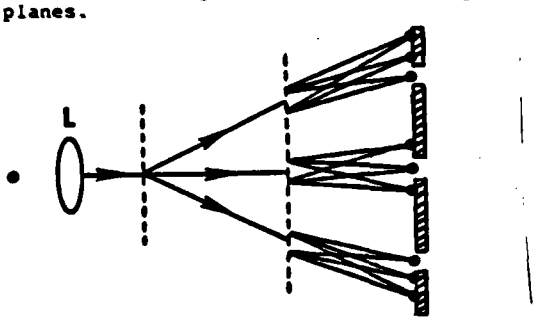

Figure 5. Gratings with spatial filtering.

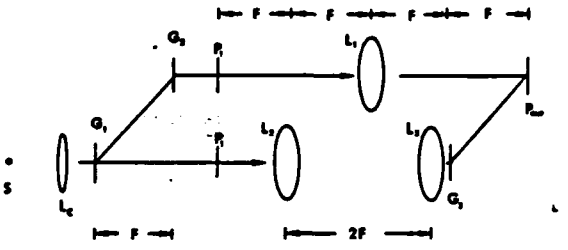

Figure 6. HOE-forming system.

For coherent light, the beams always combine coherently, and will generally produce fringes of high contrast. If the grating interferometer is illuminated with spatially incoherent light, the result is even more complex. In some planes all beams will combine coherently, even though the illumination is incoherent. The fringes in these planes will therefore be of high contrast.

Now, let the source, normally at the focal plane of a collimating lens, and therefore at infinity as seen by the gratings, instead be at a position such that the source is imaged just downstream from the second grating. At this position, a source image is formed for each of the myriad of beams produced by the two gratings. If the source extension is moderate, so that adjacent images do not overlap, we have the possibility of spatial

filtering. We can block certain images completely with stops, we can attenuate them by means of a grey scale mask, and if we become sophisticated, we can alter the phase by means of phase plates. By selecting the fringe profiles of the gratings, by judicious design of the spatial filtering masks, and by selection of the place of observation of the fringes, we can exercise considerable control over the profile of the fringe patterns. Indeed if we could completely control both the phase and amplitude of the spatial filter mask, we could achieve any desired intensity profile for the fringes, and the degree of spatial incoherence thus allowed would result in considerable noise reduction compared to the case of coherent illumination. And because the beams combine coherently, the fringe contrast would be high.

A special case of this type of fringe formation process, in which both gratings are of the same periodicity and the fringes are observed at infinity, that is, at the focal plane of a lens, was described in 1949 and became known as Lau imaging.[3] More recently, the fringes formed in incoherent light by two gratings in tandem have been described as grating images in which the first grating is imaged by the second.[4,5] The diffracted orders of the first grating represent the Fourier series components of the grating transmittance, and the diffracted orders of the second relate to what may be termed the transfer function of the second grating, considered as an imaging device. The Fourier components of grating G_1 are thus the components that, when they reach the observation plane, become the Fourier components of the fringe patterns thus formed. These components have been modified by a transfer function produced by the entire process, the free space propagation of the components, the modification by the second grating, and by the spatial filter mask we have inserted. This viewpoint is useful in describing the noise reduction capability of the process. The object (grating G_1) has a Fourier spatial frequency spectrum that consists of discrete frequencies, harmonically related, and the system transfer function is a comb filter, that is, a filter whose passband consists of only discrete harmonically related spatial frequencies that match those of the object. Noise, which has a continuous and rather flat, or uniform, spatial frequency spectrum, is thus almost completely rejected by the transfer function.

Thus, incoherent light in combination with a grating interferometer has the capability for producing, by interferometric means, diffraction gratings that are comparable to those produced by interference of coherent light, while having a lower noise background.

Diffraction lenses

Next we consider the production of diffraction lenses by interferometric means. The basic idea is that the interference between two spherical waves of different curvature (e.g., between a plane wave and a spherical wave) results in a structure akin to a Fresnel zone plate, where the fringe spacing is not uniform, but rather, decreases steadily. The zone plate, like a lens, focuses an impinging beam of light. Alternatively, the two beam interference pattern can be considered as an elementary hologram. When a hologram is illuminated with a duplicate of one of the two beams that produced it, the hologram regenerates the other beam. Thus, a hologram made by interference between a plane wave and a spherical wave can be either a collimating lens or a lens that images a collimated beam to a point image.

The diffraction lens, or holographic lens, or HOE lens, is becoming increasingly important, although it does not, compete head-on with the refractive lens, unlike the holographic grating, which does compete directly with the conventional ruled grating. But the HOE does find various niches, where it offers special advantages over the refractive lens.

The interference process is subject to the same noisiness that plagues the construction process for gratings. One would like an interference process that can produce interference between two waves of different curvature, using light that is either spatially or temporally incoherent or both. However, the grating interferometer process thus described yields only uniform fringes. Can a process be found that will produce the required tens or hundreds of thousands of fringes using light of low coherence?

This problem was addressed by Swanson, then a member of our laboratory.[6] Again, a grating interferometer was used, as shown in Fig. 6. Here, three gratings are in tandem. This arrangement has several advantages; for example, between G_2 and G_3, the two beams travel parallel paths. Also, theory shows that the distance d_2, between G_2 and G_3, drops out of the equations for fringe formation; we can let d_2 be any value we choose without affecting the fringe formation process. Thus, we can open up the spacing and place appropriate optical systems within. We must be cautious, however, that the optics thus inserted does not destroy the incoherent light fringe forming capability of the interferometer.

In the lower branch are placed two lenses separated by the sum of their focal lengths, the telescopic or afocal arrangement. A plane wave incident on the system emerges as a plane wave, with magnification equal to the ratio of the focal lengths, here taken to be the same. The upper path contains a single lens, which images the plane wave into a spherical wave. Each lens images the same plane, P_1, to the observation plane, P_{out}, where the beams overlap because of diffraction of the lower beam by G_3. Now, at plane P_1, the upper and lower beams will, if brought together, form fringes in broad source light in accordance with the basic theory of grating interferometry. These two planes, in the process of being imaged to P_{out}, do in fact combine, and therefore form fringes. We have three requirements (and one nonrequirement).

1. Both beams should image A with the same magnification, otherwise the corresponding rays will not combine.
2. Plane P_1 should be empty; it should not be a plane where a grating is located, otherwise the noise on the grating will appear in the fringe pattern.
3. We do not require that both beams have the same optical path length from P_1 to P_{out}, since the light, being very monochromatic, has a long coherence length. Thus, the two paths and the lens systems within them, do not have to be accurately matched.
4. We do, however, require that the free space, or Fresnel diffraction process be equal for the two beams. This means that the plane P should be equally distant from the source for each beam. From P_1 to P_{out}, there is only imaging, no Fresnel diffraction process.

The method is perfectly general; we may place any lens system in either arm of the interferometer, provided the above conditions are met.

Experimental results are shown in Figure 7. The improved SNR with spatially incoherent light is overwhelmingly evident. In the actual fringe pattern, the fringes are much too fine, (about 300 per millimeter) to see except under considerable magnification; hence, to produce Fig. 7, a diffraction grating of the same spatial frequency was overlain on the fringe pattern to produce a Moire pattern; the Moire pattern is in fact what is shown in Fig. 7.

Further work by the authors has shown that high diffraction efficiency is achievable, and lenses can be constructed for any set of conjugate focal planes, corresponding to either positive or negative lenses.

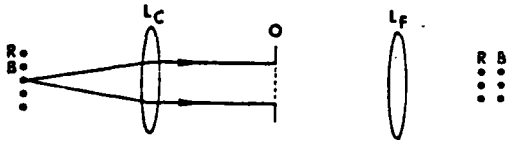

Figure 8. Fourier transformation in white light. R is red, B is blue.

Figure 7. HOEs: left-coherent; right-incoherent.

The seriousness of noise in HOEs is compounded by the bleaching process used for increasing the diffraction efficiency. In the bleaching process, an amplitude variation $t(x,y)$ is mapped into a phase structure $\exp(j\phi(x,y))$. Such a nonlinear transformation increases the noise level. This phenomenon is well known to holographers, who find that through the bleaching process, a small amount of noise, such as a weak diffraction pattern on the reference beam, is amplified into a very objectionable noise in the reconstructed image.

We next ask if HOEs can be generated from spatially coherent polychromatic light. They can indeed. A system given originally by Katyl[8] for achromatizing a Fourier transform relation, and extended by Collins[9] to fit into a grating interferometer, can be used for this purpose. The object to be Fourier transformed will then be a curved wavefront. This Fourier transforms into another curved wavefront, and the reference beam provided by the grating interferometer then yields a HOE.

We describe in a basic, heuristic way the achromatic Fourier transformation. We begin by noting that the Fourier transform, a Fraunhofer diffraction pattern of an object s, always occurs in the plane where the source is imaged (Fig. 8). However, the mask s generates new waves, which project back and form a virtual object which is wavelength scaled. We give an example; let s be a diffraction grating. Light impinging on the grating forms various orders, which project back to the source plane as additional object points, separated laterally from the actual source point. These source points have a separation proportional to wavelength. Now, the two lenses, L_C, the collimator and L_{FT}, the Fourier transform lens together reimage the source plane to form the Fourier transform. The magnification is $M = F_F/F_C$, the ratio of Fourier transform and collimator lenses, since the source is at the

focal plane of L_C and the image forms at the focal plane of L_P.

To achromatize the process, the magnification M should be inversely proportional to wavelength, to compensate for the wavelength dependence at the source plane. We let L_f be a zone plate lens, or HOE, as done by Katyl. The HOE has a focal length inversely proportional to λ: $F_P = F_{PO}\lambda 0/\lambda$ where F_{PO} is the focal length at a wavelength λ_O. The result is a Fourier transform with scale independent of λ. However, there is instead a longitudinal dispersion; for shorter wavelengths, the HOE has longer focal length, and the source image is then farther from the HOE (Fig. 8).

We now invoke the concept of the shift lens. We show (Fig. 9) two lenses, L_1 and L_2, separated by the sum of their focal lengths. For all object positions, the magnification is just the ratio F_2/F_1, the ratio of the focal lengths. Next, consider a third lens, L_S placed at the common focal plane of L_1 and L_2. This lens will cause the image to shift position, but the magnification is unaltered. This can be shown readily by simple algebra. Alternatively we can argue from physical principles. The lens L_3 is in fact a spatial filter, analagous to an electric filter. The operation it performs is linear and spatially invariant. Therefore, it can introduce no magnification, since if it did, it would not be invariant, just an electrical filter cannot change the scale of the signal passing through it.

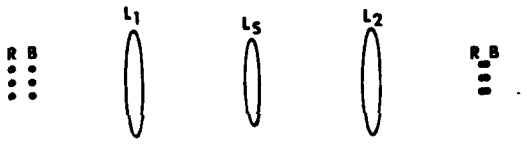

Figure 9. Principle of the shift lens. R is red, B is blue.

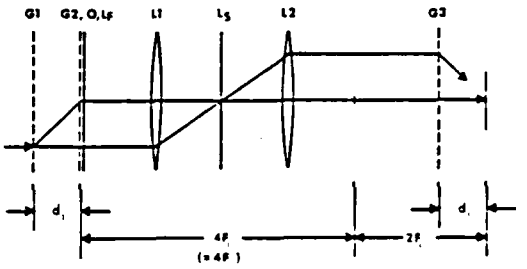

Figure 10. The complete system.

This argument should be quite compelling to those who have familiarity with spatial filters. Those not convinced by this heuristic argument may prefer just to calculate the magnification of this three lens system.

If we use a zone plate lens (HOE) for the shift lens, we can produce longitudinal dispersion, which calculations show will be proportional to wavelength. Alternatively, the already dispersed image formed by the Fourier transform lens of Fig. 8 can be compensated by this lens system. The total Fourier transform system is the units of Figs. 8 and 9 in tandem, where L_P and L_S are shown as HOES. The broad spectrum Fourier transform is displayed at P. The compensation is only approximate and is useful only over a small bandwidth, say, about 400 angstroms, since L_P disperses as $1/\lambda$, whereas the shift lens system, L_1, L_2, L_3, disperses in proportion to λ.

The final step is to insert these optical systems into a grating interferometer without destroying its fringe forming capability. This requires that both branches of the interferometer be well matched; thus, both beams of the interferometer should pass through all of the lenses. The final system is shown in Fig. 10. The lens L_P is combined with the grating G_2, as a single unit.

In order to form a HOE that acts as an off axis zone plate, or diffraction lens of positive focal length, we take the Fourier Transform of another zone plate lens of negative focal length. The HOE thus formed achieves noise reduction in two ways: first, the noise due to the intervening optical system which is always present when constructing a positive lens, is smeared due to the broadband nature of the illumination; and second, the point defects on the original zone plate being Fourier tansformed are smeared, due to the property of reciprocal spreading inherent in e Fourier transform process, that is, a point scatterer, which represents a concentration of noise, is spread by the Fourier transformation process into a low level noise of broad extent.

The capability for producing either gratings or HOES in light of reduced coherence is, we believe, of importance for applications where low noise optical diffraction elements are required. Can a HOE be made in light that is both spatially and temporally incoherent? At this time, we have not found a solution.

This work was supported by the National Science Foundation (grant NSF-G-ECS-8212472) and the Air Force (grant AFOSR 81-0243).

References

1. F. D. Bennett, "Optimum Source Size for the Mach Zehnder Interferometer," J. Appl. Phys. 22, p. 184 (1951).
2. F. O. Weinberg and N. B. Wood, Interferometer Based on Four Diffraction Gratings," J. Sci. Inst., 36, 227 (1959).
3. E. Lau, "Beugungserscheinungen an Doppelrastern," Ann. Phys. 6, 417 (1984).
4. B. J. Chang, "Grating Based Interferometer," Ph.D. thesis (The University of Michigan, Ann Arbor, Mich., 1974). University Microfilms, Ann Arbor, Mich.
5. G. J. Swanson and E. N. Leith, "Lau Effect and Grating Imaging," J. Opt. Soc. Am. 72, 552 (1982).
6. G. J. Swanson, "Interferometric Recording of High Quality Zone Plates in Spatially Incoherent Light," Opt. Lett. 8, 45 (1983).
7. G. J. Swanson, "Partially Coherent Imaging and Interferometry Based on Diffraction Gratings," Ph.D. thesis (The University of Michigan, Ann Arbor, Mich., 1983). University Microfilms, Ann Arbor, Mich.
8. R. H. Katyl, "Compensating Optical Systems. Part I: Broadband Holographic Reconstruction; Part 2: Generation of Holograms with Broadband Light; Part 3: Achromatic Fourier Transformation." Appl. Opt. 11, p. 1241, 1248, 1255, (1972).
9. G. Collins, "Achromatic Fourier Transform Holography," Appl. Opt. 18, 3109 (1981).

Miscellaneous

13.1 Journal Articles

During this reporting period, 9 journal articles were published (or prepared for publication but not yet published (or prepared for publication but not published).

13.2 Papers presented at symposia.

Most of the work described here was presented at symposia, primarily OSA and SPIE.

13.3 Persons associated with this effort

E. N. Leith (PI)
G. Collins (graduate student)
Y. Cheng (graduate student)
S. Leon (graduate student)
G. Swanson (graduate student)
I. Khoo (Professor of Physics at Wayne State University)
H. Chen (Professor of Physics at Sagninaw Valley State College)

13.4 Doctoral dissertation "Temporally and Spatially Incoherent Methods for Fourier Transform Holography and Optical Information Processing," by Gleen D. Collings, 1983.

END

FILMED

11-85

DTIC